SESSION VIII

SYSTEM DESIGN FOR NUCLEAR FACILITIES

Tuesday, August 3, 1976
CHAIRMAN: J. Murrow

THE REMOVAL OF RADIOACTIVE AEROSOLS FROM THE POST ACCIDENT ATMOSPHERE
    OF AN LWR-CONTAINMENT
                              G. Haury, W. Schoeck

GAS CLEAN-UP SYSTEM FOR VENTED CONTAINMENT
                              J. L. Kovach

STANDARDIZATION OF AIR CLEANUP SYSTEMS FOR NUCLEAR POWER PLANTS
                              E. Nicolaysen, K. E. Carey,
                              J. J. Wolak

CONTROL ROOM VENTILATION INTAKE SELECTION FOR THE FLOATING NUCLEAR
    POWER PLANT
                              D. H. Walker, R. N. Nassano,
                              M. A. Capo

EVALUATION OF CONTROL ROOM RADIATION EXPOSURE
                              T. Y. Byoun, J. N. Conway

OPENING REMARKS OF SESSION CHAIRMAN:

    In a day and a half we have heard about particulate and gaseous
collection, monitoring, fire, disposal of collected materials, effects
of natural and manmade disasters, and now we are going to learn how
systems can be, and should be, designed to further the safeguards
that Dr. Moeller spoke to us about during lunch.

THE REMOVAL OF RADIOACTIVE AEROSOLS
FROM THE POST ACCIDENT ATMOSPHERE
OF AN LWR-CONTAINMENT

G. Haury and W. Schoeck
Laboratorium fuer Aerosolphysik und Filtertechnik
Projekt Nukleare Sicherheit
Kernforschungszentrum Karlsruhe, Germany

Abstract

The computer code NAUA has been developed to model the removal of the airborne radioactive particles in the post accident atmosphere of an LWR-containment. It calculates the aerosol processes coagulation, diffusion, sedimentation and thermophoresis, the steam condensation on the particles, and significant thermodynamic effects such as heat removal by the containment spray system.

With the first version NAUA-Mod1 calculations have been done which show the dominant role of the condensation process. The number concentration and the size of the so formed droplets affect very strongly the rate of subsequent coagulation between droplets and the remaining dry particles. This effect is further enhanced by temperature decrease due to spraying.

The paper dicusses the structure and potential of the NAUA code, and presents the results of a parametric study on the important removal effects. Some problems of the physical behavior of the aerodispersed system in the post accident LWR-atmosphere are discussed which cannot be solved by the modelling alone. Therefore, the investigation of the condensation process and of the proprties of the three phase particle droplet steam system will be part of the supporting experimental program.

I Introduction

The events in the course of a hypothetical accident in a light water reactor could be divided into three main groups which are physically quite different, the release of radioactive material from the melting core into the containment, the removal of radioactivity from the atmosphere inside the containment, and the transport phenomena and radiological impact to the environment. As the amount of released radioactive material can be very high in melt down accidents following blow down, the removal processes inside the containment are of great importance as a means of mitigating the radiological consequences.

The physical and chemical properties of the radioactive material immediately suggests a classification into the groups of chemically nonreactive noble gases, volatile fission products mainly iodine compounds, and solid particulate material. The latter includes most of

the long lived isotopes as e.g. Co, Sr, Ce, and Pu.

Mathematical modelling of the time dependent behavior of the gaseous radioactive elements and compounds is not very difficult as soon as the physical and chemical processes of removal are known. In the case of the aerosolic matter, however, even if the removal processes were understood, the modelling would still remain complicated by interactions between the particles themselves and, particularly in the LWR case, by the presence of large amounts of condensable water vapor released during blow down. This water will condense on part of the aerosol, and thus introduce a third, liquid phase to the system.

The subject of this paper will be to discuss a mathematical model and results of preliminary calculations of the time dependent aerosol behavior in the post accident atmosphere of an LWR containment.

II Theoretical basis of the model

Many descriptions of aerosol removal in closed containments start from the suggestion that the decay rate of any kind of mean airborne concentration C be proportional to C itself

$$dC/dt = -\alpha.C \qquad (1)$$

which immediately leads to an exponential decay. General experience contradicts this exponential law, and the model is adjusted by introducing time dependent factors α, which are obtained empirically from experimental work. This numerically simple approach enables the model to handle multicomponent systems with moderate computation times.

The opposite approach, the one we use, is to model as closely as necessary the physical processes in the aerosol system. This leads to more complicated mathematical structures and consequently to necessary reductions in the geometrical complexity of the model containment in order to keep computation times adequately low.

We consider our approach to be more reliable for two reasons: First, in the large volumes of a reactor containment, the aerosol removal is governed by the physical aerosol processes rather than by the geometry of far off containment walls, and second, decay factors in eq.(1) are valid only for the experimental conditions from which they were deduced, and cannot be transferred to other situations with greatly different parameters. The use of experimental data should be limited to cases where the microscopic processes are well understood both in the experiment and in the calculated situation.

Starting from these considerations we constructed the NAUA code (NAUA = NAch-Unfall-Atmosphaere = post accident atmosphere) using the microscopic aerosol removal processes coagulation, sedimentation, thermophoresis, and diffusion, and the interaction process with the condensing water vapor, which is a molecular high speed process. These processes are considered to be the most important, in future versions

of the code other mechanisms, as e. g. gravitational coagulation, may be added if necessary.

The model further includes homogeneous steam and particle sources of arbitrary time dependence.

III Numerical concept of the code

In calculations of time dependences, the most important parameter of aerosols is the size of the individual particle or the size distribution of the aerosol. Sizes of irregularly shaped particles can be defined in numerous ways, we choose the mass equivalent radius as a measure, because the particle mass is proportional to the radioactivity. The effect of the irregular shape is accounted for by means of form factors whenever necessary. In discussing the structure of the model, we will concentrate on particle radius and particle properties. Detailed descriptions of the underlying physical mechanisms are given in earlier reports [1].

The code is separated into two main subunits because of numerical reasons. The first is called NAUCON, and calculates the condensation of steam on the particles and the thermodynamic properties of the gas phase. The equation given by Mason [2] is used to calculate the change of particle radii

$$r \, dr/dt = A \, (S(t) - \exp(B/r)) \tag{2}$$

where S is the degree of saturation, which is close to one in the LWR post accident atmosphere, and A and B are thermodynamic functions of the gas-steam system.

The second subunit of the code, NAUPAR calculates the aerosol removal processes. The change of the population of a size class $n(r)$ is given by

$$dn(r,t)/dt = Q(r,t) - (\alpha_S(r) + \alpha_D(r) + \alpha_T(r)) \, n(r,t)$$

$$- \int K(r,r_1) \; n(r,t) \; n(r_1,t) \; dr_1 \tag{3}$$

$$+ \iint K(r_2,r_3) \; n(r_2,t) \; n(r_3,t) \; dr_2 \, dr_3$$

Here Q is the particle source term and the alfas are coefficients for deposition by sedimentation, diffusion and thermophoresis respectively. The two integrals describe the action of coagulation. The first integral is the coagulation rate f r o m the size class under consideration to all others, the second describes coagulation i n t o this size class, where obviously $r^3 = r_2^3 + r_3^3$.

Eq.(3) is the PARDISEKO equation which was used to calculate aerosol removal in LMFBR containments [3]. In the LWR case this equation

cannot be used, because $n(r)$ is no more a continuous function and the coagulation integrals cannot be solved with the necessary precision. Thus the coagulation integrals have been replaced by a much simpler particle counting and classifying routine that, by definition, conserves the mass during coagulation. Because the new method cannot be represented by an equation of the type of eq.(3), its description will be omitted here. A detailed discussion is given elsewhere [4]. Another advantage is the higher computation speed of the new technique.

The already mentioned form factors are used in the NAUA model to account for the differences between the reality and the idealized mathematical model which e.g. always uses spherical particles. Presently three form factors are used. The first one f_m is needed in eq.(2), which is valid for condensation on water droplets only, and not on irregularly shaped solid particles. The rate of steam condensation is dependent on the degree of wetting of the particle, too, f_m thus depends on the actual radius of every individual particle. The second form factor, the aerodynamic form factor f_b describes the change in mobility due to the fluffy structure of the fuel particles. The coagulation form factor f_s, finally, accounts for the fact that the target particles are considerably larger than is represented by the mass equivalent radius.

All three factors are size dependent and unknown for fuel aerosols. Their values will be measured in the experimental part of the program. At the moment, values from pevious work on LMFBR aerosol behavior are used for f_b and f_s, f_m is set to one.

In order to test the performance of the code under varying conditions, and to identify the most relevant parameters that need experimental investigation a sensitivity study has been executed. Because the response of the aerosol system to changes in steam density is always instantaneous, it is reasonable to discuss the condensation processes and the long term removal separately, as will be done in the following sections.

IV Short term calculations of steam condensation

Steam condensation on fuel-like particles is the elementary process of the NAUA model for which the least experience exists. It has been studied intensively with variations of all possible parameters, the most important results will be discussed now.

As a result of the condensation, which acts only on the bigger particles of the initial size distribution, bimodal particle-droplet distributions are generated within a few seconds. Fig.1 shows as an example the resulting bimodal distributions that are created from an initial dry particle size distribution of log-normal shape with a mean geometric radius of 0.1 μm and a standard deviation of $\ln\sigma = 0.4$. It is apparent that the temperature of the system has little influence. This is valid for all other effects, too, which are not very sensitive to temperature, with the exception of steam density of the containment
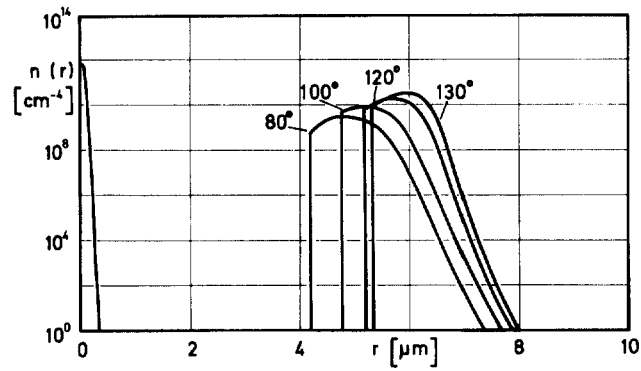
Figure 1   Bimodal size distribution developed
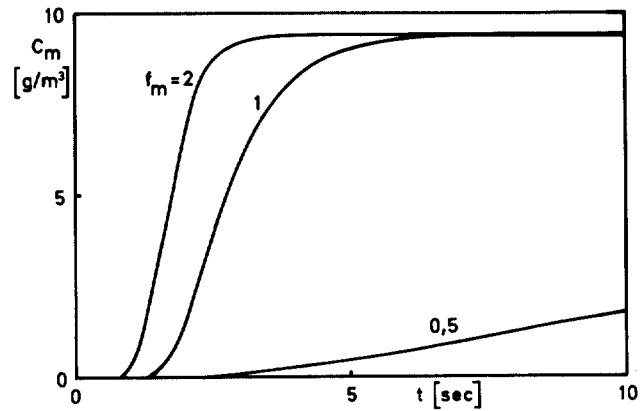at different temperatures.

Figure 2   Time dependence of droplet mass
concentration with different
condensation form factors f_m.

atmosphere. Thus temperature dependences will not be discussed in this paper, the influence of steam density, however, is shown in the next section.

A large bandwidth of particle size distribution parameters has been used in calculations of steam condensation together with various time dependent steam source terms. The differences in the resulting bimodal size distributions are great, but is was not possible to evaluate any quantitative simple law to connect input and output of the condensing steam-aerosol system. The complete model has to be employed in order to obtain reliable results.

Further calculations have been done to assess the influence of the non-sphericity of the particles on the condensation process. Since no experimental work has been published on this problem we varied the form factor f_m. Starting values for the initially dry particles are $f_m = .5$, 1, and 2. Fig.2 shows the time dependent mass concentration of the growing droplets, the total condensable steam concentration being 10 g/m^3 in all three cases. For $f_m = 0.5$ it takes more than two minutes until all the steam has condensed on the particles, in the other cases a few seconds are sufficient for the droplet formation. The great difference that is also exhibited in the number and size of the droplets emphasizes the need for exact experimental data. The steam condensation on fuel particles will be investigated closely in the first phase of the experimental program.

V Long term calculations of aerosol removal

Using an $f_m = 1$, long term calculations have been done to study the influence of the aerosol parameters and of containment spraying on the removal process. To do this it was necessary to input into the model some properties of the containment and some assumptions on the accident sequence. The containment properties are mainly geometric and thermodynamic data, and were taken from the Reactor Safety Study [5]. The temperature function T used in our calculations is shown in Fig.3. When necessary it was extended to longer times. It will be shown, however, that a further temperature decrease beyond the first 30 minutes will contribute little more to the removal of particles. Thus in most cases the temperature was held constant after the rapid decrease in the first half hour. As already mentioned, the main effect of temperature is to change the amount of condensable water vapor in the system. The density of condensable steam is shown by function C_w in Fig.3.

Among the other data the particle source term has the greatest influence on the behavior of the aerosol-steam system. On the other hand very little is known of these data, particularly when the particle size distributions and the single particle properties are required. As a rough estimate for particle sizes, we used experimental results of generation of fuel aerosols by exploding wire technique which were done in our laboratory previously [6], and by a direct arching method which was developed by one of us recently. The most reasonable values for a particle size distribution of fuel aerosol in
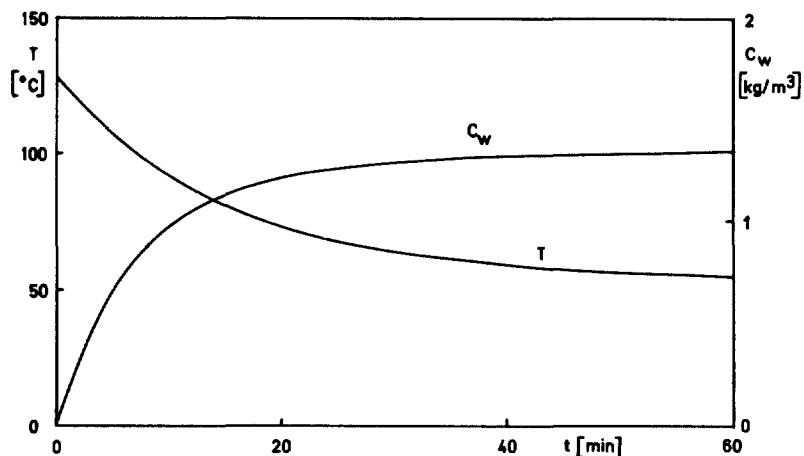
Figure 3   Time dependence of containment temperature T
            and steam density C_w used in the long term
            calculations.

the melt down and evaporation phases are a mean geometric radius of
0.1 μm and a standard deviation of 0.4, assuming a log-normal size
distribution. We have used these values in our long term calculations.
The   total   released   mass   is   1000 kg   as   given   in   [5].   In   the
calculations reported here, we assumed a source with constant rate but
with variable duration. Another removal mechanism of great importance
is   the   action   of a spray system. Its effect on particles is not yet
investigated very well, we consider the most relevant effect to be the
rapid decrease of temperature which frees large amounts of condensable
steam   (Fig.3).   Whereas   temperature   decrease   through   cold   containment
walls   mainly   leads to water condensation on the walls, the result of
the spray action as a volume effect is that the steam condenses on the
particles,   because   the surface of the particles is greater by orders
of magnitude than the surface of the containment walls or of the spray
droplets.   Thus   in   our model we assumed the action of spraying to be
that   all   condensable   steam   condenses   on   the   particles. The real
fraction   and its dependence on the various parameters will be subject
to investigations in the experimental program.

Table I   shows   the   scheme   of   parameter variations in the long term
calculations.   Case D1 is the reference case with which all others are
compared.   The   values f_k = 3.5 and f_s = 8.2 are taken from previous
LMFBR safety experiments [6].

Fig.4   shows   the   time   dependence   of   particle   number   and   mass
concentrations C_n and C_m for   the   reference   case   D1.   The   most
interesting result is that, at the end of the particle source action,

743

case #	particle source	f_b	f_s	spray
D1	30 min	3.5	8.2	off
D2	120 min	3.5	8.2	off
D3	30 min	1.0	8.2	off
D4	30 min	3.5	2.0	off
W1	30 min	3.5	8.2	on
W2	120 min	3.5	8.2	on

Table I   Scheme of parameter variations
for long term calculations.

the total released mass of 1000 kg (40 g/m^3) is airborne. It takes some hours for the coagulation process to form big enough particles, before the sedimentation becomes effective. In our case the temporal separation of the dominance of coagulation and sedimentation phases is so large that it exceeds the duration of the particle source. This can be seen clearly in Fig.5 where the cases D1 and D2 with different source term duration are compared. Only an insignificant delay of mass removal is visible, because the coagulation phase is much longer than either source term interval.

It should be emphasized, that this result was calculated with an aerosol behavior model that depends strongly on aerosol properties which are not exactly known. Fig.6 represents the results of calculations with variations of the particle properties, namely form factors f_b and f_s.

f_s acts on the coagulation rate only. Therefore, in case D4 the coagulation rate was lower than in case D1. After a prolonged coagulation phase, the aerosol removal rate finally approximates the same value as in case D1.

In case D3 the particle mobility was increased by putting f_b = 1. The factor f_b acts on all removal processes simultaneously. So an immediate beginning of the removal without a distinct coagulation phase and a much faster decay of the mass concentration is observed. Thus with an f_b = 1 also a dependence on source term duration could be expected that is more pronounced than in Fig.5.
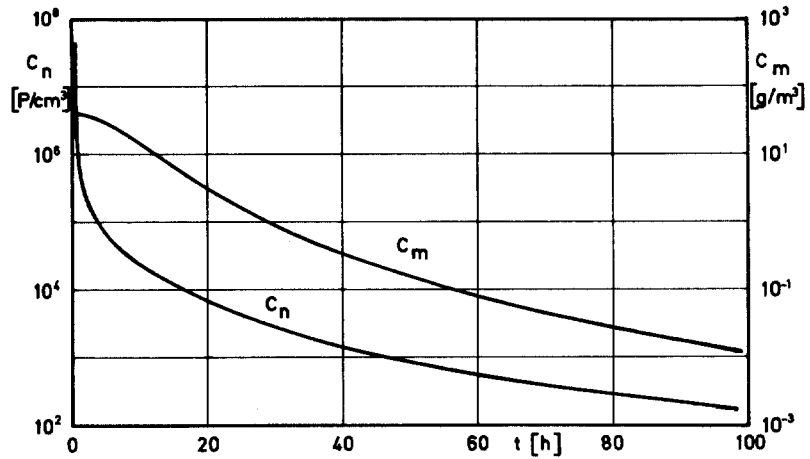
Figure 4   Time dependence of airborne particle
            mass and number concentrations C_m
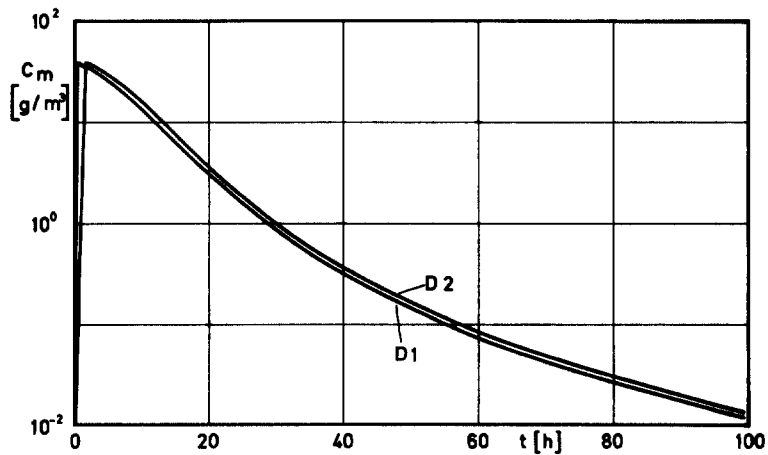   and C_n in the reference case D1.

Figure 5   Airborne particle mass concentration
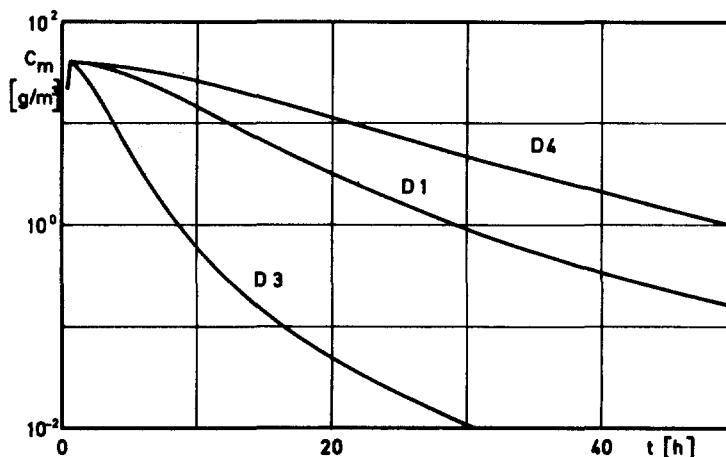   with different source term duration.

745

Figure 6   Airborne particle mass concentration
with different particle form factors.

The fact that both the influence of the source term and the long term
behavior are very sensitive to the particle form factors emphasizes
the importance of their direct experimental measurement, which will be
part of our experimental program.

So far we did not consider the effect of condensation of large amounts
of water vapor that will take place during the action of containment
spray systems. In Fig.7 the airborne mass concentration for cases W1
and W2 are shown. The time dependence is quite different from that of
the 'dry' D cases. First of all nearly the total mass consists of
condensed water droplets, as only 40 g/m^3 maximum of solid material
were released. The mass concentration closely follows the curve C_W of
condensable steam that is set free due to the temperature decrease.
After 20 minutes, the droplets have grown so big that the
sedimentation becomes noticeable. All the time the coagulation acts
only between the source particles and the already existing droplets,
and is enhanced by their great size difference. A short time after the
end of the particle source action, all particles will have vanished
due to coagulation into the droplets, and the long term decay of
airborne solid mass is determined almost only by the sedimentation of
the droplets.

This is illustrated in Fig.8 where the airborne mass of solid material
(without the condensed water fraction) for cases W1 and W2 is compared
with case D1. The difference between cases W1 and W2, that was
obscured by the great water content in Fig.7, is now clearly visible.
The decay of solid mass or of radioactivity is faster in both cases
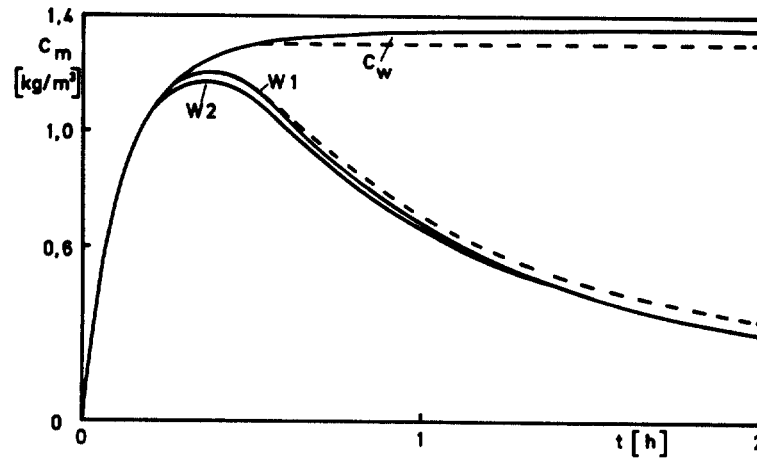
Figure 7   Airborne mass concentrations in the
            calculations with spray W1 and W2
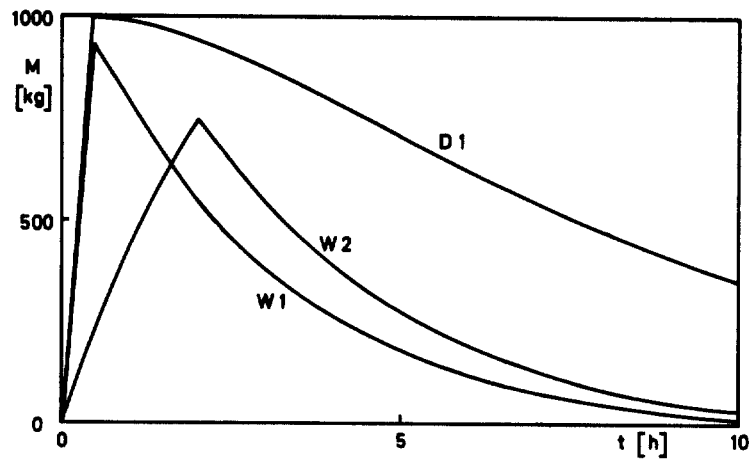   and condensable steam density C_w.

Figure 8   Total airborne mass of solid material in
            the containment for the spray cases W1 and
            W2 compared to the case D1 without spray.

than in case D1 without spray. However, the fractional content of solid matter, that is shown in Fig.8, is only a rough estimate. The measurement of the distribution of solid particulate material inside the droplets as a function of the system parameters is one of the great problems that have to be solved experimentally.

It should be noticed finally that the effect of spraying is most significant in the beginning when the temperature is still high. A shut off of the spray system after 30 minutes will cause only a short delay of the removal of airborne mass, as is shown by the dashed lines in Fig.7.

VI Experimental Program

As has been shown, some of the unknown physical parameters of the aerodispersed system have great influence on the time dependence of the airborne particle mass concentration. If the NAUA code calculations are intended to be more valuable than conservative assessments, the measurement of these parameters becomes unavoidable.

The construction of the experimental facility has been started, with which investigations of the microscopic effects such as form factors, condensation phenomena or particle distribution in the droplets can be done as well as integral experiments on spray system efficiency, wall effects and code verification. It is planned that the construction and testing of the facility will be completed in the first half of 1977. The assembling of the instrumentation and development of new measurement techniques, especially for the droplet mesurement, will be finished early enough to be used in the testing period.

References

[1] G.Haury et al, 'PNS Halbjahresberichte', No.II/1974, KFK report 2130, (1975) and No.I/1976, to be published

[2] B. I. Mason, The Physics of Clouds, Oxford, 1971

[3] H. Jordan and C. Sack, 'PARDISEKO 3, a computer code for determining the behavior of contained nuclear aerosols', KFK report 2151, (1975)

[4] G. Haury and W. Schoeck, 'Parameterrechnungen mit dem NAUA-Modell', PNS Arbeitsbericht No. 78/76 (1976)

[5] USNRC, 'Reactor Safety Study', WASH 1400, NUREG 75/014, (1975)

[6] H. Jordan, W. Schikarski, H, Wild, 'Nukleare Aerosole im geschlossenen Containment', KFK report 1989, (1974)

GAS CLEAN-UP SYSTEM FOR VENTED CONTAINMENT

J. L. Kovach
Nuclear Consulting Services Inc.
Columbus, Ohio

Abstract

Component selection and sizing analysis was performed for both operational and post accident vented containment for light water reactors.

The criteria used was the decrease of pressure and retention of significant health hazard isotopes which would be present in the containment after a loss of coolant accident.

Time-pressure curves were developed for different vent volumes together with fission product capacity for the various components of the system.

The analysis indicates that the design of post accident venting systems is feasible and the protection afforded can justify the cost of the system.

Two types of operation were analyzed; treatment external to the containment and vent to the atmosphere, and treatment external to the containment with recirculation to the containment.

I   Introduction

The ventillation systems for nuclear power stations are still primarily in the realm of sheet metal work. Although the gaseous waste treatment systems may involve chemical process technology, the expertise of the chemical solvent vapor handling techniques have not permeated the nuclear industry. The use of deep bed adsorption systems to recover solvent vapors has been practiced for over 70 years, and aspects of this process can be well suited for any major release clean-up or post accident venting of the containment. In the following, design and operation criteria for such systems is evaluated.

II   Clean-up Volumes

Figure 1 is a reproduction from WASH 1400 (1) for a typical PWR where the containment free volume is 1.8×10^6 ft^3. The volumes to be cleaned-up and vented are at the following rates:

Daily Vent % Containment Volume	CFM
100	1,250
200	2,500
300	3,750
500	6,250

Therefore even at a 2,500 cfm rate the failure pressure range will not be reached and at approximately 200 minutes after LOCA the pressure inside the containment would be decreasing even with no containment safeguards operating.

Similar values can be generated for BWRs also, however both the size and cost is less therefore, the sizing evaluation here is based on PWR only.

III Design Concept

The air (gas) motive force exists in the containment itself. The pressure differential is sufficient to result in the required flow because total pressure drop through the system is, at most, several psi. Therefore the basic clean-up process does not require blowers.

The first analysis is based on an iodine and particulate fission product removal at the 3,000 CFM flow rate corresponding to venting 3 containment volumes per day. The temperature exiting from the containment is assumed at 130°C.

The following components are considered for this application.

a) Heat Exchanger using water to lower gas temperature to ~50°C.

b) Sand Bed filters for particulate removal (99.97% Efficiency).

c) Iodine removal bed based on decay (99.99 + % Efficiency).

The cost estimates for such components in 304 stainless steel are

a) $180,000.00
b) $105,000.00
c) $285,000.00
Total: $570,000.00 redundant, code construction.

The iodine adsorption bed sizing is based on long term operating life, where the iodine may be transported through the bed; however it is decayed in a similar manner to the noble gas delay beds. The design of such bed is discussed in detail in Part VI of this paper.

For elemental iodine decay in the adsorbent bed approximately 10,000 lbs of carbon is required assuming an inlet concentration of 1.0 mg iodine FP/m^3.

The sizing data for sand beds is based on operational experience at the Savannah River Plant of USERDA (2) (3).

This mode of operation would result in venting to an outside location and the noble gases would not be delayed to an appreciable extent in the system.

If a recirculation mode is used, i.e., the particulate and iodine FP decontaminated noble gas-containing-air is reinjected into the containment, the rate of return would be approximately one third of the total gas removed because a large part of the steam is condensed. The rate of returnable gas is approximately 1000 CFM.
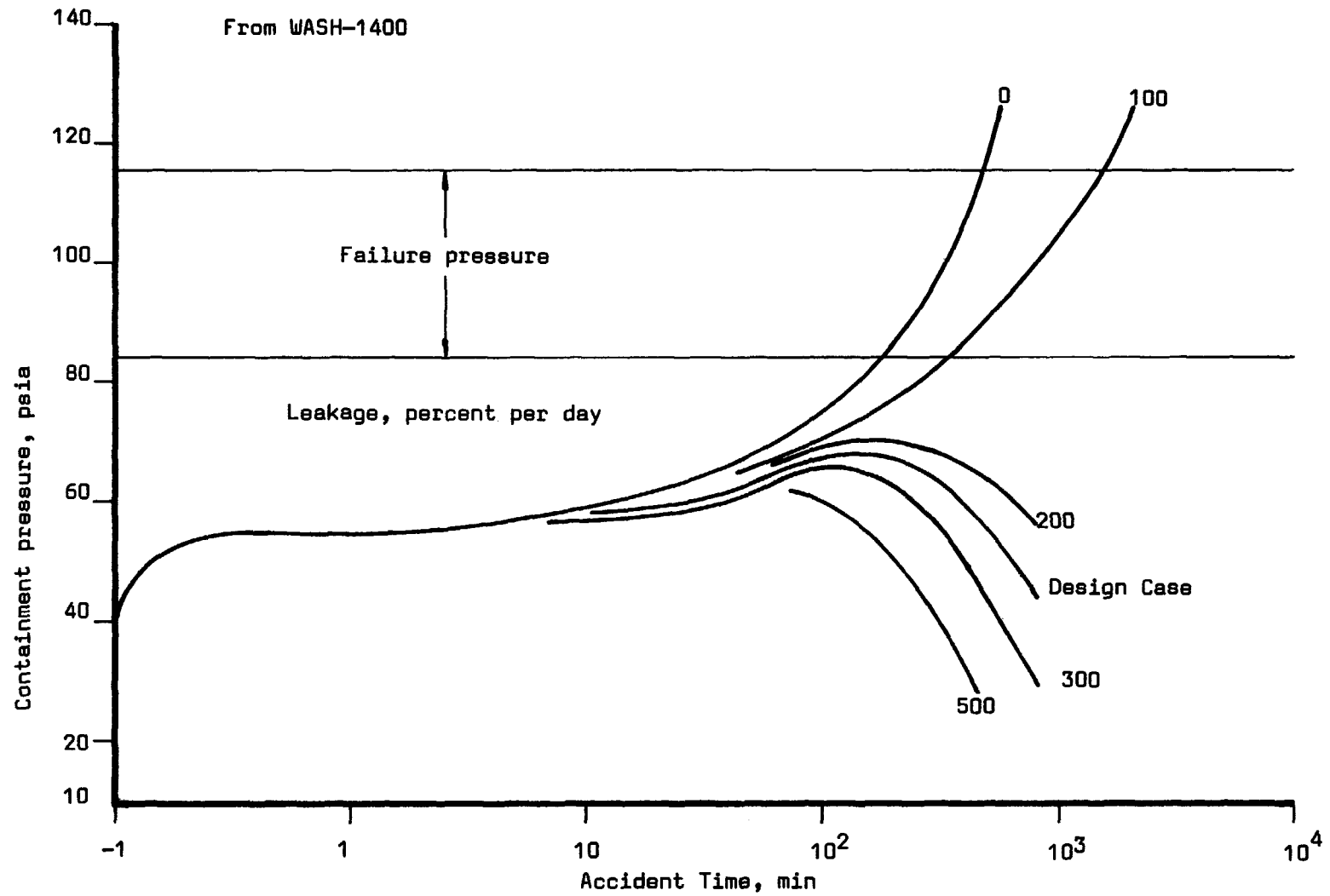
Figure 1. PWR containment pressure as a function of leak rate for an assumed LOCA with no containment safeguards.

If reinjection is used, an airmoving device capable of boosting the residual gas to approximately 60 psia is required; the cost of such a compressor is estimated at $40,000.00 each.

IV   Clean Up Components

Sand Bed Filter

Vertical bed using base grating with graduated particle size packing. Approximate gas velocity through bed at <20 FPM, bed depth 80-100 inches.   The efficiency for such beds was measured for particulate fission products and uranium or plutonium aerosol of above 99.99% (4) (5) (6).

Iodine Removal Bed

Grated bed is most beneficial where the roughing adsorber contains non-combustible 80-90% minimum efficiency packing followed by or in a separate bed with impregnated carbon or other high efficiency adsorbent.   Velocity at >40 FPM; bed volume to be sized for long-term decay type removal process, where self-regeneration takes place.   Efficiency for iodine fission products 99.99%. Detail of such sizing is discussed in Part VI of this paper.

V   Estimation of Installed Cost

Direct Costs

Equipment	$650,000
Installation (75%)	487,500
Structures and Buildings	125,000
Subtotal.	$1,262,500

Indirect Costs

Engineering Design (18%)	$227,250
Field Erection (50%)	631,250
Owner's Cost (5%)	63,125
Contingency (25%)	315,625
Interest During Construction (30%)	378,750
Subtotal.	$1,616,000
TOTAL	$2,878,500

VI   Sizing of Iodine Decay Beds

Elemental iodine is removed from contaminated atmosphere in activated carbon beds by adsorption.   In flowing air stream a concentration band is formed in the inlet side of the adsorber from 0 iodine concentration to the inlet concentration.   Once this concentration band is formed it moves along the depth of the adsorbent bed at a constant rate.

A similar concentration gradient is formed when methyl iodide is decontaminated by isotope exchange.   Both processes are controlled by bulk diffusion, i.e. intergrain diffusion in laminar flow systems, while the rate controlling

step becomes a much faster pore diffusion in turbulent flow systems. The reason for this phenomenon is that in turbulent flow, the movement of an iodine or methyl iodide molecule to the surface of the carbon grain becomes much faster.

When adsorption of a radioactive molecule takes place the above described manner of achieving equilibrium is not applicable, because as a result of the radioactive decay the movement of the concentration gradient will not stay constant but will decrease in rate as it moves along the adsorbent bed and finally will become stationary. (7)

As a result of radioactive decay the mean life of a radioactive isotope is

$$\mathcal{T} = 1/\lambda \tag{1}$$

Denoting the radioactive atom of an adsorbing molecule as X* the following will take place on the surface.

When the molecule is adsorbed, upon decay of X* a recoil nuclei will be ejected into the gas phase or into the body of the solid adsorbent. The adsorption site (active site) will be freed and may be used for the adsorption of a molecule containing the undecayed X* isotope, if the fragments of the original molecule and the daughter isotope do not interfere. (Although the possibility of new active site generation,i.e. extended surface or porosity by the radiation and the recoil atoms is indicated, its effects are not discussed here.)

The process is somewhat simplified when the decay product is only weakly adsorbed. Such is the case during the adsorption of halogen isotopes either in the form of Hal^- or $(Hal)_2$ or more specifically I^- or I_2. The decay products Kr, Xe and other noble gases are not chemisorbed at all and are only weakly adsorbed by Van der Waals forces. Therefore it can be assumed that one adsorption site is freed-up on each iodine isotope decay.

In theory, if only radioactive isotopes are present,the possibility of the "perpetual" operation of the adsorbent bed exists with complete adsorption of the continuously introduced iodine upon sites continuously freed up by radioactive decay of the adsorbed iodine and subsequent release of the daughter product into the gas phase.

At zero time the surface of the adsorbent is completely free from radioactive iodine.   At time t=0, beginning from the inlet section $x_0 = 0$,the iodine containing gas stream is passed through at a concentration of C_0 and a gas velocity of v. The superficial gas velocity is always much greater than the rate of movement of the concentration band (or adsorption wave front), therefore the iodine concentration will sharply (exponentially) decrease along the length of the adsorbent bed. Thus, initially, the radioactive iodine content of the first portions of the emerging gas stream will be negligibly low even for relatively short adsorbent depths. This initial condition is shown on Figure No. 2.

If the introduction of the iodine containing gas stream is maintained,the inlet section of the adsorbent bed is gradually filled with iodine resulting in the formation of the adsorption wave front; behind this front the adsorbent is at equilibrium with the inlet iodine concentration and in front of it there is a sharp fall to zero concentration. As the front moves forward, because of

partial freeing of the adsorbent surface as a result of decay into a weakly adsorbed molecule, the rate of movement of the front (in contrast to its movement in case of non-radioactive molecules) will continuously be slower until it stops completely at some depth of the adsorbent bed designated L.

The value for L depends on λ, the geometry of the adsorbent bed, the gas flow rate v, the capacity of the adsorbent for iodine, the temperature of the system, the relative humidity of the system, the inlet concentration C_0, and the form of the iodine species present. When the wave front has reached this section L along the adsorber a steady state system is achieved.

In the following only initial and limiting case equations are shown as a rough guide for the practical application of this design method.

By setting $C(x,t)$ to denote the concentration of the radioactive gas per unit volume of the adsorber charge at a given time t and at a given distance x from the inlet of the adsorber. The corresponding concentration of the radioactive gas adsorbed per unit volume of the adsorbent is denoted by $A(x,t)$. The maximum amount of the radioactive gas component adsorbed (at equilibrium) per unit volume of the adsorbent is denoted by N_0. The balance equation in the gas phase will be:

$$\frac{\partial C}{\partial t} = u \frac{\partial C}{\partial x} - Kf(C)\ (N_0 - A) \tag{2}$$

and in the adsorbed phase:

$$\frac{\partial A}{\partial t} = Kf(C)\ (N_0 - A) - \lambda A \tag{3}$$

where $Kf(C)\ (N_0 - A)$ characterizes the adsorption rate, i.e. the quantity of radioactive gas adsorbed per unit time per unit volume of adsorbent on the available free sites $N_0 - A$.

The value of λA denotes the rate of decay of the adsorbed iodine per unit time per unit volume of adsorbent.

At low concentration the concentration dependence $f(C)$ can be described by the Langmuir equation:

$$f(C) = \frac{C}{C + b_0} \tag{4}$$

In general b_0 is very much smaller than the inlet concentration C_0. Such function corresponds to a low dependence of the adsorption rate on the space concentration almost up to complete adsorption of the starting radioactive gas.

The value K characterizes the adsorption rate and is the reciprocal of the time required for the adsorption of the iodine by the adsorbent. Both experimental data and theoretical evaluations show that K increases in turbulent flow for the earlier described reasons.

At the initial moment t=0

$$C(x,0) \text{ and } A(x,0) = 0 \tag{5}$$

and in the inlet section at x=0

$$C(0,t) = const. = C_0 \tag{6}$$

The initial stage of the adsorption up to the formation of the stable adsorption wave is characterized by the concentration distribution illustrated in Figure No. 2. The distance 1 over which the concentration falls by a factor of two is given approximately by

$$1 = \frac{u}{K} \tag{7}$$

While the ratio of the outlet concentration C_f to the initial concentration C_0 is

$$\frac{C_f}{C_0} = \exp(-\frac{x}{1}) \simeq \exp(-\frac{Kx}{u}) \tag{8}$$

where x is the full length of the adsorber bed.

This ratio is established after a short time:

$$\tau_1 = \frac{x}{u} \tag{9}$$

which is required for the passage of a portion of the gas through the apparatus and then will increase slowly.

As a result of the high rate of adsorption, particularly in turbulent flow, the length of the adsorption wave front will be very much less than the depth of the adsorber, therefore C_f will be orders of magnitude lower than C_0.

In the next stage of the adsorption process as the adsorption wave front is established, the concentration distribution of the radioactive iodine in the gas phase and on the adsorbent is shown on Figure No. 3.

Balance equations can best be used to determine the wave front velocity u.

The amount of the radioactive iodine entering in time dt per unit section of the adsorber equals uC_0dt. The front of the adsorption wave moves by udt in the same length of time; the amount of iodine adsorbed per unit section of the adsorber equals approximately vN_0dt because the maximum adsorption capacity A_m is close to N_0.

However in the same length of time, of the adsorbed radioactive iodine $\approx$ N_0x (per unit section of the adsorber) a λdt fraction will decay. The total amount of radioactive iodine decaying equals $N_0x\lambda dt$.

Because of the law of conservation of matter:

$$uC_0 = vN_0 + N_0x\lambda \tag{10}$$

Considering that

$$v = \frac{dx}{dt} \tag{11}$$

and integrating Eq (10):

$$v = v_0 \exp(-\lambda t) \tag{12}$$

where the initial velocity of the front u_0 at $x = 0$ is

$$v_0 = u \frac{C}{N_0} \ll u \tag{13}$$

From equation (12) it follows that the motion of the front will practically cease after a time:

$$\tau \approx \frac{3}{\lambda} \tag{14}$$

which is approximately three times the half life of the radioactive iodine.

The length of the adsorption wave front can also be calculated by

$$L_a \approx \frac{v_0}{\lambda} \approx \frac{uC_0}{\lambda N_0} \tag{15}$$

from equation (10) when $v=0$.

When the movement of the adsorption wave front ceases some final concentration distribution is established in the adsorbent bed as illustrated on Figure No. 4.

In the part from the inlet section to $x=L_a$, the adsorbent is at equilibrium while the concentration in the gas phase drops to a value of:

$$C_1 \approx b_0 \tag{16}$$

Beyond this layer there is a sharp exponential fall in the concentration C and A according to equation (8). Thus the final outlet concentration is approximated by

$$\frac{C_f}{C_0} = \exp\left[-\frac{(x-L_a)}{1}\right] \tag{17}$$

Therefore near complete decay of the radioactive iodine can be achieved in approximately twice the length of the adsorption wave front:

$$x = 2L_a \tag{18}$$

Expressed on a volumetric basis, $V_a = SL_a$ is used to denote the value of the adsorbent containing the adsorption wave front and $V = Sx$ will be the adsorbent volume. From equation (15):

$$V_a = \frac{uC_o}{\lambda N_o} \qquad (19)$$

and from equation (18):

$$V = 2V_a \qquad (20)$$

Therefore the quantity of required adsorbent can be calculated to permit decay of the iodine without breakthrough.

In case of isotope exchange the number of active sites (when excess iodine is deposited on the surface, which is the case above 2% I_2 present) is approximately the same as the sites available for adsorption.

All estimates should account for poisoning of the bed by adsorption of non-iodine species on the adsorbent surface. Experimental data indicates that poisoning takes place only in a narrow inlet section of the adsorber; thus the correction should be additive and not factored into the sizing calculation.

Symbols

A = quantity of radioactive gas adsorbed at concentration C.
b = constant in Langmuir equation.
C = concentration of radioactive gas.
l = length of bed in which the concentration falls by a factor of two.
L = length of the adsorption wave.
N = quantity of radioactive gas adsorbed by unit volume of adsorbent.
S = cross section of the adsorber.
t = time.
u = velocity of the adsorption wave front.
v = superficial gas velocity.
V = volume of the adsorbent.
x = length along the adsorbent.
X* = denotes decaying isotope.
λ = decay constant.
τ = mean lifetime of decaying isotope.

Subscripts

a = properties of adsorption wave front.
f = final.
m = maximum.
o = initial.

Figure 2

Concentration of adsorbing isotope

C_o

u

u

t_1 t_2

0

Adsorbent Bed Depth

x

Figure 3

Concentration of adsorbing isotope

C_o

A

udt

N_o
A_m

$t+dt$

t

t

0

vdt

Adsorbent Bed Depth

x

Figure 4

Concentration of adsorbing isotope

C_o

N

N
A_m

b_o

0

L_a

x

Adsorbent Bed Depth
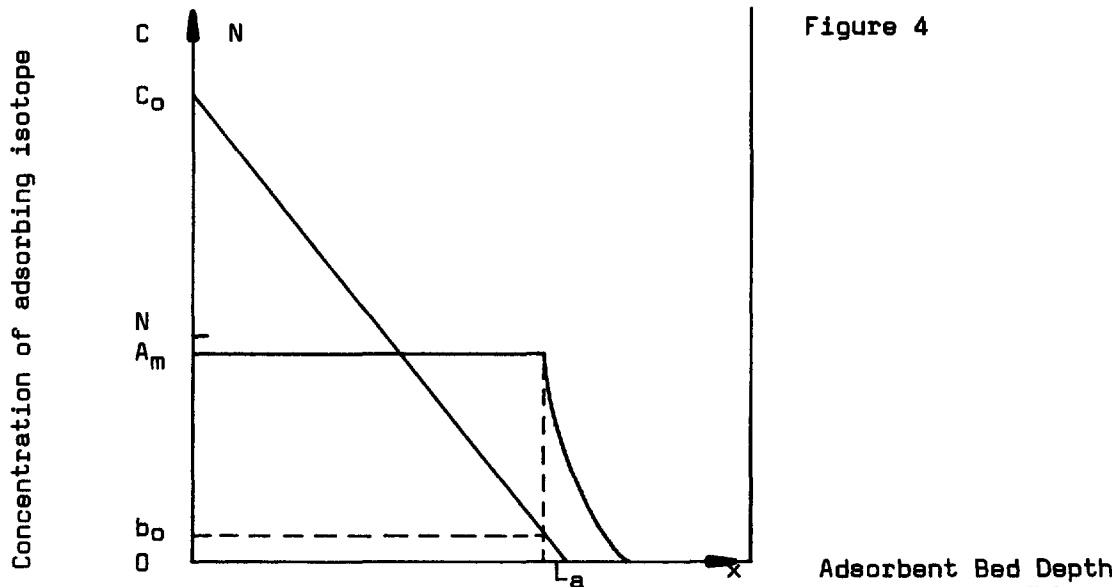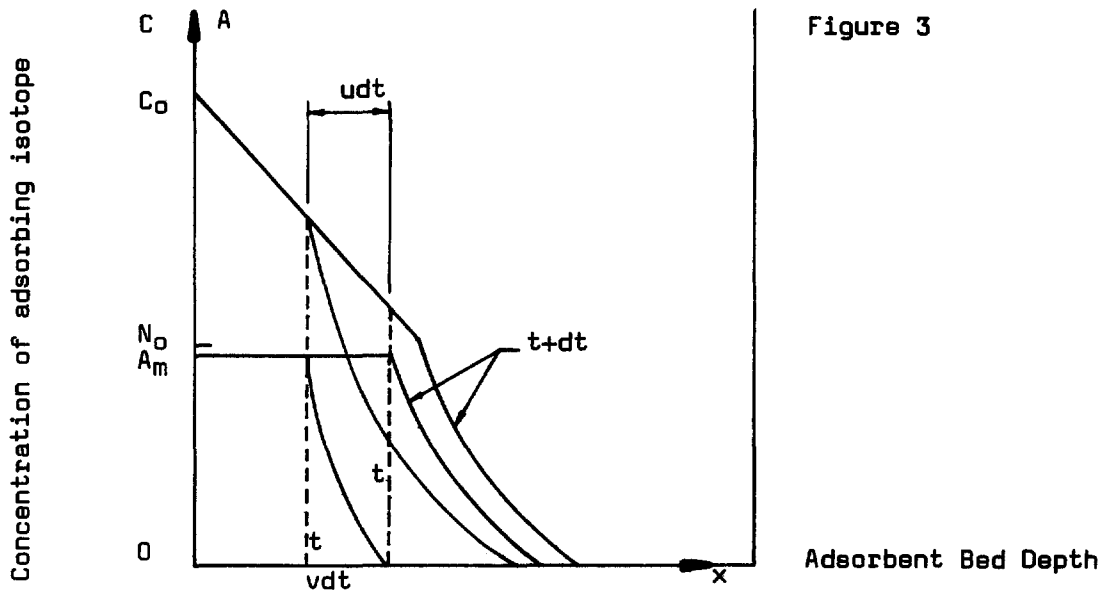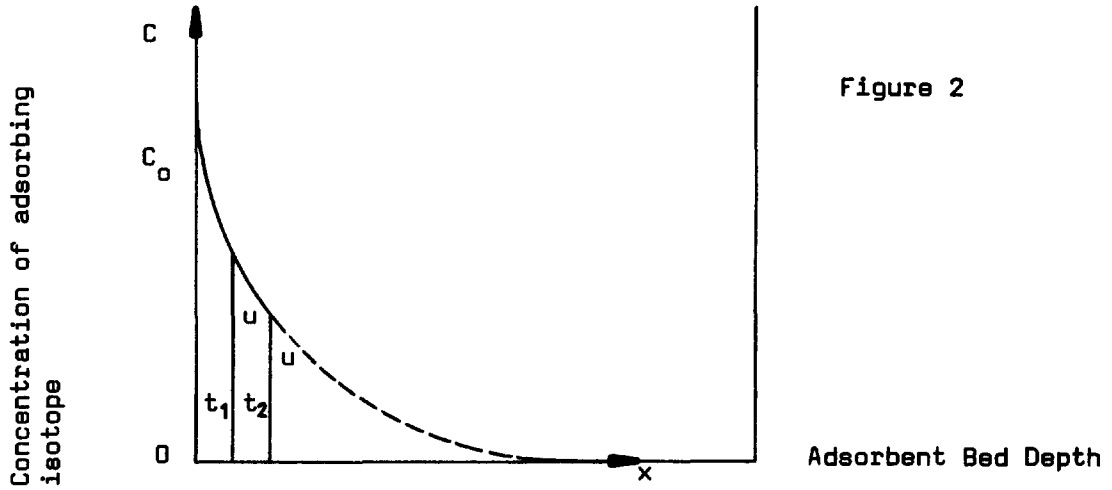
References

1. "Reactor safety study", Appendix VIII, <u>USAEC Report</u> WASH-1400 (1974)

2. Sykes, G. H. and Harper, J. A. "Design and operation of a large sand bed for air filtration." <u>Treatment of Airborne Radioactive Wastes.</u> IAEA Vienna (1968)

3. Zippler, D. B. "Evaluation of multistage filtration to reduce sand filter exhaust activity." <u>USAEC Report,</u> CONF 740807 (1974)

4. Thomas, J. W. and Yoder, R. E. "Aerosol size for maximum penetration through fiberglas and sand filters." <u>A.M.A. Arch. Ind. Health</u> Vol. 13, No. 545 (1956)

5. Kovach, J. L. and Newton, R. G. "Deep bed activated carbon for liquid, solid, aerosol and gaseous filters." <u>USAEC Report</u> CONF 700816 (1970)

6. Cheever, L. in <u>ZPPR FSAR</u> (1968)

7. Roginskii, S. Z. and Todes, O. M. "Physicochemical characterization of the dynamics of sorption of radioactive substances." <u>Radiokhimiya,</u> 4, No. 1, 39-44 (1962)

DISCUSSION

COLLARD: Did you evaluate the dimensions of a delay bed for iodine when the charcoal used is an unimpregnated one?

KOVACH: We have postulated a case where the quantity of adsorbent in the system is increased to the point where it would completely delay even xenons, if not the kryptons, in the system. Cost can determine whether it is better to use a very large external system or to pump back about a third of the total flow into the containment. On a cost basis, it looks much more economical to pump it back and allow the noble gases to decay, at least for a certain length of time, in the containment before venting to the outside.

FORSBERG: Is it correct to assume that this system could be designed so no electric power would be required for operation?

KOVACH: Electric power would be required only if you are returning the gas. If not, you don't need air motive power because the containment is pressurized. Total pressure drop for the system can be calcualted. It is about 3 psi.

LORENZ: Mention was made of very deep and, I presume, large charcoal beds. For those of you who aren't familiar with the possibilities of combustion of charcoal, a word of caution. As the size of charcoal beds increases the chance of spontaneous combustion also increases. The probability of spontaneous combustion depends upon the reactivity of the charcoal, the air supply rate, and the temperature of the bed (whether elevated by decay heat or some other means). I

refer you to a brief discussion in the 13th AEC Air Cleaning Conference paper entitled "Behavior of Highly Radioactive Iodine on Charcoal" by Lorenz, Martin, and Nagao.

KOVACH: You are correct. In the paper, we were discussing the use of inorganic non-carbon adsorbents to pick up most of the iodines and the use of mixed media for an adsorption system.

MILLER: Is the purpose of this system to more quickly accelerate the depressurization of the containment or to allow a higher containment leakage rate?

KOVACH: Either/or. This process permits you to vent under control and to depressurize the containment more than you otherwise could.

MILLER: Is it your intention to modify or replace the existing iodine safety systems in primary containment such as the spray systems?

KOVACH: We have not looked at eliminating sprays and using this type of an approach as a tradeoff.

MILLER: Is it logical to assume that you could not release the vented gases directly to the environment because of the noble gas dose?

KOVACH: Not necessarily. A dose evaluation is required for this type of safety approach. The main thing we wanted to be sure of was that all particulates and iodine, plus everything else that's volatile, except noble gases, is removed as close to 100 per cent efficiency when the contaminant is depressurized. After initial recirculation for a period, the system can be operated in the vent mode.

DIETZ: What are some approximate dimensions and quantity requirements of adsorbent for the proposed system?

KOVACH: Approximately 10,000 lbs (on carbon basis) for the postulated design case.

STANDARDIZATION OF AIR CLEANUP SYSTEMS
FOR NUCLEAR POWERPLANTS

E. Nicolaysen - Supervising Mechanical Engineer - Nuclear
K. E. Carey   - Associate Mechanical Engineer   - Nuclear
J. J. Wolak   - Associate Mechanical Engineer   - Nuclear

Gibbs & Hill, Inc.
Engineers, Designers, Constructors
New York, New York

Abstract

The Gibbs & Hill, Inc. (G&HI) approach to standardization of the air cleanup systems serving the controlled access areas in pressurized water reactor (PWR) powerplants was developed in the course of designing a succession of powerplants including Fort Calhoun Unit 1, Angra Unit 1, C.N. Almaraz Units 1 and 2, Comanche Peak Units 1 and 2, Fort Calhoun Station Unit 2 and the G&H standard plant.

The G&HI designs emphasized operability, maintainability, quality, testability, redundancy, constructability, and operation convenience at minimum cost. The later designs have been strongly influenced by Nuclear Regulatory Commission (NRC) Regulatory Guide 1.52, (1). All designs have, to some extent, been influenced by conditions related to the geographical locations of the stations.

The relationship and interplay of these factors is illustrated by discussions of the Comanche Peak Units 1 and 2, Fort Calhoun Station Unit 2, and the G&HI standard plant designs.

The features covered by this discussion are:

1. Physical and general arrangements (GA)
2. Modular design
3. Effects on total system design
4. Interrelationship with engineered safety features (ESF)
5. Compliance with NRC Regulatory Guide 1.52
6. Methods of energy conservation
7. Maintainability of the filter trains
8. Testability
9. Reliability of filter train systems
10. Economics of the design
11. Manufacturing and shipping processes

The standard plant, has to some extent, complicated the system design by requiring a design that can be built on a variety of sites. The design innovations to standardize the air-filtration system necessitated by this requirement are discussed in this paper.

Introduction

Historically, the ventilation system was a stepchild in the design of nuclear powerplants, mainly because the average design engineer did not have a full appreciation of the physical size of the air cleanup components and thus allocated insufficient floor space for this equipment. This led to designing air cleanup trains customized to fit into available spaces which resulted in adequate but less than desirable ventilation system designs. GHI was no exception in this matter as shown in Wash-1234 (2). Visits by the authors to powerplants under construction, air cleanup system vendor facilities, as well as the publication of Wash-1234 and NRC Regulatory Guide 1.52 convinced G&HI that a better approach to an air cleanup system design was needed. Four steps were taken to achieve a better design:

1. The Heating, Ventilating, and Air Conditioning (HVAC) engineer made certain that sufficient space for all the ventilation equipment had been allocated during the initial phases of the GA layout.

2. Centralization of the air cleanup units and other ventilation equipment, while maintaining separation criteria, was pursued.

3. An economic study was performed to determine if capital and operating cost of refrigeration equipment would be offset by savings in filter costs, smaller ducts, and smaller equipment sizes for sites where the available cooling water temperature was above 70 F.

4. After discussions with vendors, an economic study was performed to determine if several smaller identical air cleanup units, completely shop-manufactured and shipped intact to the jobsite, would be less expensive than larger custom built units, which were shop-assembled, then dismantled, and finally field-reassembled.

From the results of the studies and a judicious allocation of equipment space and location, G&HI arrived at a standard design, based upon use of modular air cleanup units, which we believe is unique to the power industry. The design can be applied to any size nuclear powerplants by either adding or subtracting modules.

This paper presents the standardization of the air cleanup system and gives a brief discussion of the application of the design to the system design on the Comanche Peak, Fort Calhoun Station Unit 2 and the G&HI standard nuclear powerplant. Topics include the system designs, mode of operations, maintenance and testing, economics, and the impact on the design by the NRC regulatory guides and standards, and similiar regulations.

General System Description

Air cleanup units are necessary to minimize the radioactive gaseous and particulate effluents released to the environs during normal operation (3), to remove fission products in a postaccident environment, and to protect plant operators from the accidental

release of radioactive gases (4). The ventilation systems requiring the use of air cleanup units include the controlled access area ventilation (CAAV), control room HVAC, hydrogen purge, and containment preaccess filtration.

The CAAV system encompasses the ventilation of the controlled access sections of the auxiliary building, safeguards areas, and the fuel-handling building, all known as the nuclear island. The system also provides for containment purging and ventilation during reactor shutdown.

The CAAV system uses a modular design arrangement for both the supply and exhaust. The supply is comprised of several 30,000-scfm air-filtration cooling and heating modules and the exhaust is comprised of several 15,000-scfm air cleanup modules. The supply modules, six for a single 1130-MW reactor plant such as Fort Calhoun Station Unit 2, (see Figure 1) eight for a two unit plant such as Comanche Peak (see Figure 2), are connected in parallel to a common air intake plenum. Outside air is drawn in through a missile- and tornado-protected seismic Category I intake by the supply units and discharged into a common distribution plenum. A main supply header is attached to this plenum for the auxiliary building (controlled access portions), the safeguards building, the fuel-handling building, and for containment purging. The quantity of modules is a function of plant physical size, not of plant geographical location, since the entering air is cooled to a predetermined temperature.

The exhaust modules, 12 in the case of Fort Calhoun Station Unit 2, (see Figure 1), 16 for Comanche Peak (see Figure 2), are connected in parallel to the plant vent stack plenum. Each exhaust module is also connected to a common suction plenum which contains branches for the auxiliary building, safeguards building, fuel-handling building, containment, and the condenser vacuum pump discharge. Two of the exhaust modules are classified as ESF and are maintained on a standby mode. Dampers in the common suction plenum of the exhaust allow the fuel-hanlding building exhaust to be routed through the ESF modules during refueling periods. The exhaust modules are separated into two equipment rooms which are located on different elevations, thus enabling separation of redundant modules. (see Figures 3 and 4).

The control room HVAC system is designed to insure that the habitability of the control room is maintained during all operational transients and following design basis accidents (DBA). The air cleanup equipment of the system consist of the emergency filtration and the emergency pressurization modules.

The system is provided with ductwork which supplies approximately five percent fresh makeup air from a missile-protected air intake and 95 percent of recirculation air from the conditioned space (see Figure 5). The system is provided with dampers which also allow the system to operate on 100 percent recirculation air (see Figure 6). The emergency filtration module, which is sized at 4000-scfm for a single-unit control room and at 8000-scfm for a double-unit control

room, consists of a fan and air cleanup unit; it draws a portion of the recirculation air from the return air ductwork and discharges this air to the suction side of the air-conditioning units. The capacity of the emergency filtration module is sufficient to filter the control room volume once every hour.

The emergency pressurization module, which consists of a fan and an air cleanup unit with a capacity of 1000 scfm, draws outside air in through the missile-protected intake and discharges it to the suction of the emergency filtration module. The quantity of air handled by the emergency pressurization module is sufficient to maintain the control room at a slight overpressure (.25 inches wg).

The emergency filtration and the emergency pressurization modules are provided with 100-percent standby capacity. The redundant components are physically separated, assigned to two separate and independent trains with only common supply and return ductwork.

The hydrogen purge system is designed to maintain the concentration of hydrogen within the containment below three-percent by volume following a LOCA. The purge system is provided with supply and exhaust modules. The supply module, consisting of a prefilter and supply blower, draws 1000 scfm of outside air in through a missile-protected seismic Category I intake and discharges into a supply header. The supply header routes the purge air into the containment distribution ductwork through a single penetration.

The exhaust module, also consisting of a fan and an air cleanup unit with a capacity of 1000 scfm, draws the containment atmosphere through a single penetration through a suction header. The containment atmosphere is routed to the plant vent stack through the exhaust module discharge header.

The hydrogen purge supply and exhaust modules are provided with full redundancy. The redundant modules are physically separated from each other by being located on different elevations of the auxiliary building, each having connections to the common purge supply and exhaust headers.

Additional connections on the hydrogen purge supply header and hydrogen purge exhaust header are provided in the case of the Comanche Peak Station. This enables the system to purge either one of the containments, fulfilling the protection requirements for both units with a single system.

The containment preaccess filtration system is designed to reduce the concentrations of radioactive particulate and gaseous iodine to permit limited personnel access to the containment during a hot standby or shutdown without containment purging.

The preaccess filtration modules, consisting of a fan and air cleanup units draws air from the lower levels of the containment and the discharge is routed through ductwork to the operating level. Two 50-percent modules are used, each sized for 15,000 scfm and located on the intermediate levels of the containment.

The design is based on the use of two supply module sizes, i.e., 1000 scfm and 30,000 scfm, and three air cleanup module sizes of 1000 scfm, 4000 or 8000 scfm, and 15,000 scfm.

Module Description

The air cleanup units design incorporated the guidelines of NRC Regulatory Guide 1.52 and the recommendations of ORNL-NSIC 65 (5). Specific problems in previously designed air cleanup units as shown in Wash-1234 were also considered. Particular attention was paid to adequate lighting and service space (both inside and outside of the unit) to facilitate maintenance and testing (see Figure 7). Prime consideration was given to the shortening of maintenance time thus reducing cost and exposure to the personnel.

The normal exhaust air cleanup units and fans are designed for normal operation only. These units are used in the containment pre-access filtration and CAAV systems. The components comprising the air cleanup units are as follows in sequential order: prefilter, HEPA filter, adsorber, and HEPA filters. Moisture separators and electric heaters are not used since the relative humidity does not exceed 70 percent, as shown on Figure 8. The fans are direct-drive single-inlet centrifugals. Centrifugal fans are required since the systems resistance approaches 15 inches wg with dirty filters. The direct-drive limits the amount of maintenance required for each fan. Adjustable inlet vanes are provided for each fan to maintain the design flow requirements over the range of system resistance.

ESF air cleanup units are used in the hydrogen purge exhaust, control room pressurization, control room recirculation and the controlled access emergency exhaust. The components comprising the ESF air cleanup units are in sequential order as follows: moisture separators, electric heater, prefilter, HEPA filter, adsorber, and HEPA filters. The controlled access emergency exhaust units are the only exception to this in that prefilters are not used.

Moisture separators, although inefficient when compared to prefilters used within the air cleanup modules, are used in lieu of prefilters in the CAAV ESF air cleanup modules.

The reduction in the life of the HEPA filter resulting in the use of the moisture separator is considered justified for two reasons. First, the function of the filtration units, using the moisture separator section is to act as a redundant standby to those air cleanup modules which operate normally and to operate only during refueling and in the event of an accident condition. Secondly, to maintain the same standard size of the other modular filtration units, the prefilter has been replaced by the moisture separators. It was felt that the disadvantage in shortening the HEPA life was far out-weighed by the savings realized in maintaining the same basic housing size.

The same direct-drive single-inlet centrifugal fans are used as in the normal modules. Adjustable inlet vanes are provided for each fan to maintain the design flow required.

Component Description

Moisture separators are provided in the air cleanup units and function in an adverse environment of moisture-laden air. The moisture separators are designed to remove an entrained water and steam mixture from the air entering the air cleanup modules. The removal of the water and steam mixture protects the prefilters, HEPA filters, and adsorbers from water damage and plugging. The moisture separator section of the air cleanup module is built up from a number of cartridges each capable of handling approximately 1500 scfm, and each consisting of stainless steel baffles and a stainless steel fiberglass mesh. The addition of the fiberglass enables the moisture separator to act as a medium efficiency filter. To reduce the potential of fire, the moisture separators are rated UL Class I (6).

Electric heaters are provided downstream of the moisture separator section. These heaters are designed to heat the passing airstream and reduce the relative humidity to below 70 percent, thus allowing the filters and adsorber to maintain their design efficiency. The electric heater casings are of stainless steel construction. The elements are the extended-fin type with chromized steel enclosing the resistance heating wire.

The prefilters are the first set of particulate filters located in the normal air cleanup unit. Prefilters remove the larger particulates thus extending the life of the more efficient and expensive HEPA filters located downstream by preventing premature loading. The prefilter section consists of a number of filter cartridges each capable of handling approximately 1200 scfm at one-inch wg. Prefilters are constructed of fiberglass media with a chromized steel casing. In order to reduce the potential of fire, the filters are rated UL Class I.

The second set of particulate filters located in the air cleanup modules are HEPA filters. The HEPA filters are designed to remove fine particulate from the exhaust air which may be radioactive. The third set of particulate filters are also HEPA filters. This HEPA filter section is located downstream of the charcoal adsorber and is provided for removal of potentially radioactive carbon particules released from the adsorber bed. Each HEPA filter section is comprised of a number of filter cartridges each capable of handling approximately 1500 scfm of air. The HEPA filters are of the separatorless design, constructed of a fiberglass media with a stainless steel casing. In order to reduce the potential of fire, the HEPA filters are designed to satisfy the requirements of UL-586 (7).

The adsorber section is located downstream of the first HEPA filter section. The adsorbent removes radioactive gaseous iodine (either elemental iodine or organic iodines) from the exhaust air. The adsorbent material is activated, impregnated charcoal. This material is contained in vertically oriented bed modules fabricated from stainless steel. The face of each module is either a perforated stainless steel sheet or mesh. The adsorber section is capable of handling 1000, 4000 or 8000, and 15,000 scfm, with a resulting face

velocity enabling a 0.25-second (per 2-inches of adsorbent material) residence time of the exhaust air within the adsorbent. The design of the adsorbent section allows for gravity feeding of the adsorbent through the top of the adsorber section and withdrawing of the adsorbent through drain piping located at the bottom of each bed.

Mode of Operation

The air cleanup modules, modes of operation are tabulated in Table 2. During normal plant operation for Comanche Peak, Fort Calhoun Station Unit 2 and the G&HI standard plants four of the CAAV air cleanup modules, the hydrogen purge air cleanup modules, and the control room emergency air cleanup modules do not operate.

As indicated in Table 1, during startup and normal operation, four supply and eight exhaust modules operate continuously, while the remaining CAAV modules are on standby. Following plant shutdown, one additional supply and two additional normal exhaust modules are required to function for containment purging. During the refueling mode, the operation of two exhaust modules are terminated and left on standby since the fuel-handling building exhaust filtration is accomplished by using the two emergency exhaust modules.

During startup, normal operation, and shutdown, the CAAV emergency exhaust and standby modules do not normally operate. However, periodic testing and inspection may be performed. The tests and inspections will include sequencing of dampers, unit flow tests, heater capacity tests, filter and adsorber penetration tests, adsorber efficiency tests, filter resistance tests, and visual inspection of the module.

The emergency exhaust modules are operated during refueling mode, serving as the fuel-handling building ventilation exhaust. In the event of a fuel-handling accident at least one exhaust module is capable of maintaining the fuel-handling building at a slight negative pressure thereby limiting the potential offsite release of radioactive iodine and other radioactive particulates, to the environs in accordance with 10 CFR part 50, Appendix I. The normal ventilation system is not required to operate in the event of a LOCA. In the event of a LOCA, at least one emergency exhaust unit is manually operated to maintain the controlled access areas at slight negative pressure with respect to the uncontrolled access areas and the outside.

During the winter months, both energy and filter usage are conserved by terminating the operation of several modules, thus reducing the flow through the CAAV system. Sufficient number of two-position volume dampers and flow indicating meters are located in the system to allow two system balance points, summer and winter, and still allow sufficient ventilation airflow within areas of potential radioactive leakage.

The parallel operation of 8 to 12 exhaust modules requires constant surveillance of the flow to ascertain that the modules are paralleling. This is accomplished by using flow straighteners and multi pitot-tube monitors in the inlet of each module with either

direct or remote readout so that an operator can adjust the fan inlet vanes to maintain the flow constant as the filter resistance increases because of dust loadings.

The hydrogen purge system air cleanup modules and the control room air cleanup modules are only used following a DBA. These modules all have 100-percent redundancy. The hydrogen purge system is only operated in case the containment hydrogen recombiners fail.

Maintainability, Testing, and Reliability

It should now be evident that we are dealing basically with only three different size air cleanup modules, all designed in the same manner, which is, from a maintenance point of view, a desirable arrangement. All modules in the nuclear island are identical to the containment modules which means the same maintenance procedure can be used for all. The hydrogen purge modules are identical to the emergency pressurization modules which are essentially smaller versions of the other air cleanup modules using the same components.

The air cleanup modules use cartridge-type prefilter sections with rated efficiencies of 85 percent according to the NBS dust spot method of testing. A high-efficiency prefilter is used to extend the life of the HEPA filters which decreases the frequency of filter replacement. Prefilters specified for the air cleanup system have an initial air resistance of 0.35 inches wg and are replaced when the final air resistance reaches 1 inch wg. High-efficiency prefilters of the automatic-roll type are also used in conjunction with the supply air handling units to maintain relatively clean areas throughout the power station.

Separatorless high-efficiency (99.9 percent at 0.3 micrometer as in reference (1)) particulate air HEPA filters have been used to extend the filter replacement frequency, thus reducing maintenance cost and radiation exposure to personnel. The apparent lower initial air resistance and larger dust-holding capacity of separatorless-type HEPA filters coupled with operating these filters to a final air resistance of 3.5 to 4.0 inches wg, extends the life of the filters and reduces the frequency of the maintenance cycle.

In specifying the charcoal adsorber section of the filtration unit, maintainability was an important consideration. The gasketless adsorber section using vertically oriented charcoal beds and horizontal airflow with a remote means of filling and emptying the charcoal bed was chosen. This method eliminated the need for maintenance personnel to come in direct contact with the contaminated carbon, reduced personnel exposures during adsorber replacement, and eliminated servicing gaskets to ascertain zero bypass leakage.

Air cleanup filter housings have been designed and specified in order to conform to be accessibility guidelines described in NRC Regulatory Guide 1.52 and ORNL-NSIC-65. This facilitates replacement of filters and minimizes the radiation exposure to maintenance personnel in accordance with Regulatory Guide 8.8. The units have been provided with adequately sized access doors, sufficient lighting, 5 feet of separation between filter frames and a maximum filter bank

height of six feet (three 24 inch by 24 inch filters high).

The air cleanup modules are furnished with test ports located in accessible locations on the side of each filter housing, together with portable injection and sampling grids for DOP and Freon, in order to facilitate test procedures when performing in-place testing of the HEPA filters and charcoal adsorbers. Sample adsorber canisters and local pressure gauges which monitor filter resistance are provided to maintain surveillance on each of the air cleanup modules. Permanently installed flow meters are also provided to maintain surveillance and avoid time-consuming pitot tube traversing. The test procedures and the testability requirements are in accordance with ANSI N101.1, ANSI N509, ANSI N510, and the guidelines included in NRC Regulatory Guide 1.52 and ORNL-NSIC-65.

All air cleanup modules which are designated ESF remain on standby during the normal plant mode of operation. The ESF units will operate only 10 hours a month in accordance with NRC Regulatory Guide 1.52. Therefore, it is anticipated that the proposed requirement of testing ESF atmospheric cleanup systems after 720 hours of operation will not be attained during a year of reactor operation. However, an annual test of the air cleanup modules is conducted for both the ESF and normal modules.

The feature of using only three sizes of modules allows for interchangeability of parts, enabling efficient and fast replacement of any part while a standby module is operating thus allowing overall system reliability of the highest order.

Economics

As shown earlier, there is a definite requirement to determine what the minimum temperature increase in the plant must be in order to maintain the relative humidity below 70 percent. With a maximum temperature of 104 F imposed by electrical equipment, this increase is minimum 11 F if saturated air is assumed to be entering the plant. A study determined that the use of refrigeration equipment to increase the temperature difference would be economically favorable since increased ΔT resulted in lower flow rates and hence smaller filter trains, ducts, fans and so on. The lower limit in reducing the airflow is the quantity of air required to maintain the airborne radioactivity levels below 10 CFR Part 20 maximum permissible concentrations (MPC). The Comanche Peak Station, the Fort Calhoun Station Unit 2 and the G&HI standard plant have been designed with a specific inlet air temperature. Comanche Peak and Fort Calhoun Unit 2 use chillers while the standard plant may use chillers or evaporative coolers depending upon the particular site requirements, the cooling water temperatures, and the availability of makeup water.

The modular system allows for energy conservation. By designing the system with two or more system air balancing points, i.e., for seasonal operation, the plant airflow can be reduced to cool operating equipment during the winter months by shutting down several air cleanup and supply modules and by balancing the system so that the 10 CFR Part 20 MPC requirements are met.

The modular design allows for much lower capital cost of the air cleanup trains since the engineering cost is minimal. Jigs can be used in the manufacturing process resulting in an assembly-line type arrangement.

G&HI has estimated, based on manufacturing techniques, shipping and field erection costs, that this design results in capital cost savings of approximately 20 percent over the customized design.

The Comanche Peak station uses four different air cleanup module sizes. The original design called for only three sizes but redesign of the layout in the containment deprived us of sufficient space to maintain the size desired, therefore, the containment preaccess filtration system had to be redesigned to fit into the available space. This particular problem was corrected in the Fort Calhoun and the standard plant stations.

The size of 15,000-scfm nominal was selected as the module size for the nuclear island in all three plants primarily because this size is readily shipped by truck without specific permission and routing. A 15,000-scfm air cleanup train that can be completely assembled and tested in the manufacturing plant and then shipped intact to the josite, eliminating costly field assembly, lends itself to a minimum cost system of highest reliability and maintainability.

Cost analysis showed that in the long run the gasketless air cleanup systems were less expensive and easier to maintain than the tray type. This may not be the case for the smaller systems. However, the G&HI position is that mixing of the two types of systems defeats the purpose of standardization; therefore, the tray types are not considered for the applications discussed.

In addition, the cost analysis performed to justify the use of refrigeration equipment proved that approximately $1,000,000 could be saved in filter replacement cost over 40 years for the Comanche Peak Station, due to the lesser air quantities required.

Summary

In summary, the G&HI air cleanup design can be applied to any size nuclear powerplant by either adding or subtracting modules. This fulfills the intended air cleanup function and also is the most economical approach from both the capital investment and the operating and maintenance cost points of view.

TABLE 1
AIR CLEANUP MODULE (ACM) MODE OPERATION

CAAV	Number of Modules Operative							
	Number Units Installed	Initial Startup	Startup Following Shutdown	Normal	Plant Shut-down (1)	Re-fueling	Loss of Offsite Power	LOCA
Normal Ventilation								
Supply module	6 [8]	4 [5]**	4 [6]	4 [6]	5 [6]	5 [6]	-	-
Exhaust ACM	10 [14]	8 [10]	8 [12]	8 [12]	10 [12]	8 [12]	-	-
Emergency Ventilation								
ESF exhaust module	2	2	-	-	-	2 2	1 1	1 1
Hydrogen Purge								
Supply module	2	-	-	-	-	-	-	1 1
Exhaust ACM	2	-	-	-	-	-	-	1 1
Control Room								
Emergency recirculation ACM	2	-	-	-	-	-	-	1 1
Emergency pressurization ACM	2	-	-	-	-	-	-	1 1

(1) Includes containment purging

*Numbers in brackets [ ] are for Comanche Peak Units 1 and 2. Numbers without brackets are Fort Calhoun Unit 2 and the G&HI standard plant.

**Unit 1 operating only

References:

(1)   U.S. Nuclear Regulatory Commission
       Regulatory Guides (RG)

       a)   RG 1.52, Design Testing, and Maintenance
            Criteria for Atmosphere Cleanup System Air
            Filtration and Adsorption Units of Light-
            Water-Cooled Nuclear Powerplants, 1973

       b)   RG -8.8, Information Relevant ·to Maintaining
            Occupational Radiation Exposure As Low As is
            Reasonably Achievable, 1975

(2)   U.S. Nuclear Regulatory Commission
       Wash-1234, Engineered Safety Features
       Air Cleaning Systems for Commercial
       Ligh-Water-Cooled Nuclear Powerplants, 1974

(3)   Code of Federal Regulations, 10CFR20, Appendix B,
       Concentration in Air and Water Above Natural
       Background

(4)   Code of Federal Regulations, 10CFR50,

       a)   Appendix A, General Design Criteria
            for Nuclear Powerplants

       b)   Appendix I, Numerical Guides for
            Design Objectives and Limiting Conditions
            for Operation to Meet the Criterion "As
            Low As Practicable" for Radioactive
            Material in Light-Water-Cooled Nuclear
            Power Reactor Effluents

(5)   Energy Research and Development Administration
       ORNL-NSIC-65, Design, Construction and Testing
       of High-Efficiency Air Filtration Systems for
       Nuclear Application, 1970

(6)   Underwriters' Laboratories, Inc. (UL)-900
       Safety Standard for Air Filter Units, 1971

(7)   Underwriters' Laboratories, Inc. (UL)-586
       Safety Standard for High-Efficiency Air Filter
       Units, 1971

(8)   American National Standards

   a)   N101.1, Efficiency Testing of Air
        Cleaning Systems Containing Devices
        for Removal of Particles, 1972

   b)   N509, Draft Standard for Nuclear
        Powerplant Air Cleaning Units and
        Components, 1975

   c)   N510, Standard for Testing of Nuclear
        Air Cleaning Systems, 1975
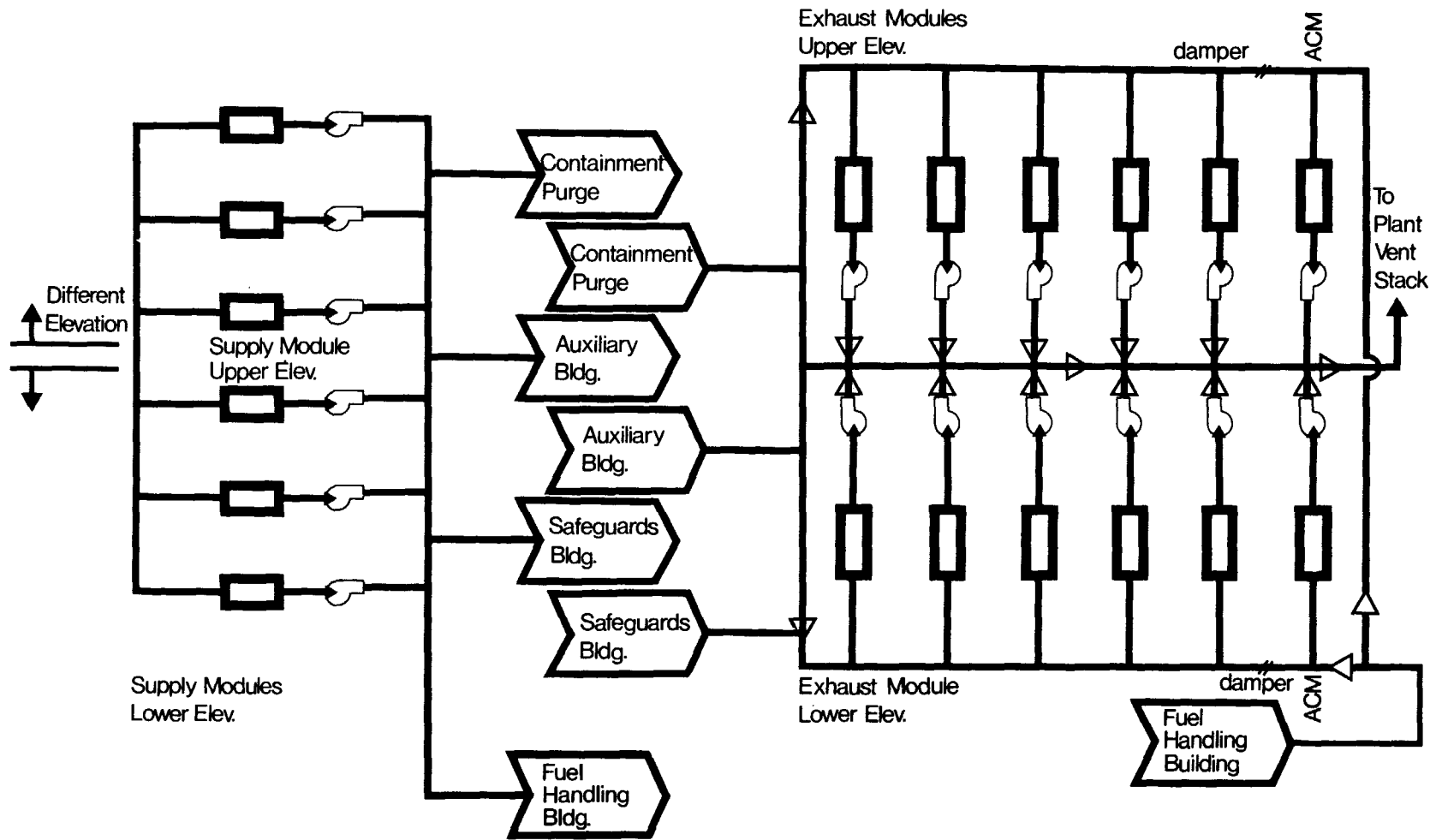
Figure 1 Controlled Access Area Ventilation Single Unit
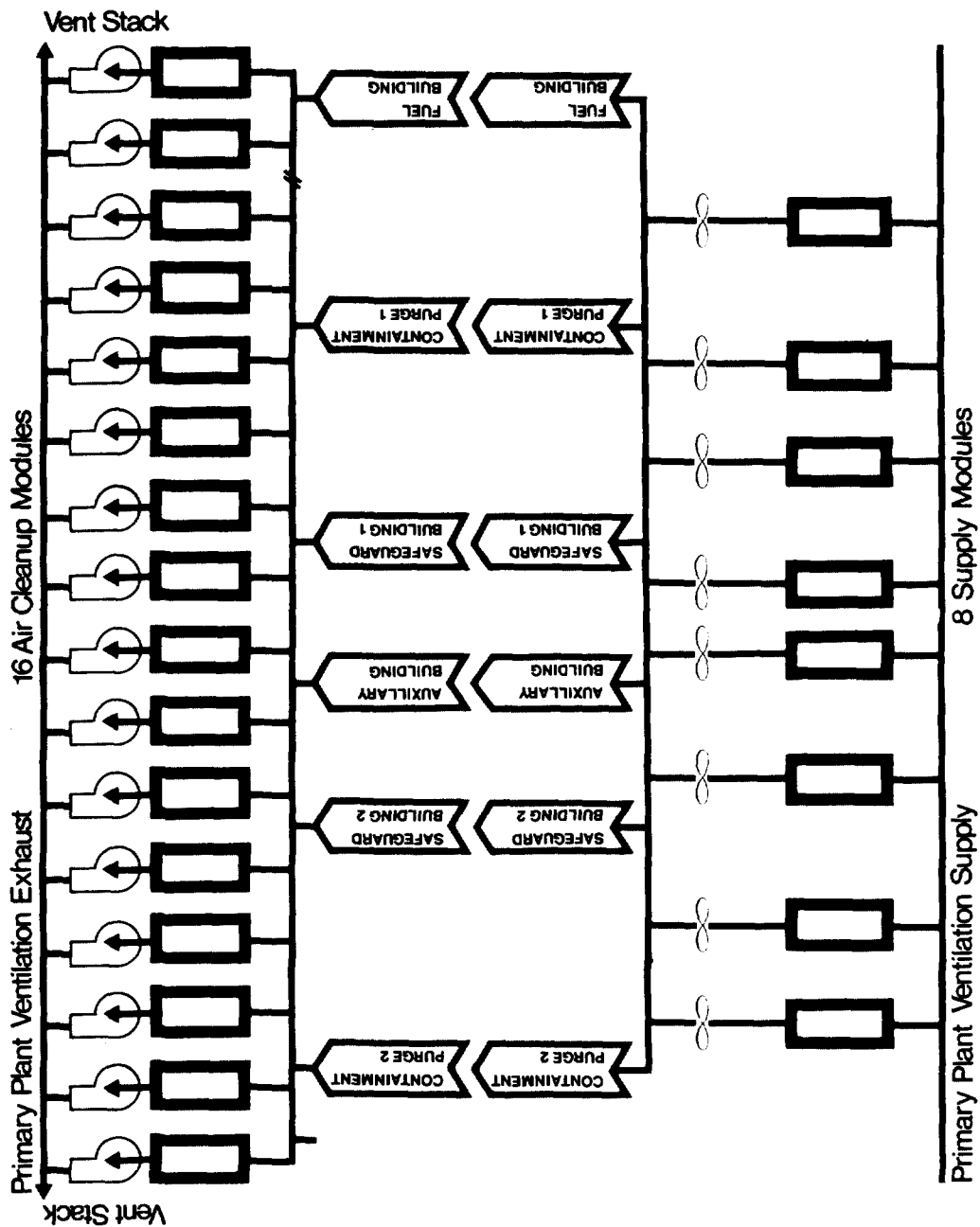
Figure 2   Controlled Access Area
Ventilation Two Unit

To
Plant
Stack

Supply Modules

Air Cleanup Modules

Outside
Air

Supply Modules

Air Cleanup Modules
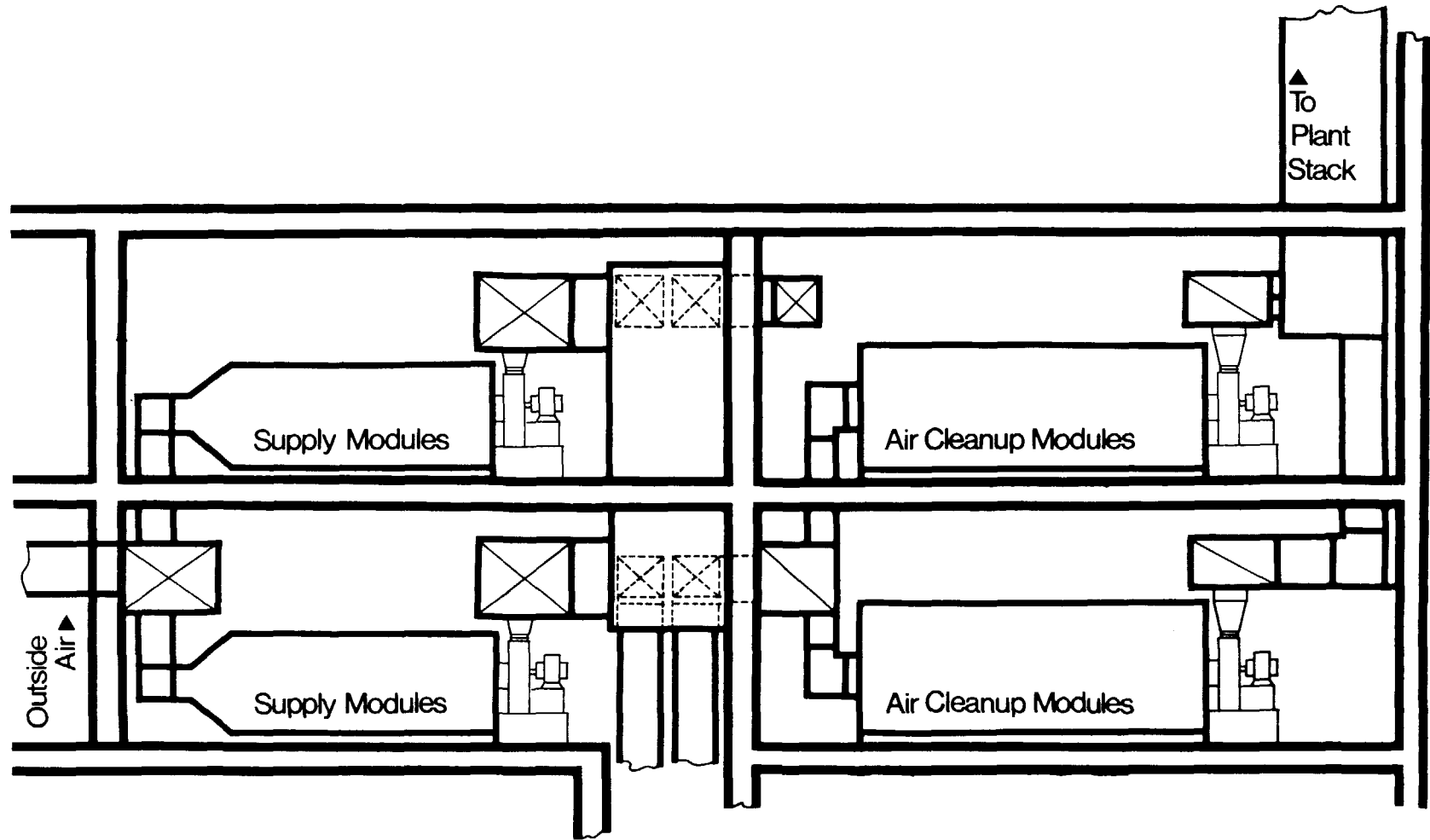
**Figure 3 Physical Arrangement
Fort Calhoun Station Unit 2**

Exhaust Modules

Supply Module
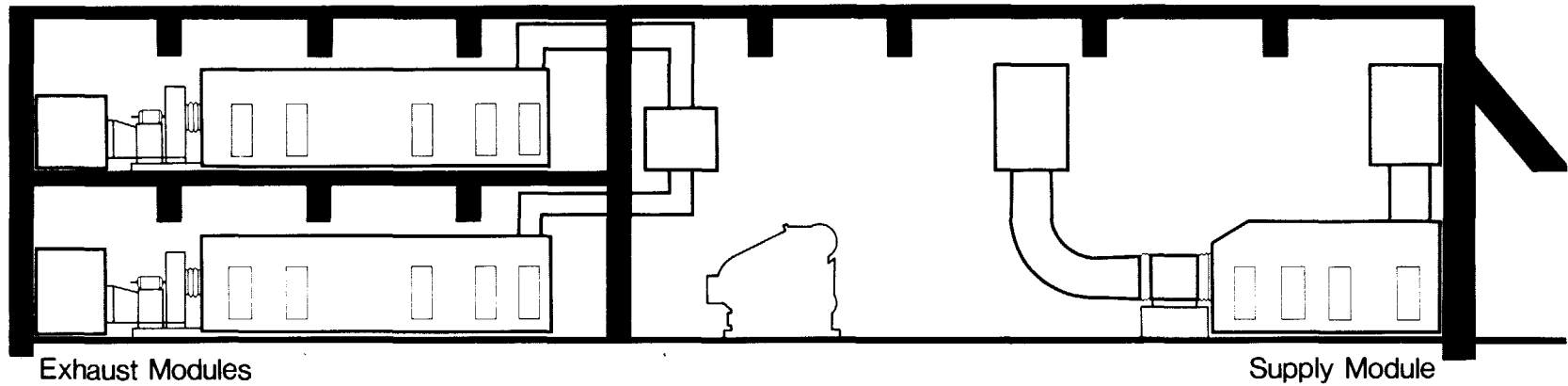
Figure 4   Physical Arrangement
Comanche Peak Units 1 & 2

Train A

Train B

Outside Air

Outside Air

Emergency Press

Emergency Press

Equipment Separation

Emergency Recirculation

Emergency Recirculation

A/C Unit

A/C Unit

Control Room Complex
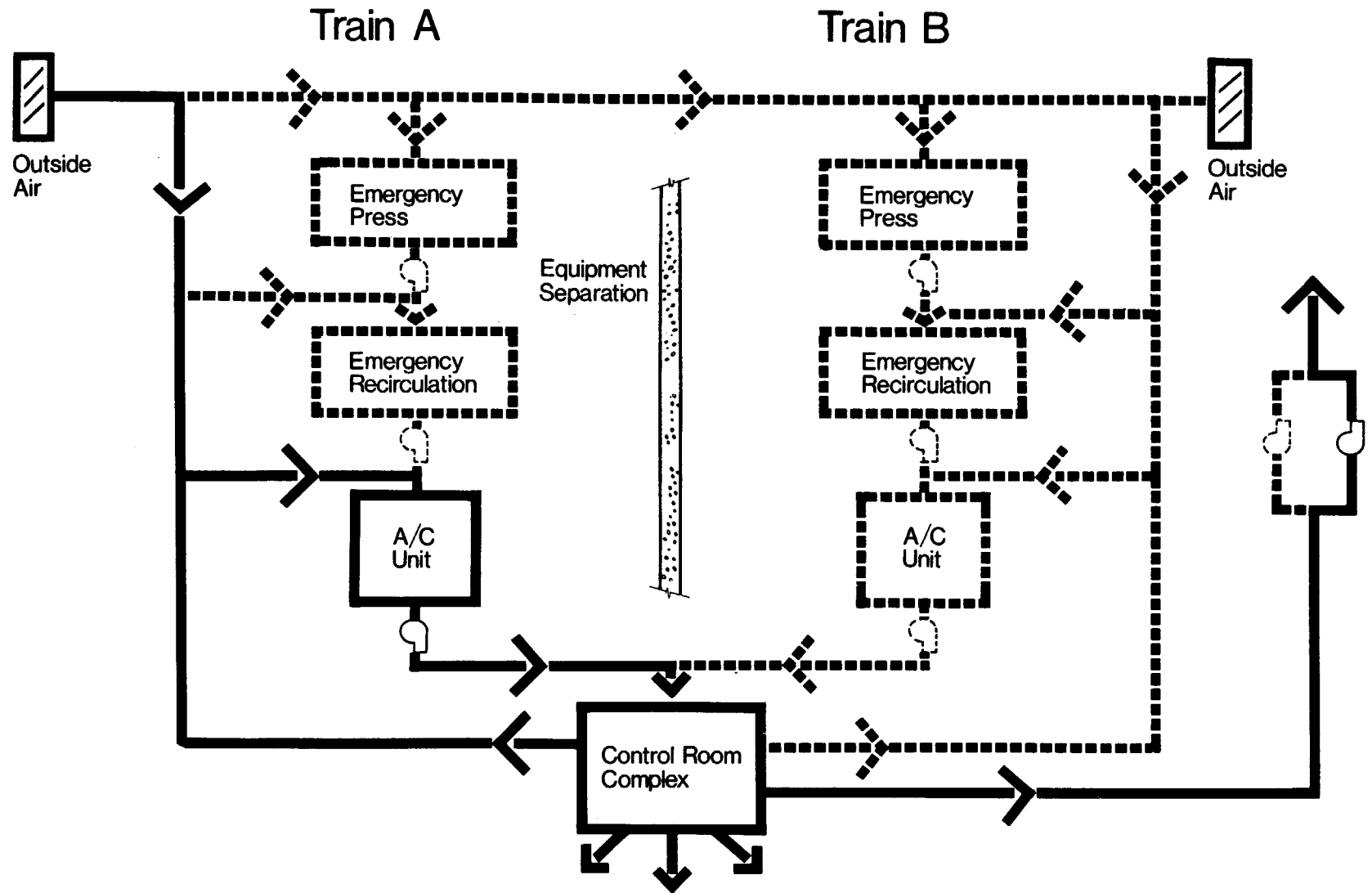
Figure 5 Control Room HVAC Normal Mode of Operation
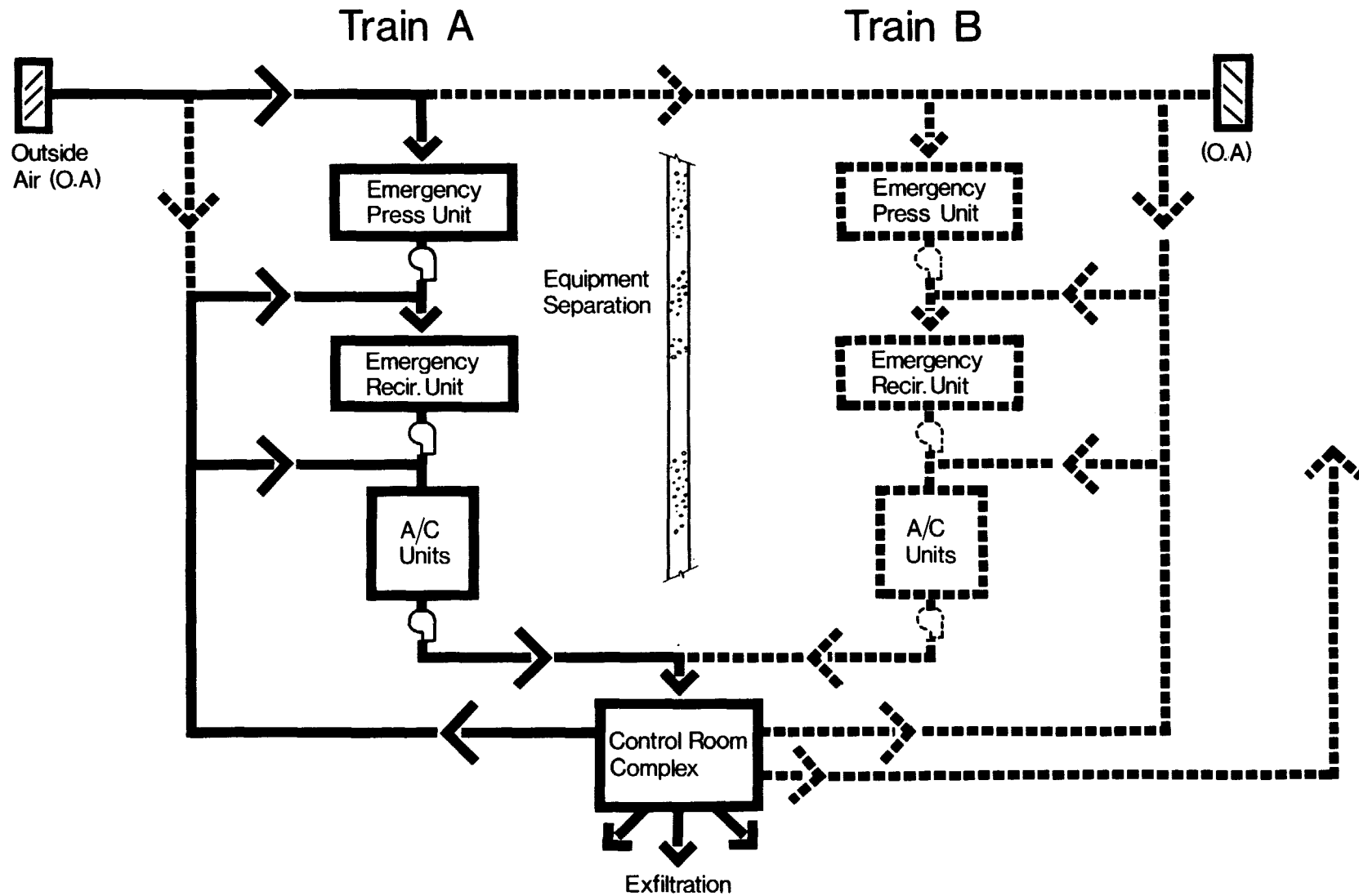
Figure 6   Control Room HVAC Emergency Recirculation Mode of Operation

Figure 7 Air Cleanup Unit

Prefilter Filter   HEPA

HEPA
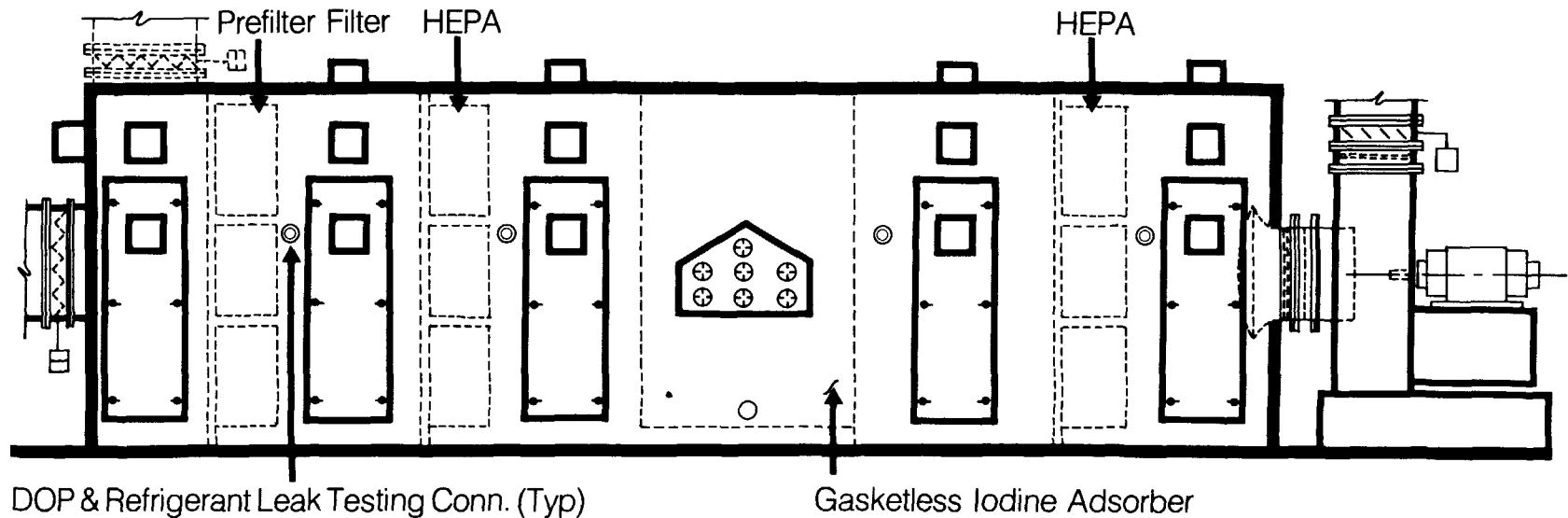
DOP & Refrigerant Leak Testing Conn. (Typ)

Gasketless Iodine Adsorber

(1) Heater & Mist Eliminator Provided for ESF
Modules to Reduce Incoming Atmosphere to
Below 70% R.H.
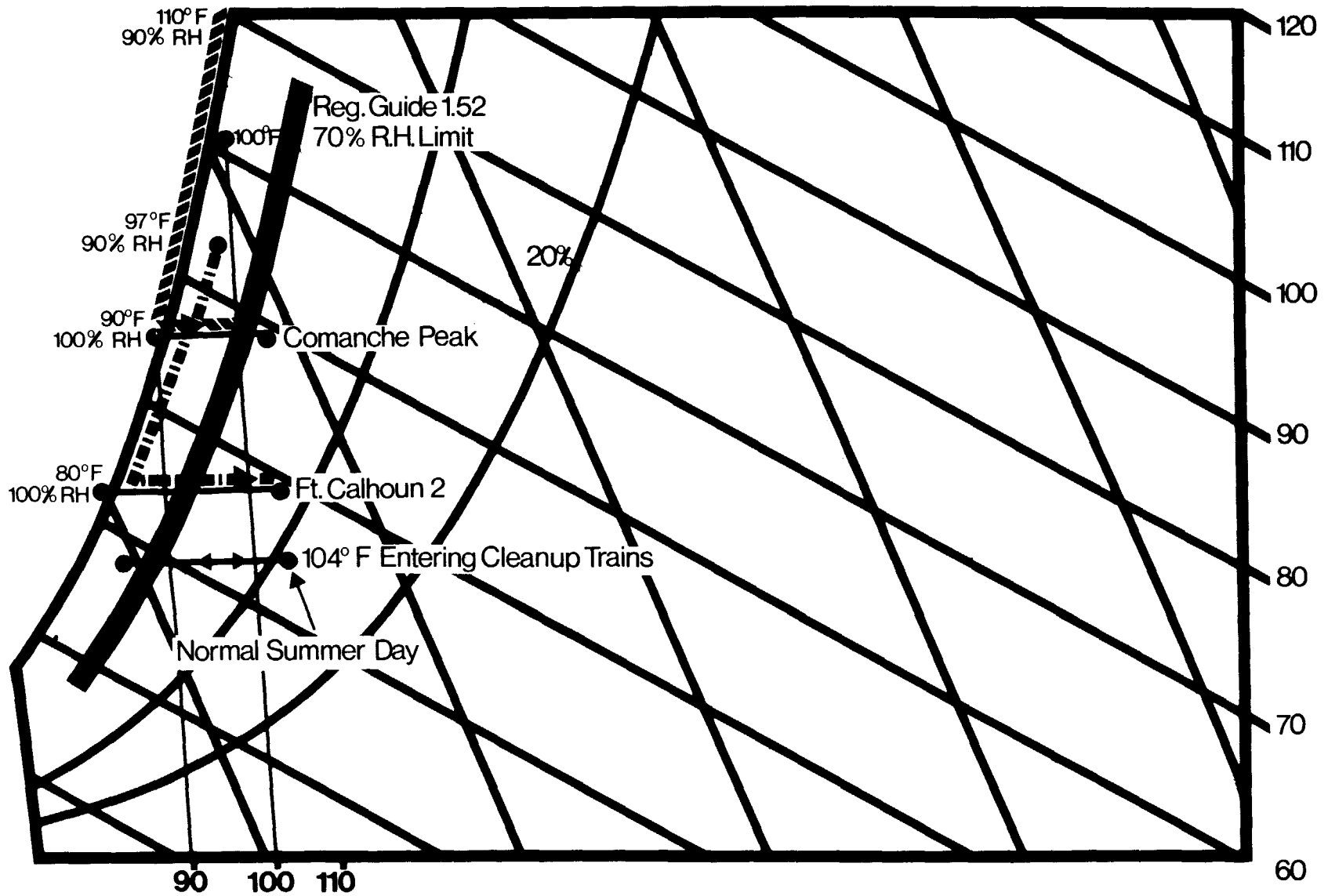
Figure 8 Design Basis for ``Saturated Air Entering Plant''

DISCUSSION

ZEIDMAN: Is it right that you were standardizing the first packages at 15,000 CFM?

NICOLAYSEN: We are using three packages of 15,000, 4,000, and 1,000 CFM. In the Comanche Peak Station we are using 8,000 CFM units for the control room since it is a twin unit station.

ZEIDMAN: That would be relatively small for us. Doesn't this lead to space problems because the modules restrict flexibility in the sense that space and equipment become "prearranged" into fixed design modules?

NICOLAYSEN: By ascertaining that sufficient space is allocated as soon as the general arrangement drawings are being prepared, we have no restrictions as to space. For the Comanche Peak Station, our two main equipment rooms were on the top elevation and could be expanded or contracted to fit the need.

ZEIDMAN: Do you recommend using the standard units even if you are up to a million CFM?

NICOLAYSEN: I would recommend cooling to reduce the airflow and the use of this design. I did a study on cost benefits on cooling. A station saved a million bucks in filter costs alone by putting in chillers.

KAHN: I was wondering why you tied the fan to a 15,000 CFM unit in your modular approach. It seems to me it would generate quite a bit of interaction between the fans of a 12-unit system.

NICOLAYSEN: We looked at the pro's and con's of using fans in parallel separate from the filter banks. It requires additional space to do it that way. Furthermore, it is much easier to compensate for the filters becoming dirty in this manner since each module contains an airflow monitoring device and variable inlet vanes for the fans. Another advantage with the fans being the 15,000 CFM size is that during the winter, when we do not require as much equipment cooling, we can shut off units and reduce the airflow. However, we must maintain sufficient airflow to stay within the M.P.C. requirements of 10 CFR 20. We conserve energy in this manner.

KAHN: In your engineering safety feature systems, do you have 100% duplication?

NICOLAYSEN: One hundred % redundancy. In the control room slide, you saw the separation. On one side of the separation wall there was the operational unit; on the other, a standby.

KAHN: The loss of a single component, such as the fan, loses the total unit?

NICOLAYSEN: Yes. It loses the unit. But using only three different sizes of fans, you can have spares on hand and in a couple of hours you have a new fan on the line.

BELLAMY: My first question pertains to how you can justify
a seismic category one, safety class three, filter housing for the
normal ventilation system modules.

NICOLAYSEN: The modules in the controlled access ventilation
system are all alike but for the replacement of the prefilter with a
moisture separator - electrical heater combination in the modules
designated ESF. Since the design is to standardize, it is just as
easy to qualify twelve as Category I as to qualify two. Furthermore,
we originally designed all the modules such that any one could be
used to exhaust the fuel building during refueling, having the mois-
ture separator and heater located within this building separate from
the modules. Then you came up with the 720 hr ESF testing requirement,
that's why the two dampers went in. In addition, the system is de-
signed already and I do not seen any reason to redesign it.

BELLAMY: My second question concerns the philosophy behind
operating the engineering safety feature modules during all modes
of refueling. Why not have them on a radiation monitoring signal
to turn them on when there is sufficient radiation in the area?

NICOLAYSEN: We could. This is part of the technical operating
procedures.

BELLAMY: That is a flexible unit.

NICOLAYSEN: According to Regulatory Guide 1.52, it is not pos-
sible to bypass. That is why we guard against it by saying, "All
right, use the ESF system during the refueling cycle."

MUNSON: I would like to inquire about the capability of
standard fans to handle the various system pressures that will occur
with different duct requirements in a custom designed station.

NICOLAYSEN: We designed the ducts to have approximately the
same pressure drop all the way through by balancing the pressure drops
in the system. The flow is also balanced by using air monitors and
balancing dampers in all major trunk lines. This is part of good
ventilation design. You have to have this, otherwise you can't bal-
ance air flow.

CONTROL ROOM VENTILATION INTAKE SELECTION
FOR THE
FLOATING NUCLEAR POWER PLANT

D. H. Walker, R. N. Nassano, M. A. Capo

Offshore Power Systems
Jacksonville, Florida

Abstract

In the event of accidents on or near a nuclear plant, it is necessary to provide sufficient protection to the plant operators in the control room to permit them to safely shut down the plant and to maintain the plant in a safe shutdown condition. One consideration in providing this protection is the adequacy of the air supply to the control room. Hazards or conditions usually considered in design of the control room air supply are release of radioactivity from the plant as a result of an internal plant accident and release of a toxic gas near the plant as a result of a nearby accident.

To assist in the design of the control room air supply for a floating nuclear plant, a comprehensive wind tunnel measurements program, employing scale models of two floating nuclear power plants located within a scale model of a typical breakwater, was performed at the Colorado State University under the direction of Offshore Power Systems. The purpose of the program was to provide data for: 1) selecting locations on the standard plant for the two alternate control room ventilation intakes, and, 2) determining applicable dispersion factors between the release locations and the selected intakes required for hazard analyses. This paper describes the measurements program and the methods employed by Offshore Power Systems in analyzing the experimental data that lead to the selection of the intake locations and the values of X/Q for control room hazard analyses.

I. Introduction

One consideration in the overall design of the control room for a nuclear power plant is to assure that the plant can be shut down and maintained in a safe shutdown condition (following certain postulated accidents). Accidents involving release of radioactivity (from the plant) or release of toxic gases (external to the plant) are usually considered in the plant design. The criteria to be met in the event of such accidents are specified by the Nuclear Regulatory Commission. [1,2,3]

Floating nuclear power plants may be sited off-shore[4] and as a result the operating crew may be required to remain on the plant for a few days following a postulated accident. It is therefore important that the air intakes be located such that an adequate air supply will be available following such an accident. The ventilation system design for the control room on the floating nuclear plant is to have dual intakes which are physically separated. The purpose of the dual intakes is to allow for drawing of outside air from a region where the concentration of radioactivity or toxic gas, if any, is relatively low. If there were to be gaseous release under very stable atmospheric conditions with low wind speed, a relatively concentrated plume of small lateral dimension could be carried toward and past one of the intakes. This condition appears to be the most severe from the standpoint of ventilation system design.

784

A wind tunnel measurements program, employing scale models of two floating nuclear power plants located within a scale model of a typical breakwater, was performed at the Colorado State University[5] under the direction of Offshore Power Systems to determine:

1. The locations on the plant for the two alternate control room ventilation intakes and

2. The dispersion factors between the release locations and the intakes for hazards analysis.

The applicability of scaled wind tunnel tests to determine the extent of mixing (at full scale) when both the release point and the intakes are located on or near complex structures is discussed by Merony[5], Halitsky[6], and in the Peach Bottom PSAR[7].

II. Description of Experiment

The model, located in the wind tunnel, included the two model power plants and the model breakwater, constructed to a linear scale of 1:450. The model is shown in Figure 1.

Ten sample ports, representing potential control room ventilation intakes, were placed on each of the side-by-side plant models during the test. Figure 2 illustrates the location of several sample ports on two isometric views of a plant. The sample ports are labeled 6 (16) through 15 (25), where the numbers in parentheses refer to the corresponding locations on an adjacent plant.

The location of simulated release points on the plant are also shown in Figure 2. These include the plant vent stack, steam relief valve vents, containment vessel surface, and the house boiler exhaust. Metered quantities of gas were vented from the release point of interest to simulate the exit velocity and to account for the bouyancy effects due to the temperature difference between the released gas and the ambient atmosphere (if any). For this purpose, helium and compressed air were mixed in metered amounts.

The floating nuclear plant design[4] has a shield building surrounding and separated from the containment. The space between the shield building and the containment is maintained at negative pressure by a ventilation system both during normal operation and during postulated accidents, such as a loss-of-coolant accident (LOCA). Radioactivity which may leak from the containment in the event of a LOCA would then be a controlled release from the plant vent stack. Some radioactivity release could also occur from the surface of the shield building as a result of bypass leakage. As shown in Table 1, each of these potential release modes was considered in the experimental program. Releases from the plant vent stack at relatively low velocity following an accident is typical of the floating nuclear plant design[8]. Some tests at higher exit velocities were performed to determine what effect increasing the stack velocity might have on dilution between the vent and potential intake locations.

III. Experimental Information

Table 1, taken from Reference 5, gives an overview of the tests performed during the experimental program. Table 1 shows that the following variables were considered: source release point on either Plant A(α) or Plant B(β), plant vent stack height, atmospheric stability (neutral, N, or stable, S), wind velocity(V_a),

stack velocity (V_c), and wind angle. The alphanumerics (eg, B3 listed in the table reference specific tests as described in the CSU data report[5].

A schematic plan view of two adjacent plants located inside a breakwater is shown in Figure 3. (While this arrangement is for the Atlantic Generating Station' Units 1 and 2, it may also be used at other sites). Figure 3 illustrates the wind angles used throughout the experimental program. Also shown are the standard intakes on each plant, as well as typical sample locations and release points.

Although experimental data were obtained for all of the experimental release points shown in Table 1, this paper deals only with the plant vent stack and containment releases and their application to potential control room hazards analysis. Data concerning potential release of toxic gas outside the plant and breakwater were also obtained during the test program. These data and these analyses are not discussed in this paper but are included in Reference 4.

Qualitative Test Results

Tests with visible plumes were performed so that overall effects could be observed qualitatively. For these visual tests, gas was bubbled through a container of titanium tetrachloride before venting. The plume was illuminated with arc-lamp beams. Figure 4 is a still photograph showing a well defined plume exiting the stack from one plant model and passing over the top of the adjacent plant model. In addition to the still photographs, a series of color motion pictures of the visual test releases was obtained.

On the basis of visual observations, the following qualitative conclusions were reached:

1. Releases from the plant vent stack at low velocity may potentially envelope the upper part of the plant structure,

2. Releases from the plant vent stack with higher exit velocities did not appear to entrain between the various building cavities.

3. Releases from the containment surface may envelope the entire structure, but are quite well mixed providing significant dilution.

4. Although wind orientation and atmospheric stratification influence the character of flow over the plants, there is no strong evidence of a "worst" situation with respect to concentration at air intakes.

Quantitative Test Results

For quantitative measurement of the extent of mixing between the release point and the sample intake location, a mixture of Krypton-85 and air was vented. Samples were collected at each of the intake locations. Subsequently the samples were analyzed by counting of radioactivity. The counts for each sample point were then transformed into concentration values. The experimental data were reported in terms of $V_a(x/Q)$, where V_a is the wind velocity and x/Q is the atmospheric dispersion factor.

The experimental concentrations are presented in Reference 5 for each test at each sample location on the plants. In addition, the test data were provided to Offshore Power Systems as computer printouts and as card data decks. The

latter data were employed in the analysis of the experimental results, described in Section IV.

IV. Analysis of Experimental Data

The experimental data were analyzed in two phases. The first phase was to select the most favorable location for an alternate air intake, considering both plants. The standard intake is located on the south side of the plant as shown in Figure 2, where the standard intake is labeled #6 for Plant A and #16 (in parenthesis) for Plant B. The second phase of the analysis dealt with derivation of the dispersion factors between the release and intake location for use in control room dose calculations.

Selection of Alternate Intake Locations

The test data were segmented into series for analysis, with a series being comprised of the data for all wind directions for release from a single release point, with other variables (stack height, wind velocity, and stack velocity) held constant. Next, the "worst" wind direction within each series was determined on the basis of the largest value (least mixing) of $(V_a X/Q)$ measured at the standard intake location. These data are presented in Tables 2 through 5. Each line or bracketed set in the tables represent a set of data. The worst wind direction and the $(V_a X/Q)$ value for the standard intake are listed in columns 5 and 6. $(V_a X/Q)$ values for other potential alternate intakes are listed in the subsequent columns. Tables 2 and 3 apply to intakes on Plant A for neutral and stable stratification, respectively. Tables 4 and 5 apply to intakes on Plant B for neutral and stable stratification, respectively.

For several test series, all concentrations were less than detectable limits at standard intake location 6 (Plant A) or standard location 16 (Plant B). For those cases (shown by ** on Tables 2 through 5), three wind directions were chosen which geometrically represent the potentially worst wind directions relative to the standard intake. Note that the source of release is given in the first column of each table. Generally, the tabulated data indicate concentration of potential second intakes for the worst condition at the standard intake (6 or 16). One would want to switch to a second intake when the conditions at the standard intake become unfavorable.

The data from Tables 2 through 5 were next reduced to the form shown in Table 6. Table 6 illustrates the most favorable second intake location for each test series analyzed. An x indicates the intakes which had the observed lowest value of $V_a (X/Q)$ for a particular test series. For some test series there is more than one preferred intake, since several sample locations had concentrations below detectable levels for a particular test series. Generally, these data show that intake #12 is the preferred second location on Plant A and intake #18 is the preferred second location on Plant B.

Floating nuclear power plants are to be of standard design, and hence the alternate air intake must be at the same location on each plant. Table 7 combines the data on preferred intake locations on Plant A and Plant B to indicate the alternate intake which is the best overall alternate location as indicated by the test program. The values in the right hand column of Table 7 were obtained by adding the appropriate totals from the bottom of Table 6 for a set of matching intakes on the two plants. From Table 7 it can be observed that the preferred combination is intake #8 on Plant A and intake #18 on Plant B. Thus, these locations on the southeast side of each plant were selected as the alternate intake

locations for design.

The next step in this analysis was to determine which of the intakes on each plant would be employed for the various wind directions. The measured values of V_a (X/Q) for the selected dual intakes for all wind directions on both Plants A and B were tabulated. These tabulations are given in Tables 8 and 9 for Plants A and B, respectively.

Only data for release from the plant stack of standard height (195 feet), and from the containment for the lower wind velocity of V_a = 5 feet/second (1.5 m/sec) (typical minimum mixing) were considered. Data for both the neutral and stable atmospheric stratification conditions were considered as shown in Tables 8 and 9. The data for the dual intakes are grouped in these two tables according to release points (stack or containment) and the plant from which release occurs. For each experimental wind angle a maximum observed value of V_a (X/Q) is listed at the bottom of the table for each of the four intakes on the two plants (intakes 6 and 16 and intakes 8 and 18) for both plant vent stack and containment releases. These maxima were plotted versus wind direction (angle) for both the plant stack and containment release points for both Plants A and B as shown graphically in Figures 5 through 8. (It should be noted that the value of V_a applicable to these data is 5 ft/sec or 1.5 m/sec.). Specifically, Figures 5 and 6 apply to intakes on Plant A, for release from the plant vent and containment, respectively; whereas Figures 7 and 8 apply to intakes on Plant B, for release from the plant vent and containment, respectively.

In the unlikely event of an accident such as a loss-of-coolant, most of the radioactivity which could affect operation in the control room is released from the plant vent stack. Therefore, data on release from the plant vent stack were the primary data used to determine which intake would be employed as a function of wind direction, Figures 5 and 7. The selection technique will be discussed using Figure 5 as the example. The maximum values of V_a (X/Q) for intake #6 are shown on Figure 5 as a dashed curve and for intake #8 as a dotted curve. The solid curve is an envelope curve based on the lower value of the two curves for all wind angles, i.e., it represents the intake providing the more favorable dilution. From Figure 5 it can be observed that on Plant A intake #8 is pre-ferred over the ranges 330° to 360° and 0° to 180° while intake #6 is preferred over the range 180° to 330°. (Referring to Figure 6, it is observed that the preferred intake as a function of direction is generally the same for the con-tainment release).

A similar technique was employed to select the preferred on-line intake for Plant B. From Figure 7, the envelope curve shows that intake #16 is preferred over the ranges 310° to 360° and 0° to 140° while intake #18 is preferred from 140° to 310°.

Figure 9 shows a plan view of Plants A and B and indicates the preferred intakes as a function of wind direction for both plants.

A wind direction indicator on each plant will be used to select automati-cally which intake should be utilized in the event of an accident. The operator can override the automatic feature if necessary.

Selection of Dispersion Factors

To calculate potential doses in the control room from airborne radioactivity

release following a hypothetical accident, dispersion factors between the release point and the intakes are needed. For the dose analysis for the floating nuclear plant, the applicable χ/Q's were developed from the experimental data.

From Figures 5 through 8, maximum values of V_a (χ/Q) were selected for the on-line intake (solid curves) for each plant and each release mode. These maximum values are summarized in Table 10. The two least favorable values for plant vent stack release and for containment release, required for dose evaluation, are 1.8×10^{-5} and 6.0×10^{-4} respectively.

V. Summary

Offshore Power Systems has employed a series of scale model wind tunnel tests for selecting the location of dual and alternate ventilation intakes for the control room on standard design Floating Nuclear Power Plants and for determining dispersion factors between the point of release and the intakes for accident analyses. The location of the alternate intakes and the accident analyses employing these dispersion factors has been approved by the Nuclear Regulatory Staff in their Safety Evaluation Report for the plant[9].

Furthermore, the dispersion values for control room dose analyses[9] for the plant vent are about a factor of 20 lower than dilution from the plant vent that would be calculated from reference 6. The atmospheric dispersion factor derived from the test data for releases from the containment was essentially in agreement with that derived via reference 6. These data demonstrate the general applicability of the methods in reference 6 for calculating dilution when releases are from the containment surface (within the building complex). The data also show the significant additional dilution attained from a release elevated slightly above the containment.

VI. References

1.   Code of Federal Regulations, 10CFR Part 50, Appendix A, General Design Criteria 19, Control Room.

2.   U.S. Nuclear Regulatory Commission, Standard Review Plan, Section 6.4, Habitability Systems, June, 1975.

3.   Murphy, K. G. and Campe, K. M., (1975), Nuclear Power Plant Control Room Ventilation System Design for Meeting General Criterion 19, 13th AEC Air Cleaning Conference, 401-428.

4.   Docket No. STN 50-437, Plant Design Report, Offshore Power Systems, May, 1973 (plus amendments).

5.   SA-1000-14A45A, (1974), Wind Engineering Study of Atmospheric Dispersion of Airborne Materials Released from a Floating Nuclear Power Plant, Merony, R. N., Cermak, J. E., Connell, J. R., and Garrison, J. A., Colorado State University.

6.   Slade, P. H., Meteorology and Atomic Energy, July, 1968, p. 221-255.

7.   Docket Nos. STN 50-277 and 50-278, Unit 2 Vent Plume Behavior, Peach Bottom Atomic Power Station, Philadelphia Electric Company, March, 1974.

8.   Docket Nos. STN 50-477 and 50-478, Preliminary Safety Analysis Reports, Atlantic Generating Station Units 1 and 2, Public Service Electric and Gas Company, March, 1974.

9.   NUREG 75/100, (September, 1975), Safety Evaluation Report Related to Offshore Power Systems Floating Nuclear Plants (1-8), Office of Nuclear Reactor Regulation, U.S. Nuclear Regulatory Commission.
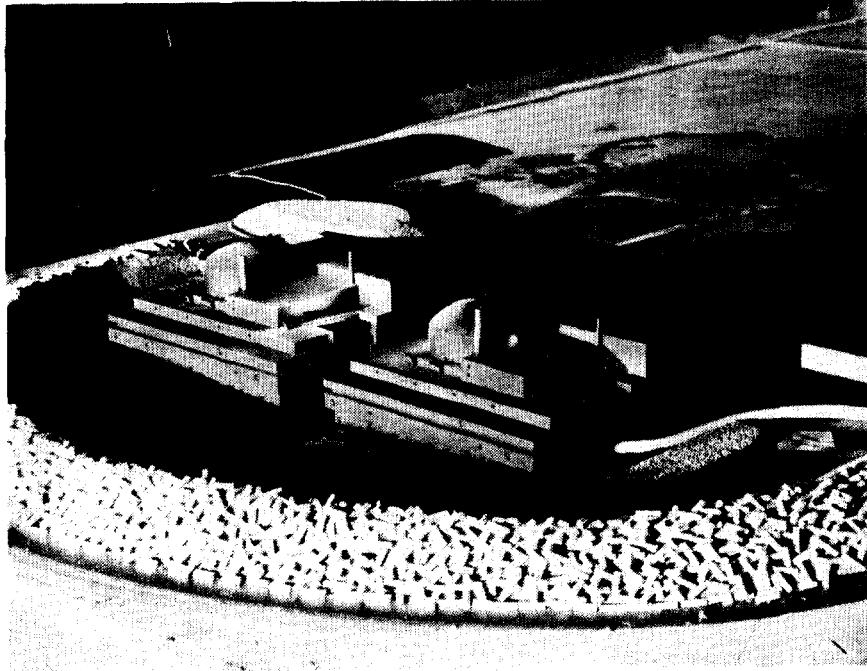
FIGURE 1

Photograph of Plant Scale Models

Enclosed Within Scale Model of

Breakwater at The Colorado State

University Wind Tunnel

Steam Relief
Valves

Plant Vent Stack

13(23)

6(16)

14(24)

15(25)

8(18)

7(17)

VIEW FROM NOMINAL SE

House Boiler Exhaust

Containment Vessel
Leak (Lower)

12(22)

11(21)

6(16)
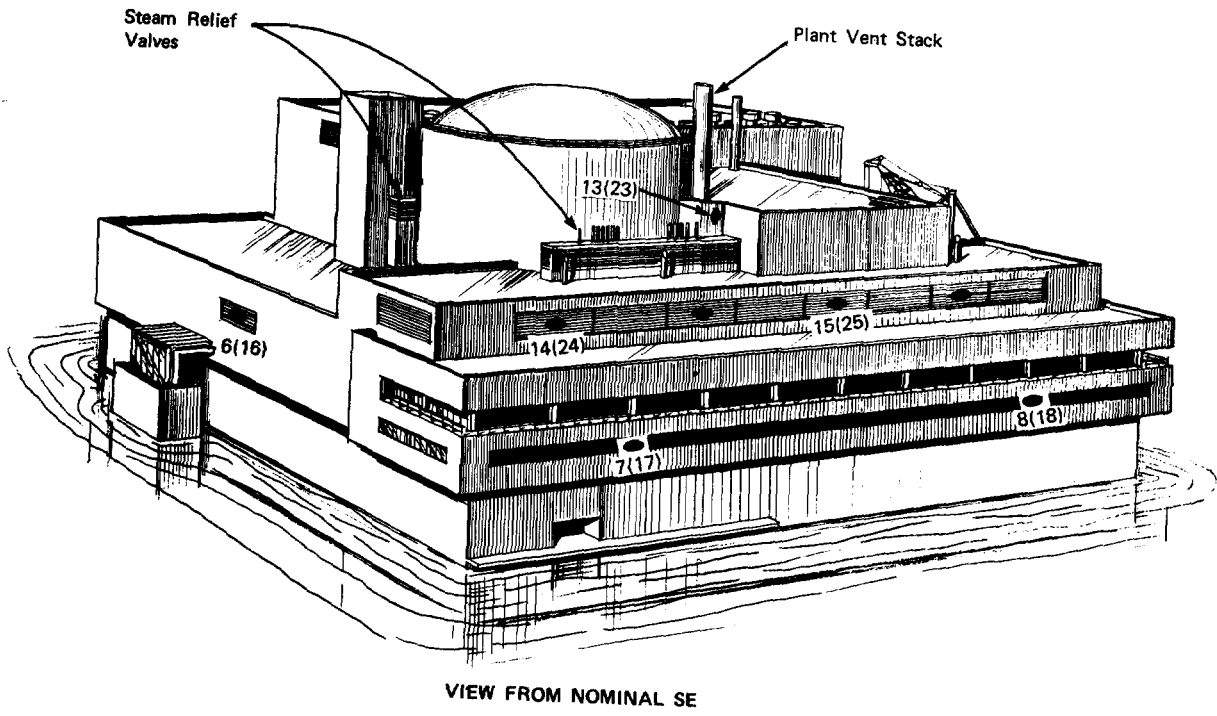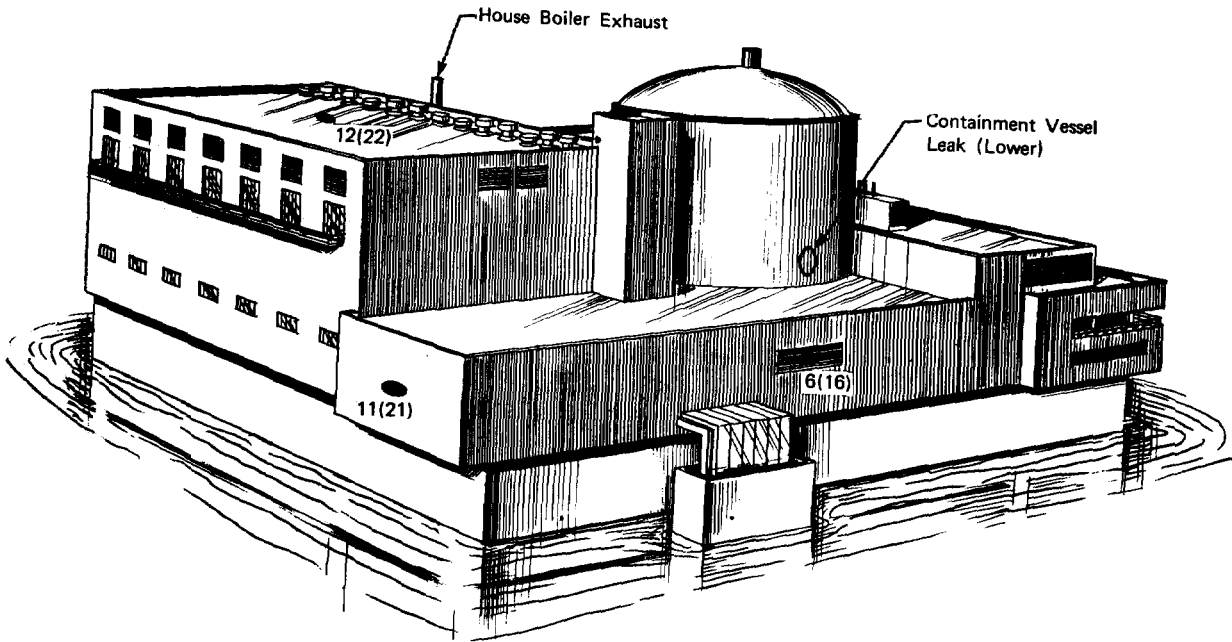
VIEW FROM NOMINAL SW

FIGURE 2

FLOATING NUCLEAR PLANT — ISOMETRIC VIEWS ILLUSTRATING
RELEASE LOCATIONS AND SAMPLING LOCATIONS

TABLE 1

SUMMARY OF TEST CONDITIONS

Source	Height (ft)	Stability	V_a (ft/sec)	V_s (ft/sec)	0°	45°	90°	90°	135°	180°	225°	270°	270°	315°
				Bldg	α	α	α	β	β	β	β	β	α	α
*Plant Vent Stack	195	N	5	.05	B1	B2	B3	B4	B5	B6	B7	B8	B9	B10
				10	B11	B12	B13	B14	B15	B16	B17	B18	B19	B20
			25	.05	B21	B22	B23	B24	B25	B26	B27	B28	B29	B30
				15	B31	B32	B33	B34	B35	B36	B37	B38	B39	B40
		S	5	.05	B41	B42	B43	B44	B45	B46	B47	B48	B49	B50
				15	B51	B52	B53	B54	B55	B56	B57	B58	B59	B60
	245	N	5	.05	B61	B62	B63	B64	B65	B66	B67	B68	B69	B70
			25	.05	B71	B72	B73	B74	B75	B76	B77	B78	B79	B80
		S	5	.05	B81	B82	B83	B84	B85	B86	B87	B88	B89	B90
				15		B180					B181			B182
*Containment Vessel	---	N	5	Lo	B91	B92	B93	B94	B95	B96	B97	B98	B99	B100
			25	Lo	B101	B102	B103	B104	B105	B106	B107	B108	B109	B110
		S	5	Lo	B111	B112	B113	B114	B115	B116	B117	B118	B119	B120
**Diesel Generator Exhaust	113	N	5	125							B121		B122	B123
			25	125							B124		B125	B126
	125		5	125							B127		B128	B129
			25	125							B130		B131	B132
**House Boiler	---	N	5	50							B133		B134	B135
			25	50							B136		B137	B138
**Steam Relief Valves	---	N	5	Hi							B139		B140	B141
			25	Hi							B142		B143	B144

* 25 Sample Locations each test
** 4 Sample Locations each test

NOTE: V_a = Wind Velocity   N = Neutral

V_s = Vent Stack Flow Velocity   S = Stable
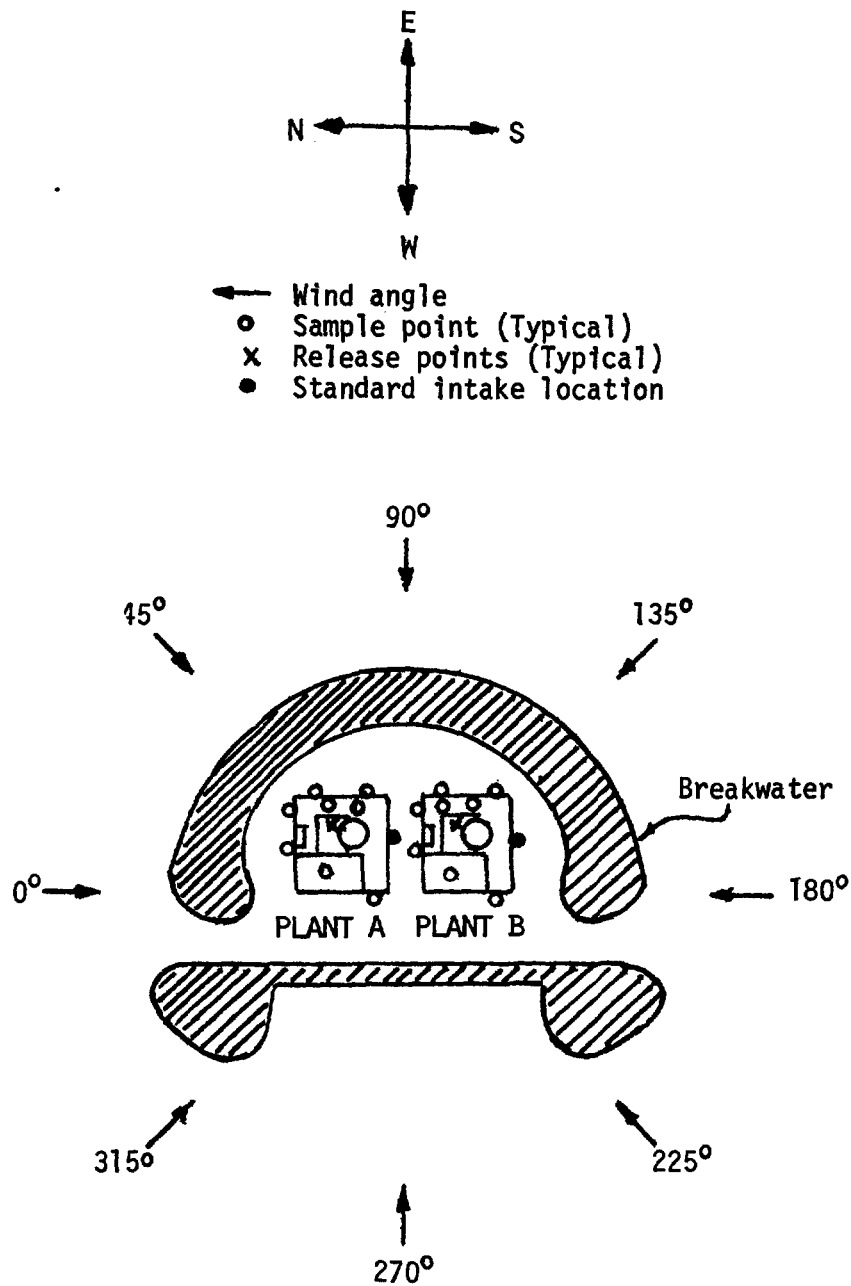
FIGURE 3

Schematic Plan View of Adjacent Plants

Inside Breakwater Illustrating Wind

Angles Employed During Test Program

(Atlantic Generating Station)
Units 1 and 2
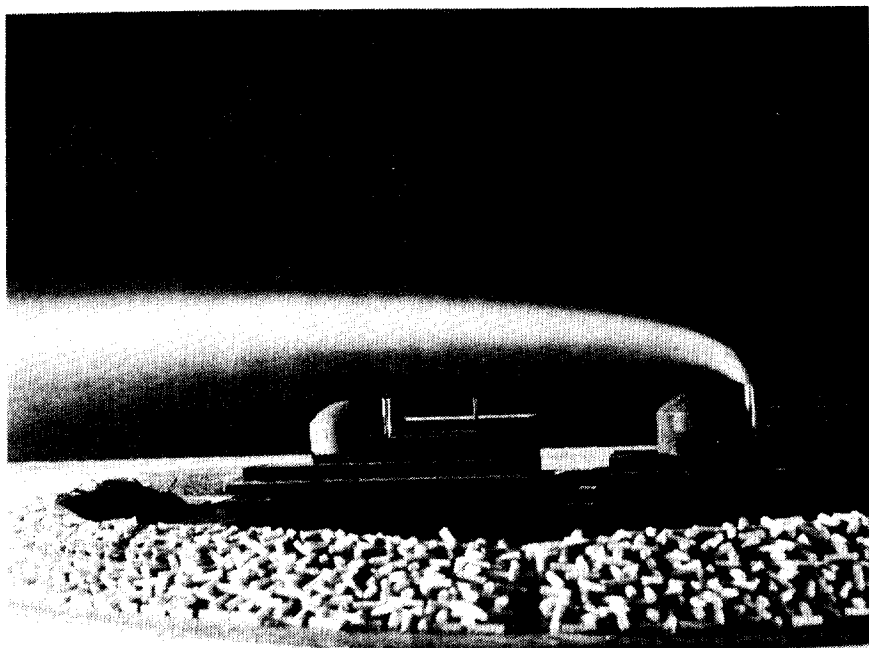
FIGURE 4

Photograph of model

During Test Illustrating

Well Defined Plume

TABLE 2

(V_aX/Q)'s AT INTAKES ON PLANT "A" FOR WIND DIRECTIONS WHICH PRODUCE HIGHEST VALUE OF PARAMETER AT INTAKE #6
NEUTRAL STRATIFICATION

Source	Stack Ht.	V_a ft/sec	V_s ft/sec	Wind Dir. *	(V_aX/Q) (M^{-2}) AT INTAKES									
					6	7	8	9	10	11	12	13	14	15
Stack-A	195'	5	.05	0°	--	--	--	--	4.2(-5)	1.3(-5)	--	--	--	--
"	"	"	"	45° }**	--	--	--	--	--	5.3(-5)	--	--	--	--
"	"	"	"	315°	--	7.5(-4)	2.5(-5)	--	--	--	--	7.3(-4)	1.0(-3)	2.7(-4)
"	"	"	10	90°	2.7(-5)	7.6(-7)	1.7(-6)	2.4(-6)	4.1(-6)	4.3(-6)	5.1(-6)	2.9(-6)	8.9(-7)	1.8(-6)
"	"	25	.05	0°	--	--	--	--	--	--	--	--	--	3.3(-5)
"	"	"	"	45° }**	--	--	--	--	--	1.7(-4)	--	--	--	--
"	"	"	"	315°	--	8.3(-4)	--	2.3(-4)	--	--	--	--	1.7(-3)	2.3(-4)
"	"	"	15	0°	2.2(-5)	3.5(-6)	1.7(-6)	2.6(-6)	1.5(-6)	4.1(-6)	3.0(-6)	2.3(-6)	2.6(-6)	2.4(-6)
"	245'	5	.05	0°	4.2(-5)	*--	--	--	--	--	--	--	--	--
"	"	25	"	270°	8.2(-6)	--	--	--	8.2(-6)	--	--	1.6(-5)	--	--
Stack-B	195'	5	.05	180°	1.6(-4)	1.4(-4)	--	3.1(-4)	1.5(-4)	1.0(-4)	--	5.7(-4)	1.9(-4)	4.3(-4)
"	"	"	10	180°	1.3(-5)	2.1(-5)	1.4(-5)	1.3(-4)	7.8(-5)	2.0(-6)	8.6(-6)	.4.5(-4)	1.6(-4)	1.7(-4)
"	"	25	.05	90°	8.3(-5)	--	--	--	--	--	--	--	--	--
"	"	"	15	180°	5.3(-5)	1.9(-4)	1.1(-4)	3.5(-4)	5.4(-4)	6.7(-6)	3.5(-5)	1.7(-3)	5.7(-4)	6.0(-4)
"	245'	5	.05	225°	4.2(-5)	--	3.3(-5)	--	--	--	--	--	--	6.7(-5)
"	"	25	"	135°	2.1(-5)	6.6(-6)	--	--	8.2(-6)	--	--	--	--	--
Cont.-A	N/A	5	1.5	0°	2.9(-4)	4.9(-6)	3.4(-6)	1.2(-6)	--	1.3(-6)	7.1(-6)	2.3(-4)	1.5(-5)	4.6(-6)
"	"	25	2.5	0°	1.0(-3)	1.1(-5)	1.3(-5)	4.4(-6)	4.3(-7)	1.7(-6)	--	1.1(-4)	2.4(-5)	1.2(-5)
Cont.-B	N/A	5	1.5	180°	5.3(-5)	2.0(-4)	1.8(-4)	2.8(-4)	7.9(-4)	4.9(-6)	4.8(-5)	8.1(-4)	8.6(-4)	7.1(-4)
"	"	25	2.5	270°	3.2(-4)	4.5(-4)	3.9(-5)	8.9(-6)	9.4(-6)	1.7(-6)	--	1.2(-4)	3.6(-4)	1.0(-4)

*   These directions were chosen from all the available data (ie. 8 different wind directions). They represent the direction which gave the largest V_aX/Q at intake #6.

** For these tests the data at intake #6 was too low to be detectable for any wind direction. Since intake #6 was south of the release point for both cases, the 0°, 45°, and 315° angles were chosen to be the worst directions

TABLE 3

(V_aX/Q)'s AT INTAKES ON PLANT "A" FOR WIND DIRECTIONS WHICH PRODUCE HIGHEST VALUE OF PARAMETER AT INTAKE #6
STABLE STRATIFICATION

Source	Stack Ht.	V_a ft/sec	V_s ft/sec	Wind Dir. *	(V_aX/Q) (M^{-2}) AT INTAKES									
					6	7	8	9	10	11	12	13	14	15
Stack-A	195'	5	.05	45°	3.4(-5)	2.4(-5)	1.4(-5)	5.0(-6)	2.5(-5)	1.9(-4)	3.2(-5)	1.5(-5)	2.0(-5)	1.4(-5)
"	"	"	15	270°	1.3(-5)	9.5(-7)	1.4(-6)	8.2(-7)	8.1(-7)	8.8(-7)	7.2(-7)	9.2(-7)	5.5(-7)	7.8(-7)
"	245'	"	.05	0° } **	--	--	--	--	--	--	--	--	--	--
"	"	"	"	45°	--	--	--	--	--	--	--	3.2(-5)	--	--
"	"	"	"	315°	--	--	--	--	3.9(-5)	--	--	3.2(-6)	2.4(-5)	--
"	"	"	15	315°	2.9(-6)	1.5(-6)	2.9(-7)	1.4(-6)	7.2(-7)	1.4(-6)	1.3(-6)	1.7(-6)	1.3(-6)	1.8(-6)
Stack-B	195'	5	.05	180°	1.0(-4)	5.7(-5)	5.1(-5)	6.5(-5)	8.7(-5)	5.9(-5)	6.6(-5)	--	2.4(-4)	--
"	"	"	15	135°	3.3(-6)	3.7(-6)	2.4(-6)	3.3(-6)	3.8(-6)	5.8(-6)	2.9(-6)	3.2(-6)	2.6(-6)	3.2(-6)
"	245'	"	.05	135° } **	--	1.3(-5)	--	1.9(-5)	7.1(-5)	3.3(-4)	--	--	--	6.3(-6)
"	"	"	"	180°	--	--	--	--	1.2(-4)	--	--	2.0(-4)	--	1.1(-4)
"	"	"	"	225°	--	--	--	--	--	--	--	6.3(-6)	--	1.3(-5)
"	"	"	15	225°	1.2(-6)	2.1(-6)	2.1(-7)	1.3(-6)	1.3(-6)	1.1(-6)	2.6(-7)	8.5(-7)	8.5(-7)	1.3(-6)
Cont.-A	N/A	5	.5	0°	3.1(-4)	9.9(-6)	8.3(-6)	1.6(-6)	4.1(-6)	4.9(-6)	2.9(-6)	5.1(-6)	3.2(-6)	3.6(-6)
Cont.-B	N/A	5	.5	180°	6.3(-6)	1.5(-5)	2.9(-5)	1.7(-4)	1.4(-4)	1.5(-4)	1.8(-4)	8.1(-4)	6.3(-4)	5.9(-4)

* These directions were chosen from all the available data (ie, 8 different wind directions). They represent the direction which gave the largest V_aX/Q at intake #6.

** For these tests the data at intake #6 was too low to be detectable for any wind direction. For these cases three directions were chosen (0°, 45°, and 315° if the intake #6 is south at the release point) or (135°, 180°, and 225°) if intake #6 is north of the release point).

TABLE 4

(V$_a$X/Q)'s AT INTAKES ON PLANT "B" FOR WIND DIRECTIONS WHICH PRODUCE HIGHEST VALUE OF PARAMETER AT INTAKE #16, NEUTRAL STRATIFICATION

Source	Stack Ht.	V$_a$ ft/sec	V$_s$ ft/sec	Wind Dir. *	(V$_a$X/Q) (M^{-2}) AT INTAKES									
					16	17	18	19	20	21	22	23	24	25
Stack-A	195'	5	.05	0°	1.1(-4)	--	--	--	--	--	--	6.7(-6)	6.7(-5)	7.3(-5)
"	"	"	10	0°	4.7(-5)	9.7(-7)	2.9(-6	3.5(-6)	2.4(-6)	2.0(-6)	4.7(-6)	1.0(-4)	6.4(-6)	5.6(-6)
"	"	25	.05	0°	4.2(-5)	--	1.9(-4)	1.3(-4)	--	--	--	3.0(-4)	--	--
"	"	"	15	0°	3.6(-4)	7.4(-6)	1.6(-5)	1.8(-5)	4.3(-5)	4.5(-5)	2.4(-5)	1.1(-3)	9.2(-5)	5.6(-5)
"	245'	5	.05	0°	6.7(-5)	--	--	--	--	--	--	1.1(-3)	--	--
"	"	25	.05	0°	2.1(-4)	6.6(-6)	--	5.2(-5)	--	--	1.6(-5)	5.8(-4)	3.3(-5)	2.0(-5)
Stack-B	195'	5	.05	180°	4.2(-5)	5.3(-5)	--	5.8(-4)	3.4(-4)	--	8.3(-5)	3.1(-4)	--	8.0(-5)
"	"	"	10	0°	2.4(-5)	1.2(-6)	4.5(-7)	1.6(-6)	3.8(-7)	4.6(-7)	5.7(-7)	8.6(-7)	1.5(-6)	--
"	"	25	.05	0°	--	--	--	--	--	--	--	--	--	3.3(-5)
"	"	"	"	45° }**	--	--	--	--	--	1.7(-4)	--	--	--	--
"	"	"	"	315° }	--	8.3(-4)	--	2.3(-4)	--	--	--	--	1.7(-3)	2.3(-4)
"	"	"	15	0°	2.2(-5)	3.5(-6)	1.7(-6)	2.6(-6)	1.5(-6)	4.1(-6)	3.0(-6)	2.3(-6)	2.6(-6)	2.4(-6)
"	245'	5	.05	0°	4.2(-5)	--	--	--	--	--	--	--	--	--
"	"	25	.05	90°	8.2(-6)	5.2(-5)	--	3.0(-5)	--	9.5(-5)	2.9(-5)	--	--	--
Cont.-A	N/A	5	1.5	315°	1.5(-4)	2.2(-4)	2.2(-4)	2.5(-4)	3.4(-4)	3.2(-5)	3.5(-4)	1.5(-4)	2.1(-4)	2.6(-4)
"	"	25	2.5	0°	2.4(-4)	1.6(-5)	4.2(-5)	1.1(-4)	1.1(-3)	1.3(-4)	1.1(-3)	4.7(-4)	1.6(-4)	1.9(-4)
Cont.-B	N/A	5	1.5	0°	2.9(-4)	4.9(-6)	3.4(-6)	1.2(-6)	--	1.3(-6)	7.1(-6)	2.3(-4)	1.5(-5)	4.6(-6)
"	"	25	2.5	0°	1.0(-3)	1.1(-5)	1.3(-5)	4.4(-6)	4.3(-7)	1.7(-6)	--	1.1(-4)	2.4(-5)	1.2(-5)

* These directions were chosen from all the available data (ie, 8 different wind directions). They represent the direction which gave the largest V$_a$X/Q at intake #16.

** For this test the data at intake #16 was too low to be detectable for any wind direction. Since intake #16 was south of the release point, the 0°, 45°, and 315° angles were chosen to be the worst directions

TABLE 5

(V_aX/Q)'s AT INTAKES ON PLANT "B" FOR WIND DIRECTIONS WHICH PRODUCE HIGHEST VALUE OF PARAMETER AT INTAKE #16
STABLE STRATIFICATION

Source	Stack Ht.	V_a ft/sec	V_s ft/sec	Wind Dir. *	(V_aX/Q) (M^{-2}) AT INTAKES									
					16	17	18	19	20	21	22	23	24	25
Stack-A	195'	5	.05	0°	8.5(-5)	2.3(-5)	2.7(-5)	2.3(-5)	9.9(-6)	1.1(-5)	2.9(-5)	5.0(-4)	6.9(-5)	3.0(-6)
"	"	"	15	315°	3.4(-6)	2.9(-6)	2.1(-6)	3.1(-6)	3.3(-6)	2.7(-6)	2.9(-6)	2.0(-6)	2.9(-6)	2.7(-6)
"	245'	"	.05	0°	3.9(-5)	--	--	--	--	--	--	1.7(-4)	--	--
"	"	"	15	45°	1.6(-6)	--	--	1.5(-6)	1.3(-6)	1.4(-6)	7.7(-7)	1.4(-6)	1.5(-6)	8.5(-7)
Stack-B	195'	5	.05	135°	5.0(-5)	4.9(-5)	3.1(-5)	1.1(-5)	3.7(-5)	3.0(-6)	3.5(-5)	9.7(-5)	4.1(-5)	2.5(-5)
"	"	"	15	315°	3.4(-6)	3.4(-6)	2.3(-6)	3.9(-6)	3.3(-6)	3.6(-6)	3.2(-6)	3.3(-6)	3.4(-6)	3.5(-6)
"	245'	"	.05	0°⎫	--	--	--	--	--	--	--	--	--	--
"	"	"	"	45°⎬**	--	--	--	--	--	--	--	3.2(-5)	--	--
"	"	"	"	315°⎭	--	--	--	--	--	--	--	2.2(-5)	--	--
"	"	"	15	315°	2.9(-6)	1.5(-6)	2.9(-7)	1.4(-6)	7.2(-7)	1.4(-6)	1.3(-6)	1.7(-6)	1.3(-6)	1.8(-6)
Cont.-A	N/A	5	.5	0°	1.1(-4)	1.5(-4)	2.7(-4)	4.4(-4)	6.9(-4)	4.5(-5)	5.5(-4)	1.8(-4)	2.1(-4)	2.4(-4)
Cont.-B	N/A	5	.5	0°	3.1(-4)	9.9(-6)	8.3(-6)	1.6(-6)	4.1(-6)	4.9(-6)	2.9(-6)	5.1(-6)	3.2(-6)	3.6(-6)

* These directions were chosen from all the available data (ie, 8 different wind directions). They represent the direction which gave the largest V_aX/Q at intake #16.

** For this test the data at intake #16 was too low to be detectable for any wind direction. Since intake #16 was south of the release point, the 0°, 45°, and 315° angles were chosen to be the worst directions

TABLE 6

PREFERRED ALTERNATE INTAKES FOR VARIOUS EXPERIMENTAL CONDITIONS

SOURCE	Stability Class	Stack Height (ft.)	Va	Vs	7	8	9	10	11	12	13	14	15	17	18	19	20	21	22	23	24	25
Plant A Stack Release	N	195	5	.05		x				x				x	x	x	x	x	x			
	"	"	"	10	x									x								
	"	"	25	.05			x		x		x	x		x			x	x	x		x	x
	"	"	"	15					x					x								
	"	245	5	.05	x	x	x	x	x	x	x	x	x	x	x	x	x	x	x		x	x
	"	"	25	.05	x	x	x			x	x		x		x		x	x				
Plant A Stack Release	S	195	5	.05		x																x
	"	"	"	15								x								x		
	"	245	"	.05	x	x	x			x	x		x	x	x	x	x	x	x		x	x
	"	"	"	15		x								x	x							
Plant B Stack Release	N	195	5	.05		x				x					x			x			x	
	"	"	"	10						x												x
	"	"	25	.05	x	x	x	x	x	x	x	x	x		x		x		x	x		
	"	"	"	15						x					x							
	"	245	5	.05	x		x	x	x	x	x	x		x	x	x	x	x	x	x	x	x
	"	"	25	.05		x	x		x	x	x	x	x		x		x					
Plant B Stack Release	S	195	5	.05							x		x			x						
	"	"	"	15		x									x							
	"	245	"	.05		x				x		x		x	x	x		x	x			x
	"	"	"	15											x							
Cont. A Release	N	N/A	5	1.5					x									x				
	"	"	25	2.5						x				x								
	S	"	5	.5			x											x				
Cont. B Release	N	N/A	5	1.5					x								x					
	"	"	25	2.5						x									x			
	S	"	5	.5	x											x						
TOTALS					7	10	9	7	8	13	6	7	6	10	13	7	9	10	8	3	5	7

TABLE 7

POTENTIAL ALTERNATE INTAKE PREFERENCE CONSIDERING TWO PLANTS

INTAKE COMBINATION		NUMBER OF PREFERENCES
PLANT A	PLANT B	FROM EXPERIMENTAL DATA
7	17	17
8	18	23
9	19	16
10	20	16
11	21	18
12	22	21
13	23	9
14	24	12
15	25	13

SELECTED ALTERNATE INTAKE: 8(Plant A); 18(Plant B)

TABLE 8

V_a (X/Q) FOR SELECTED INTAKES ON PLANT A VS. WIND DIRECTION ANGLE

Standard Intake #6
Va (X/Q) (M-2)

SOURCE	Va	Vs	STABILITY	0°	45°	90°	135°	180°	225°	270°	315°
VENT-A	5	10	N	2.4(-5)	5.7(-6)	2.7(-5)	1.2(-6)	2.7(-6)	1.9(-7)	5.9(-6)	1.3(-5)
VENT-A	5	15	S	1.2(-6)	2.5(-6)	6.4(-7)	3.2(-6)	2.2(-6)	9.4(-7)	1.3(-5)	3.4(-6)
VENT-B	5	10	N	-	-	6.4(-8)	5.2(-6)	1.3(-5)	8.3(-7)	1.7(-6)	-
VENT-B	5	15	S	-	-	3.0(-6)	3.3(-6)	3.1(-6)	1.6(-6)	5.1(-7)	-
			MAXIMUM	2.4(-5)	5.7(-6)	2.7(-5)	5.2(-6)	1.3(-5)	1.6(-6)	1.3(-5)	1.3(-5)
CONT-A	5	LOW	N	2.9(-4)	-	-	3.6(-7)	2.8(-5)	3.4(-6)	3.3(-6)	1.9(-4)
CONT-A	5	LOW	S	3.1(-4)	6.5(-6)	6.2(-6)	1.3(-6)	3.3(-6)	2.1(-6)	2.2(-6)	8.8(-5)
CONT-B	5	LOW	N	-	-	5.7(-7)	1.2(-5)	5.3(-5)	6.2(-6)	5.3(-5)	-
CONT-B	5	LOW	S	-	-	-	1.2(-5)	6.3(-4)	2.6(-7)	1.3(-6)	-
			MAXIMUM	2.9(-4)	6.5(-6)	6.2(-6)	1.2(-5)	6.3(-4)	6.2(-6)	5.3(-5)	1.9(-4)

Alternate Intake #8
Va (X/Q) (M-2)

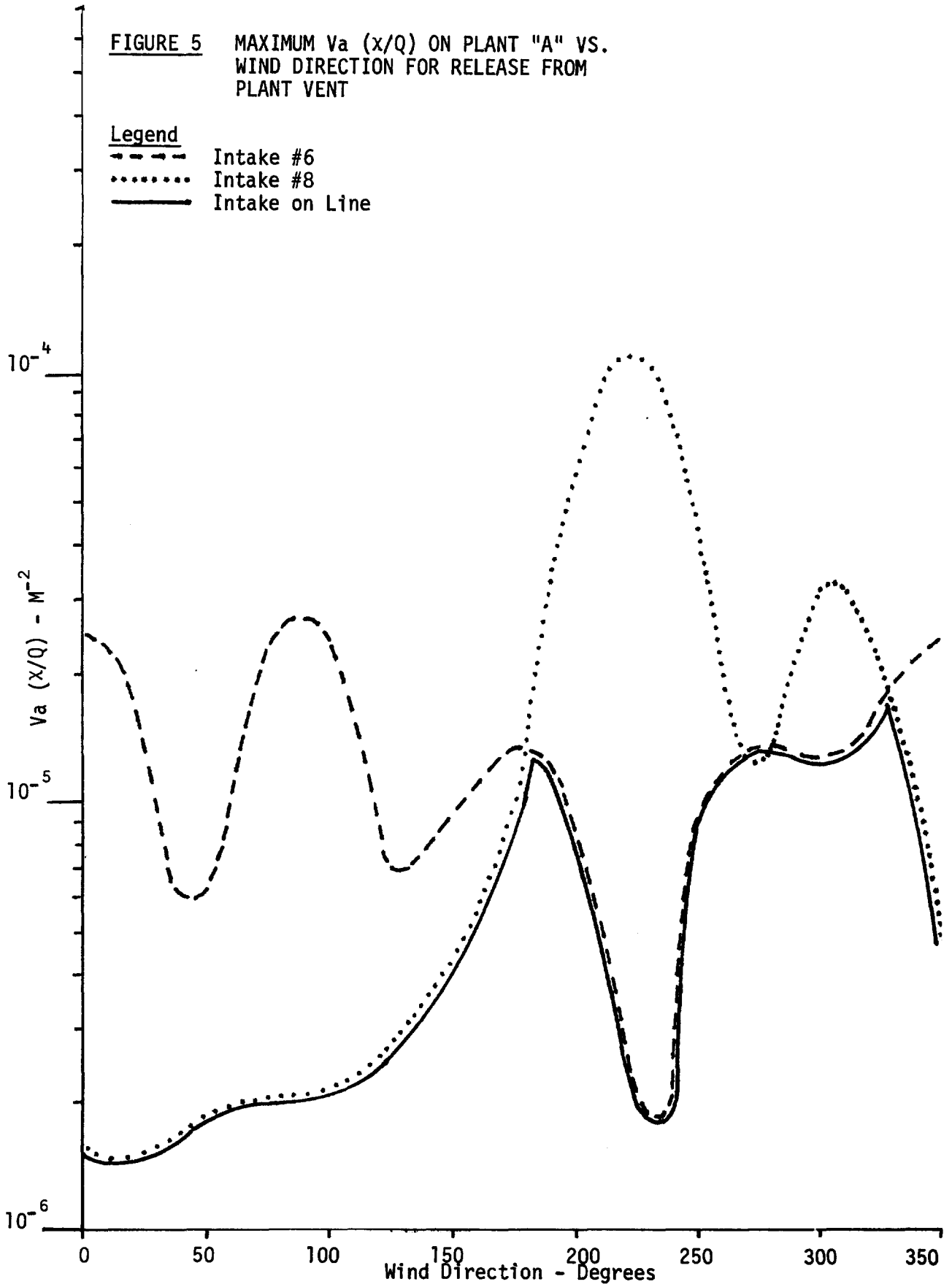| SOURCE	Va	Vs	STABILITY	0°	45°	90°	135°	180°	225°	270°	315°
VENT-A	5	10	N	4.5(-7)	1.8(-6)	1.7(-6)	1.5(-6)	3.4(-6)	1.1(-4)	1.2(-5)	3.1(-5)
VENT-A	5	15	S	1.5(-6)	1.5(-6)	4.3(-7)	3.4(-6)	1.4(-6)	2.9(-6)	1.4(-6)	2.3(-6)
VENT-B	5	10	N	-	-	-	2.5(-7)	1.4(-5)	2.5(-5)	6.9(-6)	-
VENT-B	5	15	S	-	-	2.1(-6)	2.4(-6)	2.8(-6)	1.2(-6)	1.2(-6)	-
			MAXIMUM	1.5(-6)	1.8(-6)	2.1(-6)	3.4(-6)	1.4(-5)	1.1(-4)	1.2(-5)	3.1(-5)
CONT-A	5	LOW	N	3.4(-6)	2.4(-6)	-	7.2(-7)	1.5(-4)	3.5(-5)	1.4(-4)	1.3(-4)
CONT-A	5	LOW	S	8.3(-6)	2.6(-6)	6.3(-6)	3.8(-7)	9.1(-6)	3.9(-4)	3.1(-5)	9.6(-5)
CONT-B	5	LOW	N	-	-	-	6.9(-5)	1.8(-4)	4.2(-5)	7.4(-5)	-
CONT-B	5	LOW	S	-	-	-	2.1(-6)	2.9(-5)	2.4(-4)	1.4(-5)	-
			MAXIMUM	8.3(-6)	2.6(-6)	6.3(-6)	6.9(-5)	1.8(-4)	3.9(-4)	1.4(-4)	1.3(-4)

TABLE 9

V_a (X/Q) FOR SELECTED INTAKES ON PLANT B VS. WIND DIRECTION ANGLE

Standard Intake #16
Va (X/Q) (M^{-2})

SOURCE	Va	Vs	STABILITY	0°	45°	90°	135°	180°	225°	270°	315°
VENT-A	5	10	N	4.7(-5)	4.2(-5)	5.7(-7)	-	-	-	2.4(-6)	1.7(-5)
VENT-A	5	15	S	3.2(-6)	2.7(-6)	1.8(-6)	-	-	-	1.6(-6)	3.4(-6)
VENT-B	5	10	N	2.4(-5)	5.7(-6)	-	1.1(-6)	2.7(-6)	1.9(-7)	6.4(-6)	1.3(-5)
VENT-B	5	15	S	1.2(-6)	2.5(-6)	2.6(-6)	3.2(-6)	2.2(-6)	9.4(-7)	8.1(-7)	3.4(-6)
		MAXIMUM		4.7(-5)	4.2(-5)	2.6(-6)	3.2(-6)	2.7(-6)	9.4(-7)	6.4(-6)	1.7(-5)
CONT-A	5	LOW	N	1.4(-4)	7.4(-5)	3.6(-7)	-	-	-	1.6(-5)	1.5(-4)
CONT-A	5	LOW	S	1.1(-4)	3.3(-6)	4.1(-6)	-	-	-	1.1(-5)	2.7(-5)
CONT-B	5	LOW	N	2.9(-4)	-	1.5(-6)	3.6(-7)	2.8(-5)	3.4(-6)	5.9(-6)	1.9(-4)
CONT-B	5	LOW	S	3.1(-4)	6.5(-6)	2.9(-6)	1.3(-6)	3.3(-6)	2.1(-6)	7.7(-7)	8.8(-5)
		MAXIMUM		3.1(-4)	7.4(-5)	4.1(-6)	1.3(-6)	2.8(-5)	3.4(-6)	1.6(-5)	1.9(-4)

Alternate Intake #18
Va (X/Q) (M^{-2})

SOURCE	Va	Vs	STABILITY	0°	45°	90°	135°	180°	225°	270°	315°
VENT-A	5	10	N	2.9(-6)	2.5(-6)	8.3(-7)	-	-	-	7.1(-6)	1.1(-5)
VENT-A	5	15	S	2.4(-6)	1.5(-6)	3.8(-7)	-	-	-	1.1(-6)	2.1(-6)
VENT-B	5	10	N	4.5(-7)	1.8(-6)	4.5(-7)	1.5(-6)	3.4(-6)	1.1(-4)	5.6(-4)	3.1(-5)
VENT-B	5	15	S	1.5(-6)	1.5(-6)	2.7(-6)	3.4(-6)	1.4(-6)	2.9(-6)	1.4(-6)	2.3(-6)
		MAXIMUM		2.9(-6)	2.5(-6)	2.7(-6)	3.4(-6)	3.4(-6)	1.1(-4)	5.6(-4)	3.1(-5)
CONT-A	5	LOW	N	1.4(-4)	-	-	-	-	-	4.0(-4)	2.2(-4)
CONT-A	5	LOW	S	2.7(-4)	3.6(-6)	6.3(-6)	-	-	-	2.9(-5)	3.5(-4)
CONT-B	5	LOW	N	3.5(-6)	2.4(-6)	-	7.2(-7)	1.5(-4)	3.5(-5)	2.1(-4)	1.3(-4)
CONT-B	5	LOW	S	8.3(-6)	2.6(-6)	1.3(-7)	3.8(-7)	9.1(-6)	3.9(-4)	2.8(-4)	9.6(-5)
		MAXIMUM		2.7(-4)	3.6(-6)	6.3(-6)	7.2(-7)	1.5(-4)	3.9(-4)	4.0(-4)	3.5(-4)

FIGURE 5   MAXIMUM Va (x/Q) ON PLANT "A" VS.
WIND DIRECTION FOR RELEASE FROM
PLANT VENT

Legend
- - - - -   Intake #6
• • • • • •   Intake #8
————   Intake on Line

Legend

— — —   Intake #6
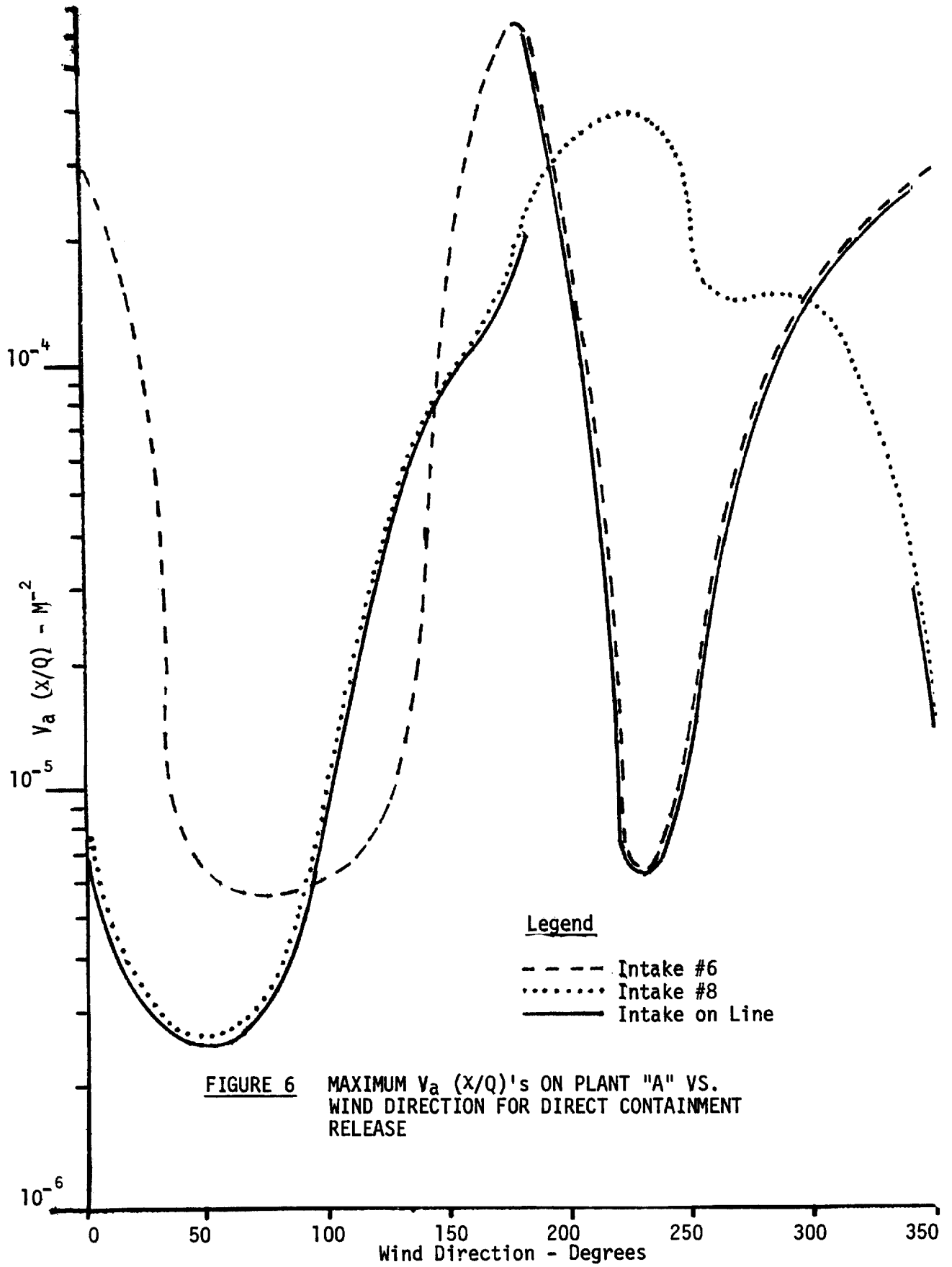· · · · · · · ·   Intake #8
————   Intake on Line

FIGURE 6   MAXIMUM V_a (X/Q)'s ON PLANT "A" VS.
WIND DIRECTION FOR DIRECT CONTAINMENT
RELEASE

FIGURE 7   MAXIMUM V_a (X/Q) ON PLANT "B"
VS. WIND DIRECTION FOR
RELEASE FROM PLANT VENT

Legend
– – – – Intake #16
. . . . Intake #18
——— Intake on Line

FIGURE 8   MAXIMUM V_a (X/Q) ON PLANT "B" VS. WIND
DIRECTION FOR DIRECT CONTAINMENT RELEASE
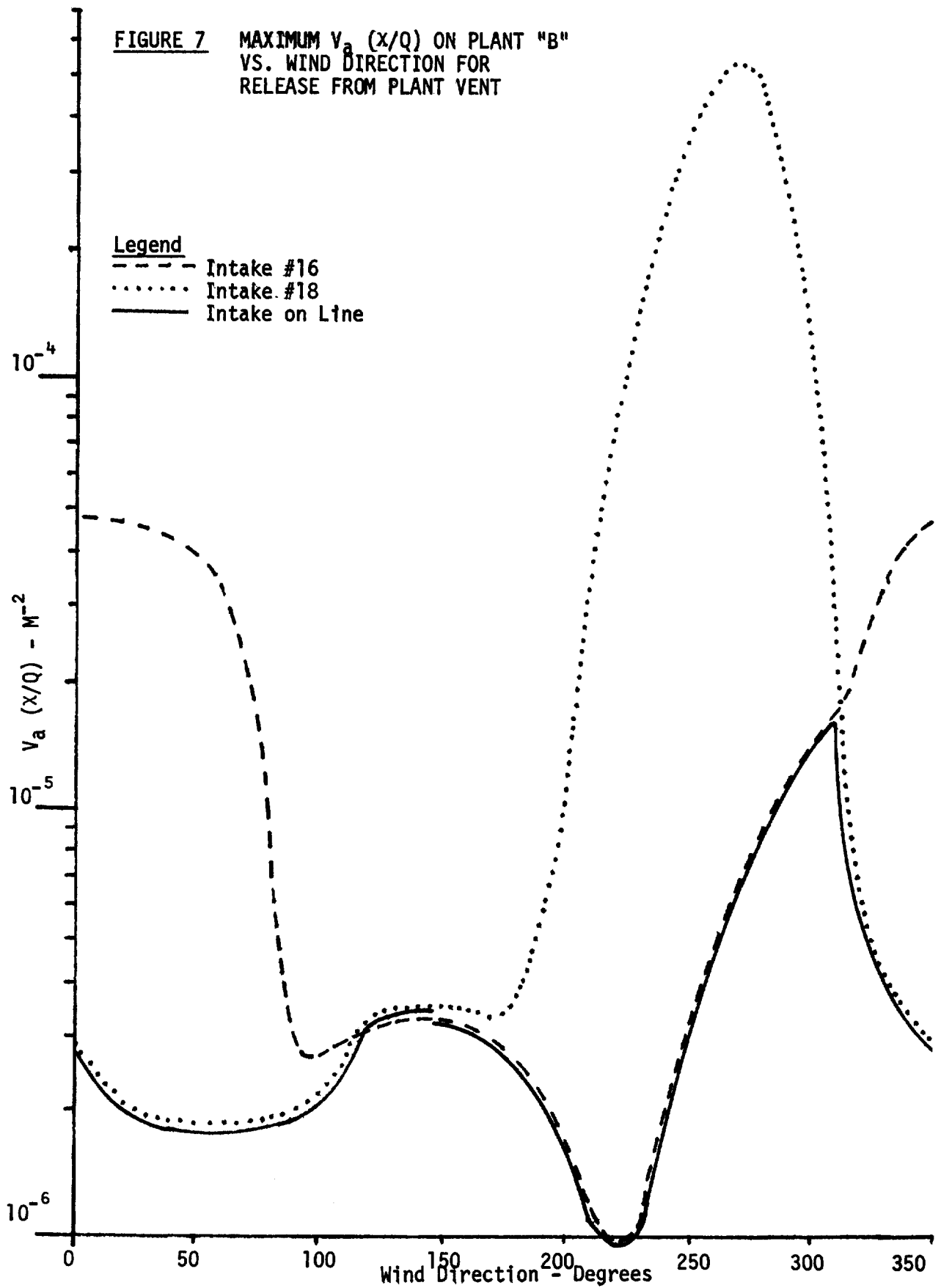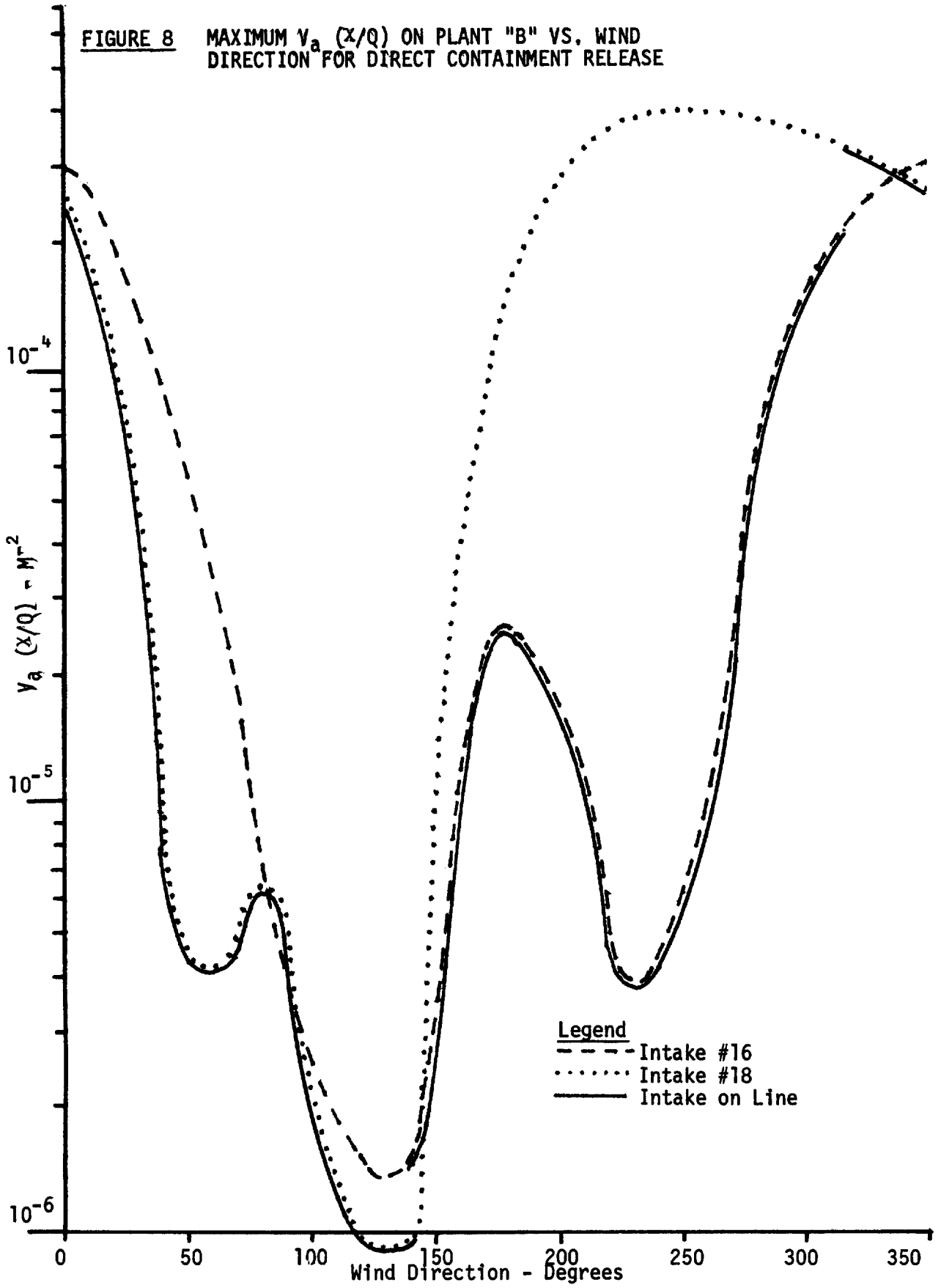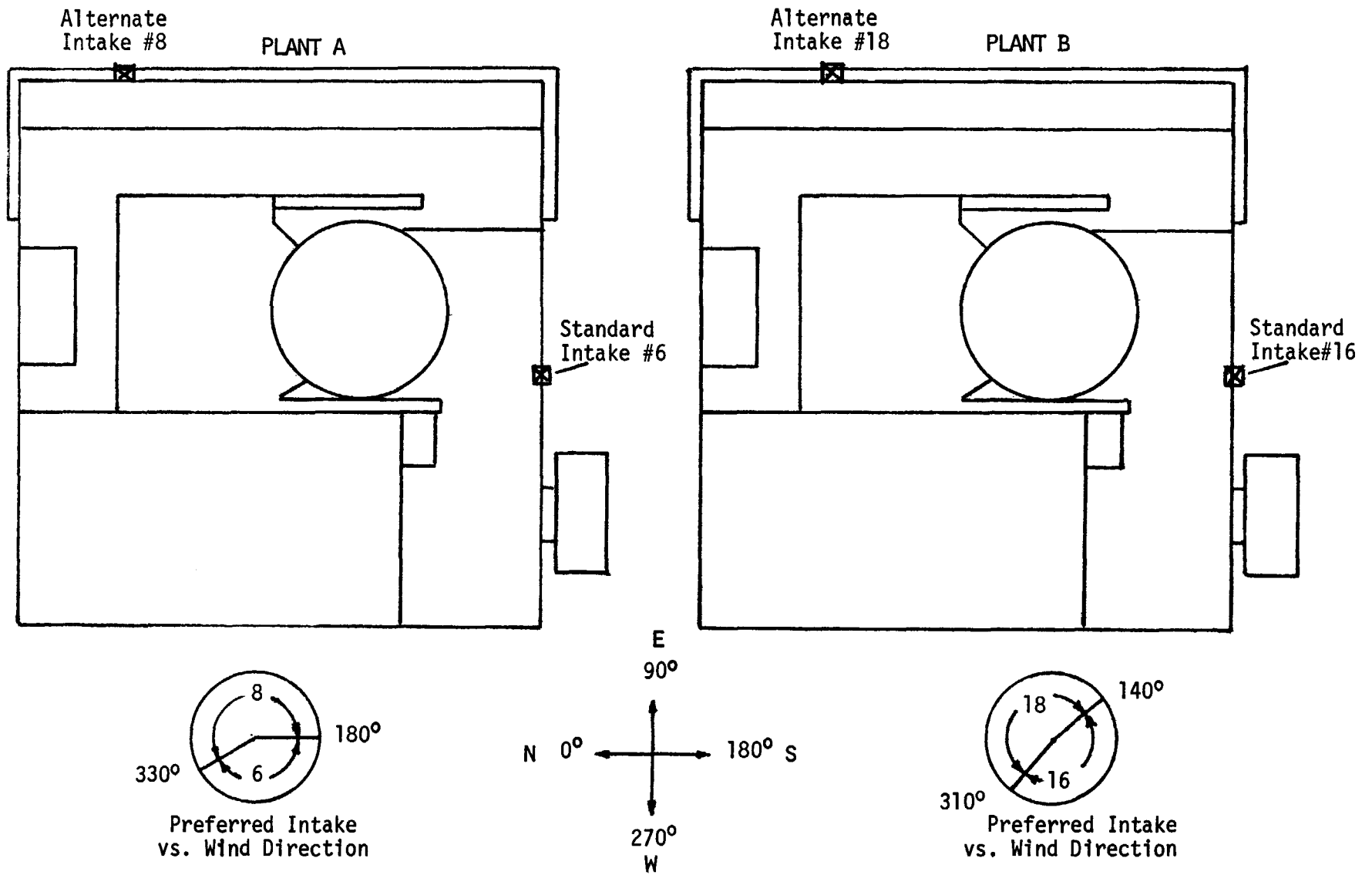
FIGURE 9   PLAN VIEW OF NUCLEAR PLANTS SHOWING STANDARD AND ALTERNATE
VENTILATION INTAKES AND PREFERRED INTAKE VS WIND DIRECTION

TABLE 10

MAXIMUM V_a (x/Q) FOR ON-LINE INTAKES

.

PLANT	STACK VENT RELEASE	CONTAINMENT RELEASE
A	1.8×10^{-5} (from Figure 5)	6.0×10^{-4} (from Figure 6)
B	1.6×10^{-5} (from Figure 7)	3.3×10^{-4} (from Figure 8)

Note: Units of M^{-2}, where $V_a = 1.5$ m/sec

DISCUSSION

SCHUERMAN: How did the Reynolds numbers compare between model and prototype?

NASSANO: The Reynolds number for the model was equal to the Reynolds number for the prototype.

EVALUATION OF CONTROL ROOM
RADIATION EXPOSURE

T. Y. Byoun and J. N. Conway
Breeder Reactor Division
Burns and Roe, Inc.
700 Kinderkamack Road
Oradell, New Jersey 07649

Abstract

This paper discusses the development, and practical
test applications of· a computer program "AID" (Accident
Inhalation Dose). The "AID" computer code calculates the
external cloud doses (gamma, whole body and beta skin) and
the resultant inhalation doses after a radiological release
based upon site meteorological data and a wide range of
possible ventilation and filtration designs.

I. Introduction

At the 13th AEC Air Cleaning Conference, a paper was
presented by K.G. Murphy and K.M. Campe of the Directorate
of Licensing entitled, "Nuclear Power Plant Control Room
Ventilation System Design for Meeting General Criteria 19."[1]
After evaluating this paper, it was apparent that it could
provide the basis for a computer code to analyze a variety
of possible ventilation and filtration options which might
be selected to meet General Design Criteria 19 of 10 CFR 50,
Appendix A. In the course of developing this code, it was
decided that it should function as a practical design tool
by permitting easy parametric changes of:

1.   Filter efficiency

2.   Filtered recirculation rate in the Control Room

3.   Filtered intake rate entering the Control Room

4.   Filtered recirculation rate in the Reactor Contain-
     ment Building

5.   Filtered exhaust rate from the Reactor Containment
     Building

6.   Source-receptor configurations

This computer code allows the user to either analyze a previously selected ventilation/filtration system or to selectively vary any of the above variables until an acceptable system is created. Since this computer code is very inexpensive to run (less than $3.00 per run), it has been our practice to fix those variables which are already frozen in the design and then to allow the computer code to optimize each of the remaining variables on successive runs. This approach allows us to see the effect on the ventilation design as each of the remaining variables is iterated until an acceptable design evolves.

II. Method of Analysis

Under a reactor accident condition, the radioactive isotopes of the core inventory may become airborne inside the containment. The continuous activity release from the containment would contaminate the air in the vicinity of the control room (CR) air intake(s) depending upon the on-site meteorological conditions. The exposure or inhalation of the airborne activity which is introduced into the CR via ventilation systems will contribute to the operating personnel radiation dose during the post-accident period.

The mathematical models incorporated into the "AID" program based on the above scenario consist of the containment model, meteorological data treatment, the ventilation system simulation for both the containment and the CR, and the time-integrated dose model. The diagrams of the system which can be handled by the "AID" are shown in Figures 1 and 2.

The time-integrated radiation exposure based on the above models can be expressed as follows:

$$D_i = F_{ij} \cdot \int_{T_1}^{T_2} A(t) \cdot {}^X\!/_Q \cdot R(t) \, dt, \tag{1}$$

where:

D_i = the time-integrated radiation exposure (Rem) due to i^{th} radioisotope

F_{ij} = effective dose conversation factors for the jth organ, that is, whole body, beta-skin, lung, bone, and thyroid

$A(t)$ = activity release rate (ci/sec) from the containment at time, t, after an accident

X/Q = effective atmospheric dilution factors (sec/m^3) based on the site meteorological data

$R(t)$ = activity dilution factor inside the CR depending upon the ventilation condition.

1. Containment Model

The term, $A(t)$, in equation (1) is the function of the containment leakage rate, ℓ, and containment cleanup system design (See Fig. 1):

$$A(t) = q_{oi} \cdot EXP\left[-\left(\lambda_i + \ell + \xi_2' \upsilon_2'/V_c\right)t\right] \cdot \ell \cdot (1 - \xi_3')$$ (2)

where:

q_{oi} = source strength (C_i) of ith isotope at time zero after an accident

λ_i = decay constant (1/sec) of ith isotope

ξ_2' and ξ_3' = filter efficiency of the containment recirculation and exhaust filter, respectively

υ_2' = in-containment recirculation rate (CFM)

V_c = free volume of the containment.

2. Control Room Filtration Systems

The activity dilution factor in the CR, $R(t)$, in equation (1) is a function of the CR filtration system design (See Fig. 1) and is shown as:

$$R(t) = \frac{\upsilon_1(1-\xi_1) + \upsilon_3}{\upsilon_1 + \upsilon_2\xi_2 + \upsilon_3} \cdot \left\{1 - EXP\left[-(\upsilon_1 + \upsilon_2\xi_2 + \upsilon_3)t/V_R\right]\right\}$$ (3)

where:

$\upsilon_1, \upsilon_2,$ and υ_3 = air-intake rate through filter (υ_1), filtered recirculation rate (υ_2), and unfiltered air infiltration rate (υ_3) in the unit of CFM

ξ_1 and ξ_2 = efficiency of the filter trains for intake and recirculation, respectively

V_R = control room free volume (ft^3).

3. Meteorological Data Treatment

The effective dilution factor (χ/Q-value) is treated as a function of site meteorological data as well as the source-receptor configuration. Adjustment factors to account for the long term meteorological averaging consist of: (1) occupancy factor, (2) wind speed factor, and (3) wind direction factor. [1]

The possible source-receptor configuration are expected to be: (a) diffuse vs. point release-point receptor, (b) ground vs. elevated release, and (c) single vs. multiple air-intake arrangements. Three different formula for the χ/Q evaluation are incorporated into the "AID" program depending upon the above source-receptor configurations.

(3.A) Evaluation of Diffusion Coefficients

Standard deviations for both horizontal crosswind (σ_y) and vertical crosswind direction (σ_z) are based on the Pasquill's diffusion curves. [2] For the desired Pasquill's stability condition (from Type A to Type G), the program "AID" estimates the coefficients by using the interpolation formula given below: [2]

$$\sigma_y(x) = \alpha \cdot x^\beta , \tag{4}$$

$$\alpha = \ln\left\{ \sigma_y(x_2)/\sigma_y(x_1) \right\} / \ln\left(x_2/x_1 \right) \tag{4a}$$

$$\beta = \sigma_y(x_1) \cdot x_1^{-\alpha} \tag{4b}$$

where:

$\sigma_y(x)$ = standard deviation of the gas concentration in the horizontal crosswind at distance, X , from the release point

$\sigma_y(x_1)$ and $\sigma_y(x_2)$ = standard deviations σ_y , at reference distances X_1 and X_2 which are permanently stored into the program as a function of the stability condition.

The coefficient for vertical crosswind direction, σ_z , is evaluated by using the same equations given above.

(3.B) X/Q -Values as a Function of Source-Receptor Configuration

(B.1) Volume Source Formula[2]

$$\frac{X}{Q} = \frac{1}{\pi u_o \Sigma_y \Sigma_z} \cdot \exp\left(-\frac{h^2}{2\Sigma_z^2}\right) \tag{5}$$

where:

u_o = five percentile wind speed in meter/sec

h = effective height of source (meters)

$$\Sigma_y = \left(\sigma_y^2 + a/2\pi\right)^{1/2} \tag{5a}$$

$$\Sigma_z = \left(\sigma_z^2 + a/2\pi\right)^{1/2} \tag{5b}$$

a = the cross-sectional area of the containment (m^2)

The above equations are for general cases, such as volumetric release, elevated releases, or point-ground level releases.

(B.2) Diffuse Release and Point Receptor[2]

$$\frac{X}{Q} = u_o^{-1} \cdot \left\{\pi \sigma_y \sigma_z + a/(K+2)\right\}^{-1} \tag{6}$$

where:

$$K = 3/(s/d)^{1.4} \quad \text{for single air-inlet arrangement} \tag{6a}$$

$$K = 0 \quad \text{for dual inlets} \tag{6b}$$

s = distance between the containment surface and receptor (meters)

d = containment diameter in meters.

Equation (6) could be applied for the following cases: [1]

(1) Diffuse release-point receptor, or vice versa

(2) Point release-point receptor with source-receptor elevation difference greater than 30% of containment height

(3) Dual air-inlets located on the major plant structures contiguous to the CR (see eq. 6b)

(B.3) Remotely-Placed Dual Inlets[1]

$$\frac{X}{Q} = \frac{0.16}{L u_o X} \tag{7}$$

where:

X = distance from source to the closest inlet (meters)

L = vertical mixing layer in meters taken as the containment height divided by 2 for the consideration of building wake factor.

Equation (7) could be applied when the dual inlets are placed about 180 degrees apart from the release point and each inlet is located well away from the major structure.[1]

(3.C) Long Term Meteorological Data Averaging

The five percentile $\frac{X}{Q}$ calculated from equations (5) to (6) is reduced on the basis of long term averaging considerations. These consist of: (1) wind speed factors, w_s , (2) wind direction factors, w_d , and (3) occupancy factors, w_o .

The first step to calculate the wind speed and wind direction factors is to determine the number of 22.5^o wind sectors that result in receptor exposure.[1]

$$
\begin{aligned}
n &= 10 && \text{if} && 0.0 \le s/d \le 0.38 \\
n &= 8 && \text{if} && 0.38 < s/d \le 0.50 \\
n &= 7 && \text{if} && 0.50 < s/d \le 0.63 \\
n &= 6 && \text{if} && 0.63 < s/d \le 0.82 \\
n &= 5 && \text{if} && 0.82 < s/d \le 1.24 \\
n &= 4 && \text{if} && 1.24 < s/d \le 2.47 \\
n &= 3 && \text{if} && s/d > 2.47.
\end{aligned}
\tag{8}
$$

Notations used in eq. (8) are described previously in eq. (6a).

The wind speed factor for the "p"-percentile wind speed, w_s, is given by using the annual joint frequency data of wind direction and speed shown in Table 1, and the following equations:

$$w_s = \frac{u_o}{u_p} \tag{9}$$

$$p = \sum_{i=N_1, j=1}^{i=N_2, j=\ell} f_{ij} \Big/ \sum_{i=N_1, j=1}^{i=N_2, j=8} f_{ij} \tag{10}$$

$$u_p = (u_\ell - u_1)/2 \tag{11}$$

where:

u_o and u_p = wind speeds of five percentile and "p"-percentiles, respectively

f_{ij} = annual joint frequency data for i^{th} wind sector and j^{th} wind speed as shown in Table 1

ℓ = ℓ^{th} wind speed column in Table 1 which would give "p"-percentile speed

N_1 and N_2 = N_1^{th} and N_2^{th} $22.5°$ wind sectors which are calculated by using eq. (8). (Winds blowing from $N_1 \sim N_2$ sectors will result in the receptor exposure.)

p = the wind speed percentile to be used for different time intervals.

The wind speed percentiles, p , applicable during subsequent time intervals after an accident are: (1) 5% during 0-8 hr. period, (2) 10% during 0-24 hr. period, (3) 20% for 1-4 days, and (4) 40% during 4-30 days period.[1]

The wind direction factor, W_d , is given by evaluating the fraction of time frequency of the receptor exposure (See Table 3),[1]:

$$F_d = \sum_{i=16, j=8}^{i=N_2, j=8} \sum_{i=N_1, j=1} f_{ij} \tag{12a}$$

$$\sum_{i=1, j=1} f_{ij} = 1 \tag{12b}$$

Based on the above fraction of time of wind blowing from source to receptor, the wind direction factors, W_d ,[1] during subsequent time intervals after an accident are used:

W_d = 1 for 0-8 hrs. period $\tag{13a}$

W_d = $0.75 + 0.25 \cdot F_d$ for 0-25 hrs. period $\tag{13b}$

W_d = $0.5 + 0.5 \cdot F_d$ for 1-4 days period $\tag{13c}$

W_d = F_d $\tag{13d}$

4. Dose Models

The "AID" program calculates the external cloud doses (gamma, whole body and beta-skin) and inhalation doses (thyroid, lung, and bone dose). Effective dose conversion factors, F_{ij} , in equation (1) are illustrated below:

(4.A) External Whole Body (WB) Dose[2]

$$F_{ij} = 0.25 \, E_{\gamma i} \tag{14a}$$

for the WB dose based on the semi-infinite cloud model

$$F_{ij} = 0.25 \cdot E_{\gamma i} \cdot V_R^{0.338}/1173 \tag{14b}$$

for the external WB dose due to the activities dispersed inside the control room (CR).

where:

$E_{\gamma i}$ = total gamma ray disintegration energy (MeV/sec) of ith isotope[4]

$V_R^{0.338}/1173$ = Geometry factor for the immersed cloud in the CR based on 0.733 MeV of average gamma energy.[1]

(4.B) Beta-Skin Dose[2]

The beta-skin dose calculation in the "AID" code has two options; with and without taking a credit of dead skin depth:

$$F_{ij} = 0.23 \bar{E}_\beta \; ; \text{ for surface dose} \tag{15}$$

$$F_{ij} = 0.23 \bar{E}_\beta \cdot \alpha \cdot \left\{ c^2 \left[3 - \exp(1 - Vd/c) \right] - \frac{Vd}{c} \left(2 + \ln \frac{c}{Vd} \right) + \exp(1 - Vd) \right\} \tag{16}$$

for the depth beta dose[2]

where:

$\bar{E}_\beta$ = average beta energy per disintegration (MeV/dis)

$$\bar{E}_\beta = 0.33 \cdot E_\beta^{max} \cdot \left(1 - z^{1/2}/50 \right) \cdot \left\{ 1 + \left(E_\beta^{max} \right)^{1/2}/4 \right\} \tag{16a}$$

z = number of electrons per atom

E_β^{max} = maximum beta disintegration energy (MeV/dis)

d = dead skin depth in gr/cm^2

c = 2   for 0.17 MeV $< E_\beta^{max} <$ 0.5 MeV

c = 1.5 for 0.5 MeV $\le E_\beta^{max} <$ 1.5 MeV

c = 1   for 1.5 MeV $\le E_\beta^{max} <$ 3   MeV

$$\alpha = \left[3c^2 - (c^2 - 1)e \right]^{-1} \tag{16b}$$

$$\nu = 37.2 / \left(E_\rho^{max} - 0.036 \right)^{1.37} \tag{16c}$$

$$\left[3 - \exp\left(1 - \frac{\nu d}{c}\right) - \frac{\nu d}{c} \cdot \left(2 + \ln \frac{c}{\nu d}\right) \right] = 0 \ \text{if} \ d \geq \frac{c}{\nu} \tag{16d}$$

(4.C) Inhalation Dose

Inhalation doses which can be estimated by "AID" program are thyroid, bone, lung, and whole body doses.

$$F_{ij} = \langle BR \rangle \cdot \overline{W}_{ij} \tag{17}$$

where:

$\langle BR \rangle$ = standard man's breathing rate (m^3/sec)

$\overline{W}_{ij}$ = j^{th} organ inhalation dose conversion factors (Rem/c_i-inhaled) due to i^{th} isotope[3]

5. "AID" -- Flow Diagram

The simplified flow diagram of the "AID" program is shown in Fig. 3.

The main input data required for "AID" program consist of:

(1) Containment leakage and geometry data (containment diameter, height, free volume),

(2) site meteorological data -- annual joint frequency data as a function of wind direction and speeds (See Table 1),

(3) initial activity data as a function of isotope,

(4) source-receptor configuration,

(5) filtration system conditions for both containment and control room based on the desired model shown in Fig. 2,

(6) option control card.

III. Discussions

A series of parametric studies on the control room(CR) accident dose analysis is usually required to develop acceptable alternate CR filtration system design which meet the regulatory requirements. The CR habitability system design features which are impacted by the above dose analysis are mainly:

(1) CR filter efficiency requirements,

(2) filtered recirculation rate(CFM) requirements for the control room or for the reactor containment,

(3) single air-inlet vs. multiple inlet arrangements including the location of the inlets,

(4) leak tightness of the control building to prevent the unfiltered infiltration of the radioactivities and to minimize the air-intake rate required for the pressurization of the CR.

The "AID" program is a practical tool for these parametric studies since it enables the designer to make a timely decision on the above design in the preliminary design stage. The special features of the "AID" code are as follows:

(1) Built-in routine for the versatile treatment of the meteorological data, including wind sector averages, and the long term X/Q -value adjustment factors, with minimum input requirements.

(2) Various options for different source-receptor configurations.

(3) Options for the site boundary analysis and activity concentration analysis in a certain cell due to the activity release from an adjacent cell.

(4) Several options in choosing the filtration system models for the containment and the control room are available (See Fig. 2).

(5) Time-dependent containment leakage rate can be handled.

(6) A library of 295 isotopic data including the organ dose conversion factors.[3,4]

(7) Automatic updating routines for different control room/containment recirculation rates, source-receptor distances, and time intervals.

IV. Conclusion

The "AID" program has proven itself to be an extremely valuable tool which we have used for both the scoping and detailed analyses that must be performed for a nuclear power plant to determine the control room vertilation design. This program is presently be used for this purpose for the Clinch River Breeder Reactor Plant. Results of a typical sample problem are included.
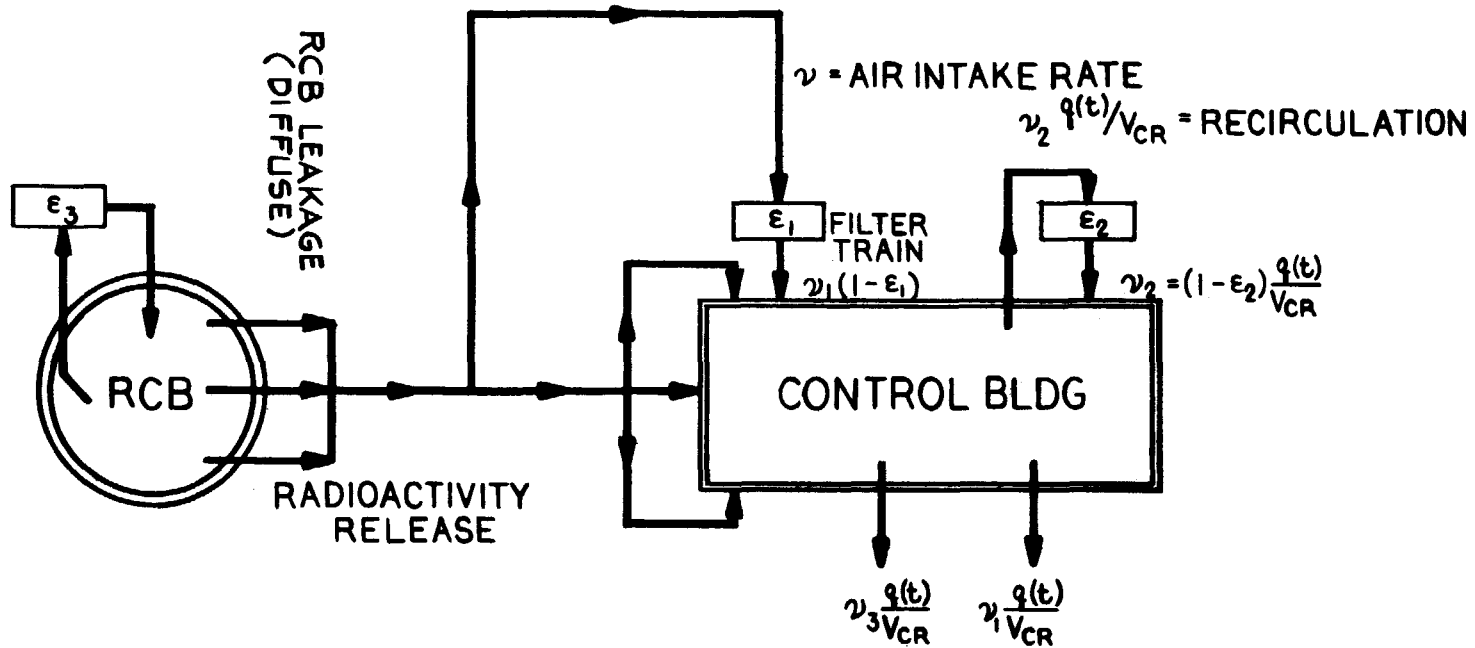
References

(1)   K.G. Murphy and K.M. Campe, "Nuclear Power Platn Control Room Ventilation System Design for Meeting General Criterion 19": Proceedings of the 13th AEC Air Cleaning Conference, Vol. 1, CONF-740807, pp. 401-430, August, 1974.

(2)   D.H. Slade, Editor, "Meteorology and Atomic Energy", TID-24190, pp. 102-113, 331-332, and pp. 406, July, 1968.

(3)   E. Specht, et. al., "Description of the COMRADEX-II Code". TI-001-130-048, pp. 41-70, Atomics International, February, 1975.

(4)   Nuclear Data Group ORNL, D.H. Horen, et. al., Editor, "Nuclear Level Schemes A=45 through A=257", Academic Press, Inc., 111 Fifth Ave., N.Y., N.Y. 10003, 1973.

v = AIR INTAKE RATE

$v_2 \dfrac{q(t)}{V_{CR}}$ = RECIRCULATION

FILTERED RECIRCULATION INSIDE THE RCB

ϵ_3

RCB

RCB LEAKAGE (DIFFUSE)

RADIOACTIVITY RELEASE

ϵ_1 FILTER TRAIN

$v_1(1-\epsilon_1)$

ϵ_2

$v_2 = (1-\epsilon_2)\dfrac{q(t)}{V_{CR}}$

CONTROL BLDG

$v_3\dfrac{q(t)}{V_{CR}}$ $v_1\dfrac{q(t)}{V_{CR}}$

NOTE:

V_{CR} = TOTAL FREE VOLUME OF THE CONTROL ROOM

$q(t)$ = AMOUNT OF CONTAMINATED AIR INTRODUCED TO THE CONTROL ROOM AS A FUNCTION OF TIME AFTER ACCIDENT

ϵ_1, ϵ_2 = FILTER EFFICIENCIES

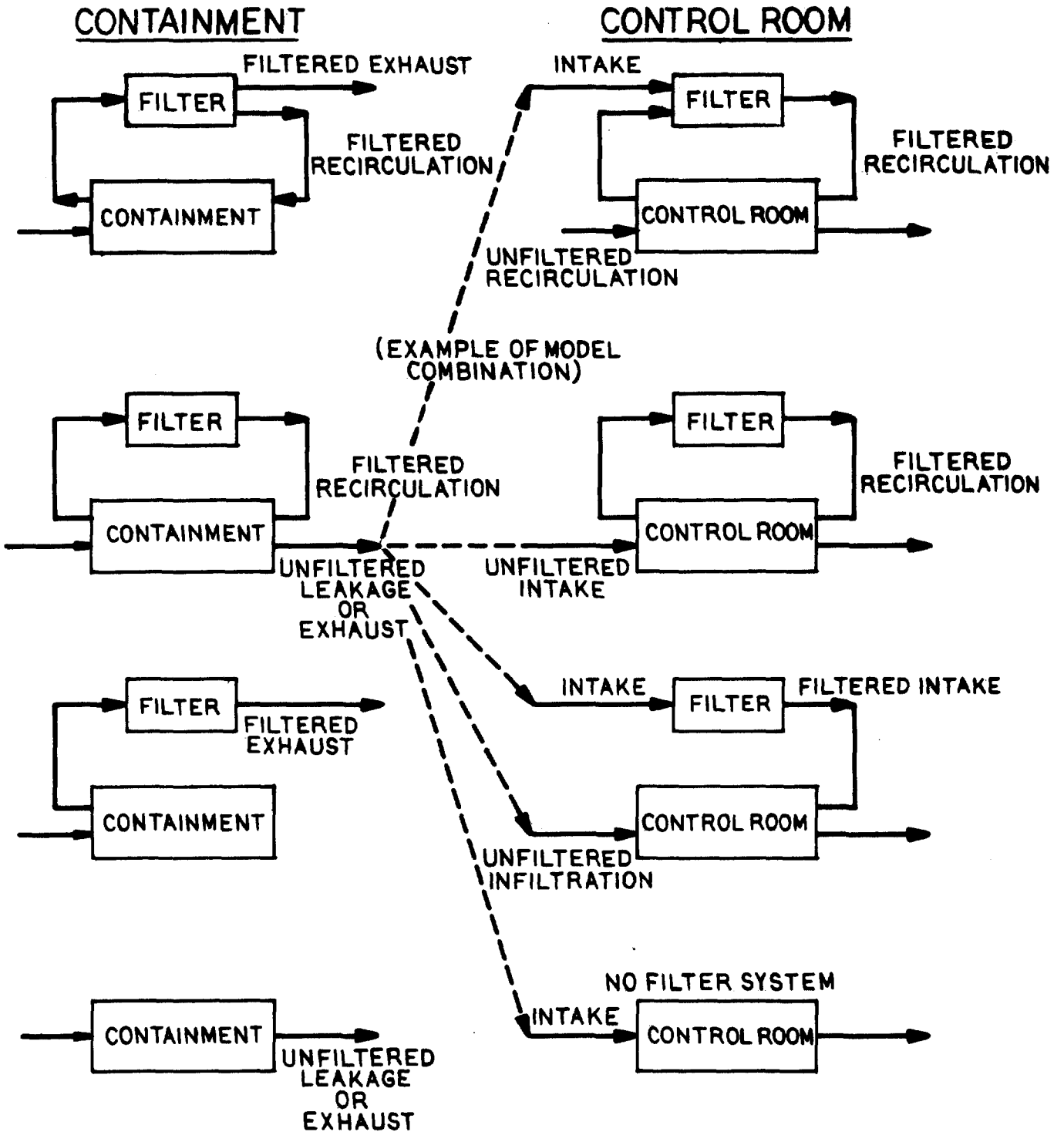FIG. I CONTROL BLDG EMERGENCY VENTILATION SYSTEM MODEL

FIG. 2 "AID" OPTIONS OF FILTER MODELS FOR CONTAINMENT AND CONTROL ROOM

FIGURE 3 - SIMPLIFIED FLOW DIAGRAM OF THE COMPUTER CODE "AID" (ACCIDENT INHALATION DOSE)
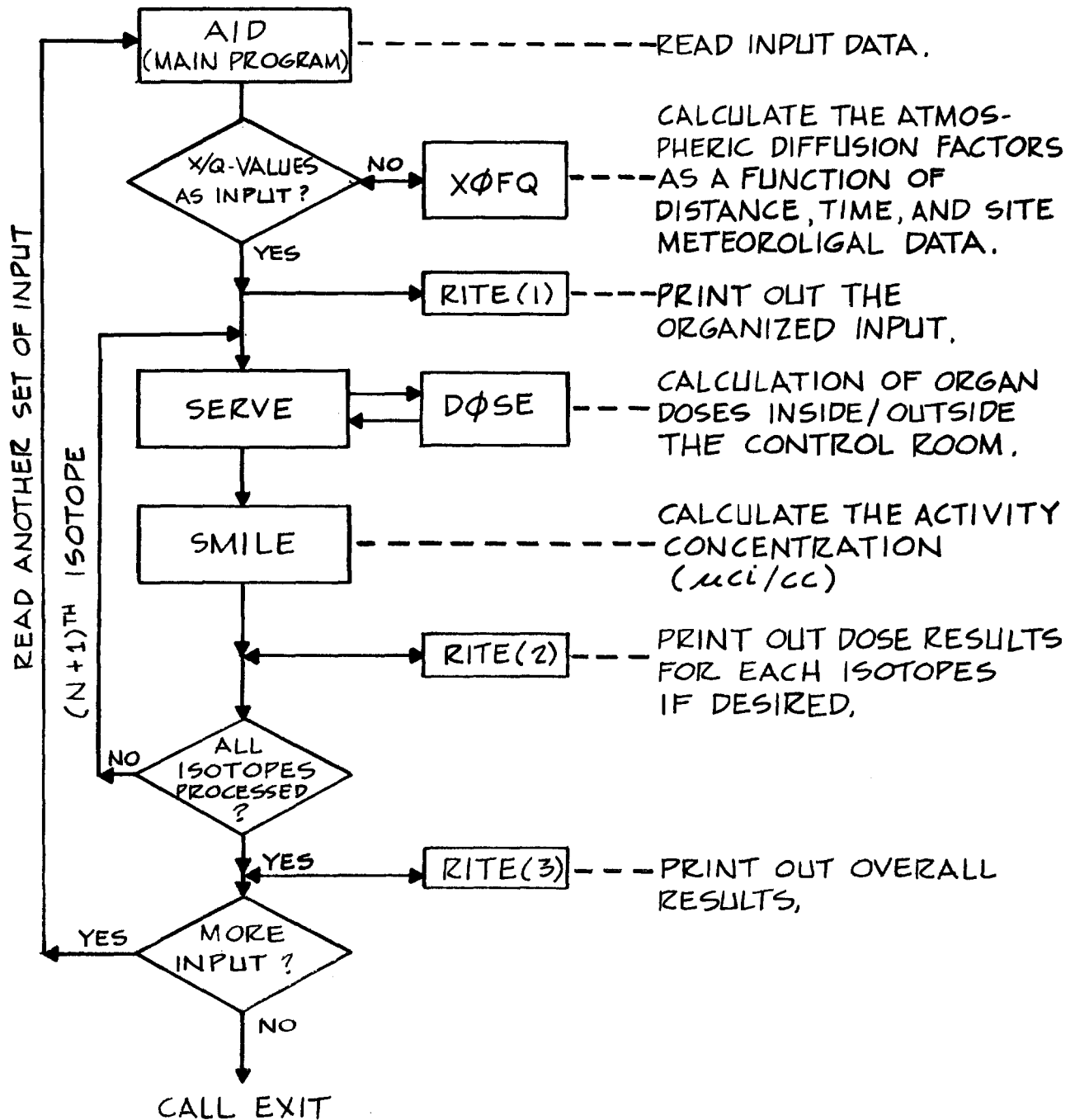
TABLE 1 - <u>ANNUAL JOINT FREQUENCY OF WIND DIRECTION</u>
<u>AND WIND SPEED (MEASURED DATA)</u>

WIND SPEED (U_j) / WIND DIRECTION (i)	ANNUAL JOINT FREQUENCY DATA $(F_{,ij})$ AS FUNCTIONS OF WIND DIRECTION (*) AND WIND SPEED (**)						
	U_1	U_2	.	.	.	U_7	U_8
N (i = 1)$^{(*)}$	$f_{1,1}$	$f_{1,2}$	.	.	.	$f_{1,7}$	$f_{1,8}$
NNE (i = 2)	$f_{2,1}$	$f_{2,2}$	.	.	.	$f_{2,7}$	$f_{2,8}$
NE (i = 3)	.	.	.	.	.	.	.
.	.	.	.	.	.	.	.
.	.	.	.	.	.	.	.
.	.	.	.	.	.	.	.
NW (i = 15)	.	.	.	.	.	$f_{15,7}$	$f_{15,8}$
NNW (i = 16)	$f_{16,1}$	$f_{16,2}$	.	.	.	$f_{16,7}$	$f_{16,8}$

(*) N (i = 1): WIND DIRECTION BLOWING FROM 22.5 DEGREE SECTOR OF THE NORTH
DIRECTION (i = 1,2, ... 16)

(**) U_j : j^{TH} WIND SPEED (KNOTS OR METER/SEC)

SAMPLE PROBLEM

Based upon a radiological release from the Reactor Containment, "AID" runs were made for Case I - Single Control Room Intake and for Case II - Dual Control Room Intakes. The only variable used was the Control Room filter recirculation rate. The initial "AID" run defined the threshold recirculation rate necessary to meet the Guideline Dose for each organ.

FOR CASE I - A&B (SINGLE CONTROL ROOM INTAKE)

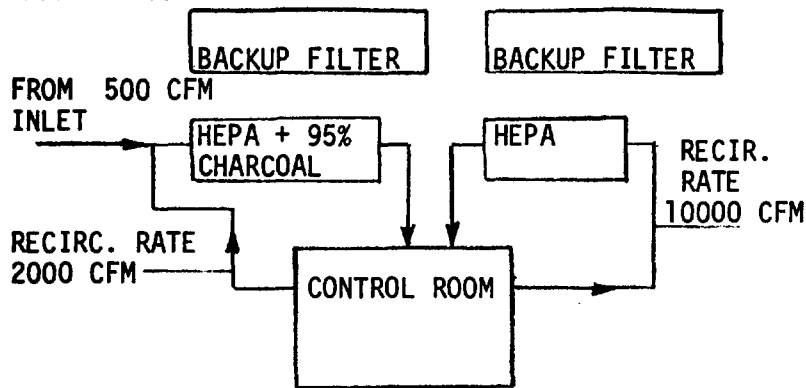| ORGAN NAME	THRESHOLD RECIRC. RATE (CFM) TO MEET GUIDELINE DOSE FOR EACH ORGAN	DOSE RESULTS (REM) CORRESPONDING TO THE THRESHOLD RECIRCULATION RATE FOR EACH ORGAN				
		WHOLE BODY	BETA-SKIN	THYROID	LUNG	BONE
WHOLE BODY	2,000	4.0	4.1	11.3	17.0	140.
BETA-SKIN	2,000	4.0	4.1	11.3	17.0	140.
THYROID	1,000	6.9	4.1	18.7	30.6	252.
LUNG	4,000	2.3	4.1	6.3	9.1	74.
BONE	12,000	1.0	4.1	2.3	3.2	26.

Based upon the above information two options were selected for further evaluation. Specific runs were made for each option with the results as shown below.

CASE A. SINGLE INTAKE AND SINGLE FILTER TRAIN:
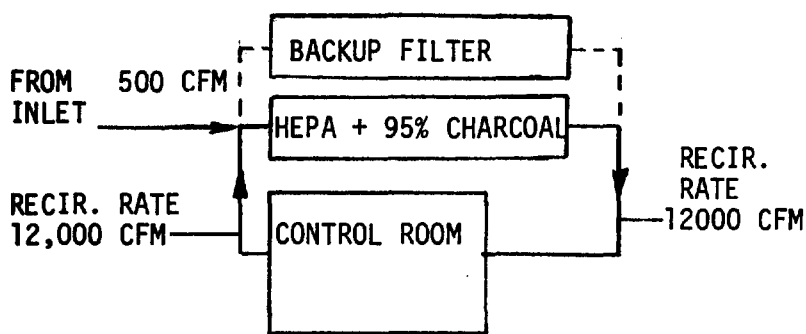
ORGANS	DOSES (REM)
WHOLE BODY	1.0
BETA-SKIN	4.1
THYROID	2.3
LUNG	3.2
BONE	26.0

CASE B. SINGLE INLET AND COMBINED FILTER TRAINS:

ORGANS	DOSES (REM)
WHOLE BODY	1.0
BETA-SKIN	4.1
THYROID	11.3
LUNG	3.2
BONE	26.0

## FOR CASES II - A&B (DUAL CONTROL ROOM INTAKES)

| ORGAN NAME	THRESHOLD RECIRC. RATE (CFM) TO MEET GUIDELINE DOSE FOR EACH ORGAN	DOSE RESULTS (REM) CORRESPONDING TO THE THRESHOLD RECIRCULATION RATE FOR EACH ORGAN				
		WHOLE BODY	BETA-SKIN	THYROID	LUNG	BONE
WHOLE BODY	1,000	4.5	1.2	7.4	20.2	170.
BETA-SKIN	1,000	4.5	1.2	7.4	20.2	170.
THYROID	1,000	4.5	1.2	7.4	20.2	170.
LUNG	2,000	2.4	1.2	4.2	10.6	89.
BONE	8,000	0.7	1.2	1.2	2.8	23.2

Based upon the above information two options were selected for further evaluation. Specific runs were made for each option with the results as shown below.

CASE A. DUAL INLETS AND SINGLE FILTER TRAIN:
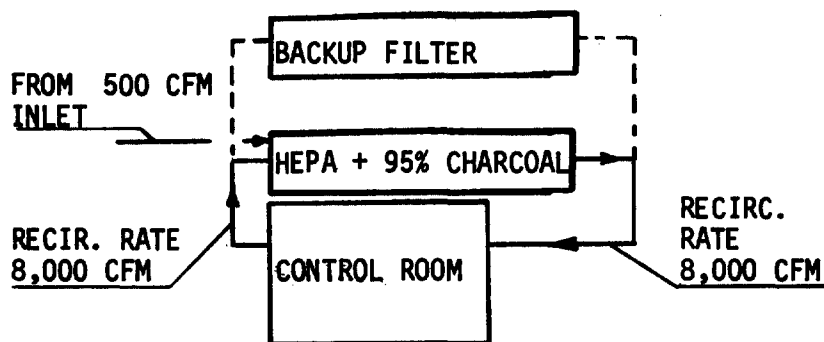
ORGANS	DOSES (REM)
WHOLE BODY	0.7
BETA-SKIN	1.2
THYROID	1.2
LUNG	2.8
BONE	23.2

CASE B. DUAL INLETS AND COMBINED FILTER TRAINS:
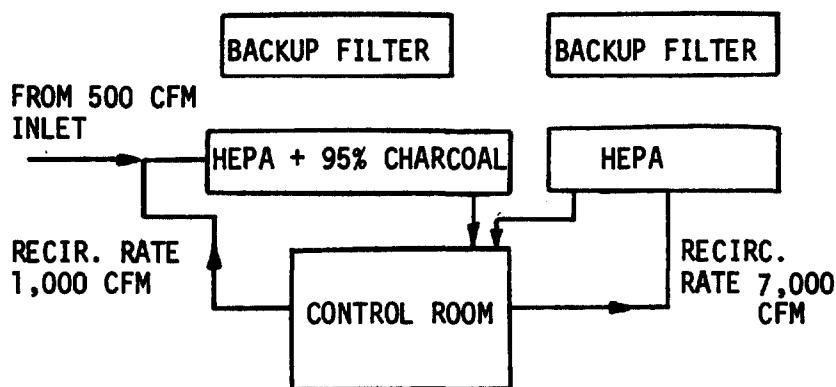
ORGANS	DOSES (REM)
WHOLE BODY	0.7
BETA-SKIN	1.2
THYROID	7.4
LUNG	2.8
BONE	23.2

DISCUSSION

MUNSON: I would like to inquire about the recirculated HEPA
filter. What is it doing?

CONWAY: In our case, it is reducing the average concentration
in the control room. We needed it because of plutonium. It was a
specific requirement there.

MUNSON: Is this requirement directly related to the outdoor
intake air cleanup by-pass that must be assumed in the dose calcula-
tion? I am sort of surprised to see particulate in the control room.

CONWAY: It was our initial intent not to have recirculation,
but we found that we couldn't handle it by any other mechanism. We
had run outside air quantities down to 500 CFM. We decided it was an
absurdity and below the amount we needed to pressurize the load. At
that point, there was no other avenue open to us.

MUNSON: Is that the assumed amount that you have to consider?

CONWAY: Yes, and it really hurt us. In this calculation, we
went to the minimum number that is allowed by NRC. I believe it was
in the order of 3 CFM. That alone was significant.